

**ROLE OF WASTE HYDRAULIC PROPERTIES ON
LANDFILL ENGINEERED SYSTEMS**

By

Lukas Novy

A Thesis submitted to the Faculty of Graduate Studies of
The University of Manitoba
in partial fulfilment of the requirements of the degree of

MASTER OF SCIENCE

Department of Civil Engineering
University of Manitoba
Winnipeg, Manitoba
R3T 5V6
Canada

Copyright © Lukas Novy, 2007

THE UNIVERSITY OF MANITOBA

FACULTY OF GRADUATE STUDIES

COPYRIGHT PERMISSION

ROLE OF WASTE HYDRAULIC PROPERTIES ON

LANDFILL ENGINEERED SYSTEMS

BY

Lukas Novy

A Thesis/Practicum submitted to the Faculty of Graduate Studies of The University of

Manitoba in partial fulfillment of the requirement of the degree

MASTER OF SCIENCE

Lukas Novy © 2007

Permission has been granted to the University of Manitoba Libraries to lend a copy of this thesis/practicum, to Library and Archives Canada (LAC) to lend a copy of this thesis/practicum, and to LAC's agent (UMI/ProQuest) to microfilm, sell copies and to publish an abstract of this thesis/practicum.

This reproduction or copy of this thesis has been made available by authority of the copyright owner solely for the purpose of private study and research, and may only be reproduced and copied as permitted by copyright laws or with express written authorization from the copyright owner.

ABSTRACT

Hydraulic design and operation of liquid injection systems and retrofitted vertical extraction wells were analyzed in this study. A two-dimensional unsaturated fluid flow model was used to simulate the hydraulic interactions that occur during liquid injection and drainage from a liquid injection system into refuse. Results from the numerical model analysis suggested that the rate of pressure increase and subsequent decrease in flow rate within a perforated injection pipe is inversely proportional to the refuse hydraulic conductivity. An injection trench positioned within refuse with a low hydraulic conductivity resulted in rapid saturation and decrease in the injected volume when compared to a high hydraulic conductivity. A set of empirical equations were present to predict the pressure development within a trench and injection volume for a range of refuse hydraulic properties and pipe hydraulic configurations were presented.

Field scale pump and recovery tests and slug injection tests were conducted at the Brady Road Landfill located in Winnipeg Manitoba to provide insight into the movement of liquid and pressure responses in a landfill and to assess refuse hydraulic properties. The well extraction rate and well specific capacity were measured and pressure responses during pumping and recovery were monitored in an array of piezometers. Pressure responses from the pump tests suggest that low permeability layers within a landfill may limit vertical liquid movement. Drawdown pressure responses were simulated using analytical methods for an unconfined aquifer and a double aquifer analytical model, recovery response data and slug test data were analyzed with analytical methods for an unconfined aquifer. Deduced refuse transmissivity from all the selected analytical methods ranged from 0.16 to 9.65 m²/day and the storativity ranged from 10⁻¹ to 10⁻³, an

unconfined aquifer analytical model deduced a specific yield that ranged from 0.13 to 0.14.

DEDICATION

This thesis is dedicated to my wonderful family for their endless love, guidance and support. I greatly appreciate all the sacrifices that were made.

Natalie, Mom and Dad
I love you all

ACKNOWLEDGMENTS

First and foremost I would like to thank my advisor Dr. Jamie VanGulck, I am not sure if I can put into words the amount I learned under his support and guidance. I will always value his patience and willingness to discuss any questions, and I am very thankful for the opportunities that are now in place for my career because of his efforts. I would like to furthermore thank Dr. Jamie VanGulck and his wife Michelle Quick for welcoming me in their home during my initial arrival to Winnipeg and countless times thereafter, I am pleased to call them both as good friends. I would like to gratefully acknowledge Dr. Grant Ferguson at St. Francis Xavier University for his timely research inputs and suggestions. How could I ever forget my fellow landfill partner and friend Stanislaw Lozecnik? I will always cherish the many friendships formed during my time in Manitoba. Whether it being squash, volleyball, or beverages and fun at Celebrity Place, there was never a lack of things to distract me from my research, thanks to all who were involved, of particular notoriety (if not already mentioned elsewhere): Bartek Puchajda and Dominika Celmer, Irmgard Nikkel; Natalie Joyce, Tim Krahn and Dalila Seckar, Greg and Sonya Siemens, Neil Privat and his family, Mike Head and Dagmara Cenkowski, Jared Baldwin, German Circo, Alexander Knop, Clifford Dyck and Catherine Gerbasi, Kevin Stevens , Rob Craig. Lastly there are numerous people inside and outside of the University that directly helped with my thesis research that require mentioning and they are as follows: Summer students Adam Moore and Dave Kruz,, Kerry Lynch from the Geotechnical Engineering Laboratory, Colin Potter and Tony Kuluk from the Winnipeg Solid Waste Division, Lyod Peacock from Physical Plant Services, Ricky Langlois and Gord Boychuk from Paddock Drilling Ltd.

TABLE OF CONTENTS

ABSTRACT	II
DEDICATION	IV
ACKNOWLEDGMENTS.....	V
TABLE OF CONTENTS.....	VI
LIST OF TABLES.....	IX
LIST OF FIGURES.....	XI
CHAPTER 1: INTRODUCTION.....	1
1.1 PROBLEM DEFINITION.....	1
1.2 SCOPE OF THESIS.....	3
1.3 THESIS OUTLINE.....	4
1.4 REFERENCES.....	5
CHAPTER 2: LITERATURE REVIEW.....	6
2.1 INTRODUCTION.....	6
2.2 REFUSE HYDRAULIC PROPERTIES.....	8
2.2.1 Saturated Hydraulic Conductivity.....	8
2.2.1.1 Methods of Determination.....	8
2.2.1.2 Reported Values.....	10
2.2.2 Field Capacity and Specific Yield.....	10
2.2.2.1 Methods of Determination.....	11
2.2.3 Reported Values.....	13
2.2.4 Unsaturated Characteristics of MSW.....	13
2.2.5 Role of Overburden Pressure and Compaction Efforts.....	16
2.2.5.1 Methods of Determination.....	16
2.2.5.2 Reported Values.....	17
2.3 CONCLUSIONS.....	19
2.4 REFERENCES.....	22
CHAPTER 3: HLIS NUMERICAL SIMULATIONS.....	42
3.1 INTRODUCTION.....	42
3.2 FIELD CASE STUDY.....	44
3.2.1 Methodology.....	46
3.2.2 Model Domain and Boundary Conditions.....	47
3.2.3 Pipe Hydraulic Configurations.....	48
3.2.4 Pipe Hydraulic Boundary Conditions.....	49
3.2.5 Refuse and Backfill Hydraulic Properties.....	51
3.3 HLIS NUMERICAL SIMULATIONS.....	53
3.3.1 Effect Of Refuse Properties on Liquid Injection.....	53
3.3.2 Influence of Pipe Hydraulic Configurations.....	55
3.3.3 Validity of Pipe Perforation Boundary Conditions.....	56
3.3.4 HLIS Zones of Liquid Saturation.....	57
3.3.5 Liquid Injection Schedule Analysis.....	59

3.4	DESIGN IMPLICATIONS	60
3.4.1	Empirical Correlations	61
3.4.1.1	Empirical Design Methodology	63
3.5	CONCLUSIONS	64
3.6	REFERENCES	66
CHAPTER 4: BRADY ROAD LANDFILL WELL EXTRACTION TESTS.....		82
4.1	INTRODUCTION.....	82
4.2	LEACHATE EXTRACTION WELL FIELD STUDIES	83
4.2.1	Iowa Sanitary Landfills, United States, Hentges et al. (1993)	84
4.2.2	Buckinghamshire and Cambridgeshire, England, Burrows et al. (1997).....	84
4.2.3	Chianni Landfill, Pisa, Italy, Giardi (1997)	85
4.2.4	New Jersey, United States, Oweis et al. (1990)	86
4.3	THEORETICAL BACKGROUND INFORMATION.....	86
4.4	BRADY ROAD FIELD STUDY	87
4.4.1	Field Study Hydrogeology	89
4.4.2	Leachate Extraction Pump and Slug Tests	90
4.4.3	Pump and Recovery Test Pressure Behaviour	91
4.4.4	Refuse Hydraulic Properties Method of Analysis.....	94
4.4.4.1	Neuman (1974) Unconfined Aquifer Drawdown Pumping Response..	95
4.4.4.2	Moench (1984) Dual Porosity Drawdown Pumping Response	96
4.4.4.3	Theis (1935) Recovery Analysis	96
4.4.4.4	Bouwer and Rice (1976)	97
4.4.5	Deduced Refuse Hydraulic Properties	98
4.4.5.1	Transmissivity	99
4.4.5.2	Storativity and Specific Yield	100
4.4.5.3	Anisotropy.....	101
4.5	DESIGN IMPLICATIONS	102
4.6	CONCLUSIONS	103
4.7	REFERENCES	104
CHAPTER 5: CONCLUSIONS AND RECOMENDATIONS.....		122
5.1	INTRODUCTION.....	122
5.2	SUMMARY AND CONCLUSIONS	122
5.3	PRACTICAL FINDINGS AND RECOMMENDATIONS.....	124
APPENDIX A NUMERICAL STABILITY ANALYSIS		126
A.1	NUMERICAL STABILITY ANALYSIS OF HLS MODEL	127
A.2	NUMERICAL STABILITY ANALYSIS OF VERTICAL EXTRACTION WELL MODEL ...	127
APPENDIX B HLIS EMPERICAL CORRELATIONS.....		129
APPENDIX C BRADY ROAD LANDFILL FIELD STUDY SURVEY		138
APPENDIX D ANALYTICAL SOLUTIONS FITS		141
APPENDIX E EXTRACTION WELL NUMERICAL ANALYSIS		151
E.1	REFUSE ANISOTROPY NUMERICAL ANALYSIS.....	152
E.1.1	Model Domain and Boundary Conditions	152
E.1.2	Refuse Hydraulic Properties	153

E.1.3 Vertical Extraction Well Numerical Simulations	154
E.2 REFERENCES	156

LIST OF TABLES

Table 2.1: Summary of refuse hydraulic conductivity measurements conducted in the laboratory	33
Table 2.2: Summary of refuse hydraulic conductivity measurements conducted in the field.....	34
Table 2.3: Summary of reported refuse hydraulic conductivity using alternative methods	35
Table 2.4: Summary of refuse initial water content, field capacity, porosity and specific yield using field and laboratory methods	36
Table 2.5: Summary of refuse initial water content, and porosity using alternative methods	37
Table 2.6: Summary of literature reported values of the power law empirical parameters for refuse.	38
Table 2.7: Summary of influence of compaction effort on the reported refuse unit weight. (modified from a summary compiled by Oweis and Khera (1986) and Rowe and VanGulck (2004))......	39
Table 3.1: Summary of the three selected pipe hydraulic configurations.	70
Table 3.2: Summary of designated, saturated refuse hydraulic conductivities, pipe hydraulic configurations, and pipe perforation boundary conditions for a series of six HLIS numerical simulations.....	70
Table 3.3: Summary of the time required to fill a HLIS, the pressure head at the bottom of the trench (h_p) volume of liquid injected (V), and the deduced maximum horizontal (x), upward vertical (z_{up}), and downward vertical (z_{down}) distances for 4, 8 and 24 hours of liquid injection simulation respectively.	71
Table 3.4: Summary of the selected variable saturated refuse hydraulic conductivity, the initial drainage trench bottom pressure (h_p) and volume injected (V), and the time duration to drain a trench for each series of liquid drainage simulation.	72
Table 4.1: Summary of deduced transmissivity and storativity values for all extraction wells used by Hentges <i>et al.</i> (1993) (modified from Hentges <i>et al.</i> (1993)).	108
Table 4.2: Saturated refuse depth, deduced values for refuse transmissivity, hydraulic conductivity, specific yield, and sustainable yield from Burrows <i>et al.</i> (1997) Buckinghamshire and Cambridgeshire, England (modified from Burrows <i>et al.</i> (1997)).	109
Table 4.3: Summary of extraction well depth, ground elevation, piezometric surface, extraction rate, and deduced transmissivity for drawdown and recovery from Chianni Landfill, Italy (modified from Giardi (1997)).	110
Table 4.4: Summary of the top casing elevation, bottom elevation, and depth for installed extractions wells and piezometers at the Brady Road Landfill.	111
Table 4.5: Summary of the maximum measured drawdown with radial distance from the extraction for the 9.1 m, 6.1 m and 3.0 m deep piezometers during pump Test 1 and Test 2.	112

Table 4.6: Summary of the deduced refuse transmissivity, specific yield and anisotropy from drawdown and extraction rate data collected from Pump Test 1 and Test 2 using the Neuman (1974) solution for an unconfined aquifer.	113
Table 4.7: Summary of the deduced refuse transmissivity and storativity using the Theis (1935) recovery method.	113
Table 4.8: Summary of selected spherical block diameter and deduced refuse transmissivity and storativity using the dual porosity spherical block model of Moench (1984).	114
Table 4.9: Summary of initial displacement after slug injection, and deduced refuse transmissivity using the slug tests method of Bouwer and Rice (1976).	115
Table B.1: Deduced values for the a_v and b_v and a_{hp} and b_{hp} derived coefficients for a refuse hydraulic conductivity of 10^{-8} m/s and selected model refuse inlet hydraulic head (h_p), and , normalised perforation flux (q_{seep}).....	130
Table B.2: Deduced values for the a_v and b_v and a_{hp} and b_{hp} derived coefficients for a refuse hydraulic conductivity of 10^{-8} m/s and selected model refuse inlet hydraulic head (h_p), and , normalised perforation flux (q_{seep}).....	131
Table E.1: Summary of selected anisotropy ratio, refuse hydraulic conductivity, and aquifer compressibility for the conducted vertical extraction numerical simulations.....	157

LIST OF FIGURES

Figure 2.1: Hydraulic conductivity as a function of vertical stress within a landfill.	40
Figure 2.2: Hydraulic conductivity as a function of refuse depth with a landfill.	40
Figure 2.3: Hydraulic conductivity as a function of the refuse unit weight.	41
Figure 2.4: Change in field capacity, saturated water content and specific yield with induced vertical stress as measured by Powrie and Beaven (1999).	41
Figure 3.1: Typical injection flow and pressure head response (modified from Townsend and Miller 1998).	73
Figure 3.2: Schematic representation of uniform pipe perforation discharge, backpressure, and liquid drainage into surrounding refuse for: (a) partially filled trench and (b) completely filled trench.	73
Figure 3.3: (a) Numerical model boundary conditions and problem domain, (b) detailed trench configuration and numerical model boundary conditions.	74
Figure 3.4: Perforation backpressure and model perforation flux relationship for the described three hydraulic pipe scenarios.	75
Figure 3.5: Baseline configuration pressure head increase at the trench base during liquid injection for refuse saturated hydraulic conductivities of 10^{-4} m/s, 10^{-6} m/s and 10^{-8} m/s with variable and constant hydraulic conductivity with suction.	75
Figure 3.6: Deduced perforation liquid injection flux for baseline configuration (a) and cumulative volume of liquid (b) for simulated liquid injection for refuse saturated hydraulic conductivities of 10^{-4} m/s, 10^{-6} m/s and 10^{-8} m/s with variable and constant hydraulic conductivity with suction.	76
Figure 3.7: Pressure head deduced at the trench base during liquid injection for refuse saturated hydraulic conductivities of 10^{-4} m/s, 10^{-6} m/s and 10^{-8} m/s with a high perforation flux and high perforation pressure head pipe configuration.	76
Figure 3.8: Deduced perforation liquid injection flux (a) and cumulative volume of liquid (b) for simulated liquid injection for refuse saturated hydraulic conductivities of 10^{-4} m/s, 10^{-6} m/s and 10^{-8} m/s for the high perforation flux and high perforation pressure head hydraulic scenarios.	77
Figure 3.9: Pressure head deduced at the trench base during liquid injection for variable refuse saturated hydraulic conductivities of 10^{-4} m/s, 10^{-6} m/s and 10^{-8} m/s with a head dependent flux, constant flux, and constant pressure perforation hydraulic boundary condition.	77
Figure 3.10: Cumulative volume of liquid for simulated liquid injection for refuse saturated hydraulic conductivities of 10^{-4} m/s, 10^{-6} m/s and 10^{-8} m/s for a head dependent flux, constant flux, and constant pressure perforation hydraulic boundary condition.	78
Figure 3.11: Deduced pressure head decrease at the trench base from liquid drainage into variable refuse hydraulic conductivities of 10^{-6} and 10^{-8} m/s for an 8 hour liquid injection schedule using the baseline pipe hydraulic configuration.	78
Figure 3.12: Developed zones of saturation after 8 hrs of liquid injection into a variable refuse hydraulic conductivity of a) 10^{-4} , b) 10^{-6} and c) 10^{-8} m/s hydraulic conductivity using the baseline pipe configuration.	79

Figure 3.13: a_{hp} and b_{hp} pressure head development coefficients for liquid injection using range of inlet hydraulic head and normalised perforation flux with saturated refuse hydraulic conductivity of 10^{-6} and 10^{-8} m/s.	80
Figure 3.14: a_v and b_v liquid volume coefficients for liquid injection using range of inlet hydraulic head and normalised perforation flux with saturated refuse hydraulic conductivity of 10^{-6} and 10^{-8} m/s.....	81
Figure 4.1: Plan view schematic of extraction well and piezometer layout (not to scale)	116
Figure 4.2: Measured average liquid elevations with radial distance from three piezometers located at depths of 3.0 m, 6.1 m and 9.1 m within the Brady Road Landfill.	116
Figure 4.3: Observed landfill composition during drilling: (a) clay cap material and (b) grayish to black slurry waste material.....	117
Figure 4.4: Field test location and the surrounding landfill cell at a higher elevation... ..	118
Figure 4.6: Pressure response in 9.1 m deep peizometers at radial distances of 1.0 m, 1.4 m, 3.0 m and 3.2 m away from the extraction for two pump tests.....	119
Figure 4.7: Recovery response for 9.1 m deep peizometers at radial distances of 1.0 m, 1.4 m, 3.0 m and 3.2 m away from the extraction for two pump tests.....	120
Figure 4.8: Example of a) Neuman (1974) and b) Moench (1984) solution fit to measured drawdown for Test 2 and P6A.	120
Figure 4.9: Example of Theis (1935) solution fit to measured recovery response at piezometer P6A after Pump Test 2.	121
Figure 4.10: Example of Bouwer and Rice (1976) solution fit to slug removal test at piezometer P6A.	121
Figure 4.11: Deduced transmissivity for 6.1 m and 9.1 m depth piezometers using the slug method of Bouwer and Rice (1976).	121
Figure A.1: Pressure head deduced at the trench base during liquid drainage injection for a refuse saturated hydraulic conductivities of 10^{-6} m/s the baseline pipe configuration and two specific model input scenarios.	128
Figure A.2: Original simulated drawdown response at radial distance of 1 m and refuse depth of 8.8 m for a vertical to hydraulic anisotropy ratios of 1, refuse compressibility of 5.5×10^{-5} kPa ⁻¹ , and refuse hydraulic of 6.3×10^{-7} m/s, and for and two specific model input scenarios.....	128
Figure B.1: Simulated and predicted a) pressure head at the trench base and b) volume injected for liquid injection into a saturated refuse hydraulic conductivity of 10^{-6} m/s, a normalized model perforation discharge of 5×10^{-5} m ³ /s/m, and an inlet hydraulic head of 2 to 50 m.....	132
Figure B.2: Simulated and predicted a) pressure head at the trench base and b) volume injected for liquid injection into a saturated refuse hydraulic conductivity of 10^{-6} m/s, a normalized model perforation discharge of 3×10^{-5} m ³ /s/m, and an inlet hydraulic head of 2 to 50 m.....	133

Figure B.3: Simulated and predicted a) pressure head at the trench base and b) volume injected for liquid injection into a saturated refuse hydraulic conductivity of 10^{-6} m/s, a normalized model perforation discharge of 1×10^{-5} m ³ /s/m, and an inlet hydraulic head of 2 to 50 m.....	134
Figure B.4: Simulated and predicted a) pressure head at the trench base and b) volume injected for liquid injection into a saturated refuse hydraulic conductivity of 10^{-8} m/s, a normalized model perforation discharge of 5×10^{-5} m ³ /s/m, and an inlet hydraulic head of 2 to 50 m.....	135
Figure B.5: Simulated and predicted a) pressure head at the trench base and b) volume injected for liquid injection into a saturated refuse hydraulic conductivity of 10^{-8} m/s, a normalized model perforation discharge of 3×10^{-5} m ³ /s/m, and an inlet hydraulic head of 2 to 50 m.	136
Figure B.6: Simulated and predicted a) pressure head at the trench base and b) volume injected for liquid injection into a saturated refuse hydraulic conductivity of 10^{-8} m/s, a normalized model perforation discharge of 1×10^{-5} m ³ /s/m, and an inlet hydraulic head of 2 to 50 m.....	137
Figure C.1: Survey of Site Layout and elevations conducted by the City of Winnipeg, Solid Waste Division.....	139
Figure C.2: Summary of piezometer and extraction well elevations, conducted by the City of Winnipeg, Solid Waste Division.....	140
Figure D.1: Generated Neuman (1974) solution fit to measured drawdown data for piezometers at locations P1A and P6A.	142
Figure D.2: Generated Neuman (1974) solution fit to measured drawdown data for piezometers at locations P2A and P7A.	143
Figure D.3: Generated Moench (1984) solution fit to measured drawdown data for piezometers at locations P1A and P6A.	144
Figure D.4: Generated Moench (1984) solution fit to measured drawdown data for piezometers at locations P2A and P7A.	145
Figure D.5: Generated Theis (1935) solution fit to measured recovery data for piezometers at locations P1A, P2A, P6A and P7A.	146
Figure D.6: Generated Bouwer and Rice (1976) solution fit to measured slug recovery data for piezometers at locations P1A,P1B, P2A and P2B.	147
Figure D.7: Generated Bouwer and Rice (1976) solution fit to measured slug recovery data for piezometers at locations P3A, P3B, P4A and P4B.	148
Figure D.8: Generated Bouwer and Rice (1976) solution fit to measured slug recovery data for piezometers at locations P5A, P5B, P6A and P6B.	149
Figure D.9: Generated Bouwer and Rice (1976) solution fit to measured slug recovery data for piezometers at locations P7A, and P7B, P6A.	150
Figure E.1: Numerical model boundary conditions and problem domain for vertical extraction well analysis.	158

Figure E.2: Simulated drawdown response at radial distance of 1 m and refuse depth of 8.8 m for a refuse hydraulic of 1.5×10^{-7} m/s and vertical to hydraulic anisotropy ratios of 0.04, 0.19 and 1..... 158

Figure E.3: Simulated drawdown response at radial distance of 1 m and refuse depth of 8.8 m for a refuse hydraulic of 6.3×10^{-7} m/s and vertical to hydraulic anisotropy ratios of 0.04, 1 and 4. 159

CHAPTER 1: INTRODUCTION

1.1 PROBLEM DEFINITION

Modern landfills are designed with a significant amount engineered infrastructure to safeguard the environment. Effective disposal and control of leachate generated at a landfill is an operational issue that requires consideration at the design stage of the facility. Leachate is primarily rainwater that comes into contact with refuse as it percolates through solid waste. A relatively recent method of leachate management that has been employed involves collection and injection back into the refuse. Among other things, the design of collection and liquid injection systems requires consideration given to the refuse hydraulic properties, as well as, the operation characteristics of the system. Bioreactors landfills are an emerging management strategy aimed to enhance microbial processes within the landfill and thereby accelerate waste degradation and reduce the contaminating lifespan of a landfill (Reinhart and Townsend 1997). Generally, compared to conventional landfilling practices, bioreactor landfills include the addition of liquid (e.g., water or leachate) in order to increase the refuse moisture content to conditions that enhance waste degradation (Reinhart and Townsend 1997). Compared to the other methods of liquid injection, horizontal liquid injection systems (HLIS) provide the advantage of being able to inject large volumes of liquid, a relatively low material cost, easy integration into landfill operations, and reduced odor and aesthetic problems (Reinhart and Townsend 1997, Warzinski *et al.* 2000). HLIS normally convey liquid through a trench, embedded within the refuse, which contains perforated plastic pipe surrounded by a high permeability material (e.g., gravel or tire chips).

HLIS are installed during landfill operation by digging a trench into the refuse at select vertical waste lift heights and horizontal spacings to uniformly wet the refuse within the refuse cell. A change in the hydraulic performance of the HLIS during liquid injection can potentially affect the uniform infiltration of liquid into the refuse and therefore, the desired, uniform waste degradation. A HLIS field study by Townsend and Miller (1998) reported a change in HLIS performance (decrease in the injection flow rate and increase in delivery pressure) during liquid injection. The observed changes in hydraulic performance of the injection pipe during liquid injection is currently unknown but is likely a function of the design of the perforated pipe, trench, refuse hydraulic properties, system operation, and the hydraulic interactions between the pipe, trench, and refuse.

Leachate collection systems have been incorporated in the design modern landfills to collect and remove leachate from the landfill. Collection system design varies depending on specific design requirements, but generally are comprise of a perforated collector pipe surrounded by a high permeability material that is located below the refuse and above any low permeability liners. In older dumps and landfills with no, or clogged, leachate collection systems, a leachate mound will develop with time at the base of the landfill. A high leachate mound creates several environmental dangers, such as increased potential for surface water and groundwater contamination. In situations where there is no or ineffective leachate collection systems, extraction wells have been installed within the refuse to remove leachate and control the height of the leachate mound (Rowe and Nadarajah 1996).

Extraction wells typically consist of a plastic pipe casing that is screened over a specified depth interval and surrounded by a filter pack material. The performance of an extraction well to a reduce leachate mound is dependent on the bulk hydraulic conductivity

of the refuse and cover materials, as well as, the physical and operating characteristics of the well. The in situ bulk hydraulic conductivity of refuse and cover material in a landfill can be highly variable and depend on spatial location, cover material applied, and age of the refuse. Presently extraction well designs have utilized analytical and numerical studies that are subjected to certain assumptions and limitations. As such, optimum performance of these systems to effectively reduce leachate levels in the landfill may not be achieved.

1.2 SCOPE OF THESIS

The first component involves a numerical analysis of fluid flow from a HLIS into surrounding refuse. The second component consists of deducing the in situ saturated hydraulic conductivity from a well controlled pump test on a leachate extraction well conducted within a municipal solid waste landfill.

The specific objectives of the research undertaken are to:

- Develop a transient unsaturated-saturated fluid flow model to characterize the influence of spatial and temporal hydraulic properties of refuse, pipe hydraulic characteristics, and the liquid injection boundary condition applied at pipe perforation on the fluid flow from a HLIS and the increase in pressure within a HLIS with time.
- Investigate the movement of liquid and pressure drawdown responses with time in refuse through a large scale field pump test conducted at the Brady Road Landfill in Winnipeg, Canada.
- Assess the ability of conventional aquifer ground water analytical formulas to capture the measured spatial decrease in water pressure within the refuse during a pump test and to quantify refuse hydraulic conductivity.

1.3 THESIS OUTLINE

Chapter 2 reviews field and laboratory methodologies that have been used to obtain refuse hydraulic properties. Chapter 3 describes the results of numerical simulations that characterize the effects of various hydraulic conditions on HLIS performance. Chapter 4 describes results and analysis large scale field pump test conducted at a municipal solid waste landfill. Lastly, Chapter 5 presents conclusions and recommendations for future work.

1.4 REFERENCES

- Reinhart, D.R. and Townsend, T.G. (1997) *Landfill Bioreactor design and operation*, CRC Press LLC, FL, USA
- Rowe, R.K. and Nadarajah, P. (1996) Estimating leachate drawdown due to pumping wells, *Can. Geotech J.*, 33:1-10.
- Townsend, T.G. and Miller, W.L. (1998) Leachate Recycling Using Horizontal Injection, *Advances in Environmental Research*, 2(2):129-138.
- Warzinski, J., Watermolen, B.T., Torresani, M.K., and Genthe, D.R. (2000) A Superior Approach To Recirculation, *Waste Age*, 31(2):

CHAPTER 2: LITERATURE REVIEW

2.1 INTRODUCTION

Landfilling continues to be used as a common method around the world to dispose municipal and industrial wastes. Modern landfills are normally constructed with a low permeability liner(s) in combination with a leachate collection system in order to reduce the contaminant migration into subsurface aquifers (Rowe 2004). A cover system normally comprised of soil or a geosynthetic is applied after landfill cell closure in order to control liquid infiltration into the refuse and gas release into the atmosphere. When water percolates through refuse it picks up the constituents of the waste and is called leachate.

Recently liquid management methodologies in landfills have incorporated large amount of engineered infrastructure to safeguard the environment from harmful leachate contaminant concentrations. Bioreactor landfills are an example of relatively new liquid management strategy. Bioreactors normally employ leachate injection to increase waste moisture and biological activity within the refuse in attempts to enhance gas production, accelerate waste stabilization rates, store and treat leachate within the landfill, and reduce the contaminating lifespan of the landfill (Reinhart and Townsend 1997). Another liquid management strategy in landfills are to utilize leachate extraction wells to decrease and control leachate mound that can develop in dumps and landfill with no or clogged leachate collection systems (Rowe and Nadarajah 1996).

The successful design and operation of bioreactor landfills that employ leachate recirculation and leachate extraction can be greatly influenced by the refuse hydraulic properties; specifically, the saturated refuse hydraulic conductivity, and the refuse field

capacity and specific yield. The refuse hydraulic conductivity is critical to characterize the potential rate of moisture movement within refuse from a liquid injection system or to an extraction well. The refuse field capacity and the specific yield help evaluate the liquid storage capabilities of refuse as they quantify the expected liquid volumes that can be absorbed and released by refuse, respectively. Correct assessment of refuse hydraulic properties has generally proven to be difficult (Pohland 1975, Oweis and Khera 1986, Reinhart and Townsend 1997, Qian *et al.* 2002) as there are many factors that can influence the hydraulic properties of refuse, as follows (adapted from Rowe and VanGulck 2004):

- **Composition of waste** – The relative grain size and porosity of the refuse and cover material will effect the hydraulic conductivity
- **Degree of Compaction** – More heavily compacted refuse will displays lower hydraulic conductivity due to a reduction in porosity of the refuse (e.g. Landva and Clark 1990, Zeiss and Major 1993)
- **Overburden pressure** – Increasing the overburden pressure decreases the hydraulic conductivity due to reduction in refuse porosity (e.g. Bleiker *et al.* 1993, Powrie and Beaven 1999)
- **Waste Age** – The degradation process tends to increase the refuse density and decrease the porosity (Powrie and Beaven 1999)

Testing of the refuse hydraulic properties in the laboratory has an advantage of controlling these listed influencing factors; however, laboratory testing can not effectively account for large-scale waste heterogeneity. Field testing for refuse hydraulic properties can employ a much larger sample size compared to laboratory testing and therefore may provide more representative results of a bulk refuse matrix. However a disadvantage of field test is that one cannot control the listed influencing factors, thereby making analysis of field testing results difficult to analyze and compare to laboratory studies.

The objective of this chapter is to summarize the field and laboratory studies that have been conducted to assess refuse hydraulic properties.

2.2 REFUSE HYDRAULIC PROPERTIES

The following section presents current field and laboratory techniques that have been conducted to assess refuse hydraulic properties; specifically, the saturated hydraulic conductivity, field capacity, and specific yield. Additionally, this section will also present laboratory studies and field measurement that have analyzed the unsaturated refuse characteristics and changes in the refuse hydraulic conductivity, density, porosity and moisture content due to increases in vertical stress and compaction.

2.2.1 Saturated Hydraulic Conductivity

There has been some debate on whether the conventional Darcian flow model is valid for refuse, and several studies have discussed the possible effects of a non channel flow within refuse due to preferential flow paths (Bendz and Flyhammar 1999, Bendz *et al.* 1997, Zeiss and Major 1993, Zeiss and Ugucioni 1995) but it has been generally accepted that Darcy's Law is a valid in analysing the flow of liquid within saturated refuse (Rowe and VanGulck 2004).

2.2.1.1 Methods of Determination

In order to obtain representative results for the saturated refuse hydraulic conductivity of a heterogeneous waste matrix, the creation of new testing apparatus has often been required. For example, Beaven and Powrie (1995) and Powrie and Beaven (1999) constructed a large scale (2 m in diameter and 3 m high) Pitsea compression cell that can measure vertical and horizontal hydraulic conductivities at various applied

vertical stresses. Another common method to assess refuse hydraulic conductivity is to measure the transient rate of liquid infiltration through large diameter columns containing refuse. Zeiss and Major (1993) and Zeiss and Ugucioni (1995) constructed large columns (0.57 m diameter and 1.8 m high), packed with refuse, to quantify the effects of refuse compaction and channeled flow on the refuse hydraulic conductivity. Conventional laboratory testing equipment with modifications for a larger sample size has also been employed to assess the hydraulic conductivity. For example, Landva *et al.* (1998) used a consolidometer of 447 mm diameter by 540 mm deep to evaluate vertical hydraulic conductivity and a 760 mm diameter by 450 mm deep consolidometer to evaluate the horizontal hydraulic conductivity.

Conducting pump tests, slug injection, and falling head tests on geological formations in the field and the using conventional ground water analytical solutions (Theis 1935, Boulton 1963, Cooper and Jacob 1946, Neuman 1972, Driscoll 1986) to asses the in siturefuse hydraulic properties has been an effective and commonly employed method (Kruseman and de Ridder, 1994). Several such pump studies have been attempted on municipal refuse, most notably by Burrows *et al.* (1997) who conducted a total of fifty four pump tests on twenty full penetrating and fully screened wells with four landfill locations in Southern England. Recently, Jain *et al.* (2006) estimated the saturated hydraulic conductivity of initially unsaturated refuse at twenty three locations at a solid waste landfill in Florida using the borehole permeameter testing method. A borehole permeameter test is conducted such that a constant head of water is maintained in an excavated borehole until a steady infiltration rate is reached. Assessing the applicability of using conventional ground water analytical formulae to analyze the

removal or injection of liquid into refuse has been challenging due to the inconsistent and heterogeneous composition of refuse which can vary in its hydraulic properties with time and location within the landfill (Fasset *et al.* 1994). Measurement of the rate of liquid infiltration through large scale test pits has also been used (Oweis *et al.* 1990, Landva *et al.*, 1998) to evaluate the insitu refuse hydraulic conductivity.

2.2.1.2 Reported Values

The reported values of refuse hydraulic conductivity measured in the laboratory, field, and back calculated with numerical models or alternative methods are provided in Tables Table 2.1, Table 2.2, and Table 2.3, respectively. Based on the literature reported values, the saturated refuse hydraulic conductivity ranges from about 10^{-4} m/s to 10^{-11} m/s. Limited data has been collected on the anisotropy ratio between horizontal (K_H) and vertical (K_V) saturated hydraulic conductivity. Landva *et al.* (1998) measured an anisotropic ratio of $K_H = 8 K_V$ using a large scale vertical (0.44 m diameter) and horizontal (0.76 m diameter) consolidometer. Hudson *et al.* (1999) documented an anisotropic ratio with a range $K_H=2 K_V$ to $K_H= 5 K_V$.

2.2.2 Field Capacity and Specific Yield

The volumetric moisture content definition (θ_{vol}) of refuse is defined as a ratio of volume of water (V_w) to the total volume (V_t) of a sample. Fresh in place refuse will initially contain some moisture in the range of 0.15 – 0.35 (Straub and Lynch 1982). Depending on landfill practices, it is possible that the water content of the in-place refuse will increase with time as a result of rain water infiltration and liquid injection. As volumetric water content increases, it will approach and possibly exceed the total

absorptive capacity (field capacity, θ_{fc}) of the refuse. When the volumetric water content exceeds the field capacity, gravity drainage conditions will occur. The saturated refuse water content, θ_{sat} represents a flooded condition where the void spaces of the refuse are filled with liquid. Ignoring minimal residual air saturation and non-connected pores, the saturated water content can be assumed to be equal to the porosity of refuse. Refuse water contents in excess of the field capacity will result in liquid drainage of the pores until the refuse water content once again reaches its field capacity. The specific yield θ_{sy} , or the drainable porosity, n_e , are used to quantify the volume of liquid that would drain from refuse in a flooded condition to the refuse's field capacity. The refuse field capacity and the specific yield signify the expected liquid volume that can be absorbed and released by refuse, respectively, and as such they are very important parameters in the design of liquid extraction and injection systems.

2.2.2.1 Methods of Determination

The volumetric water content of refuse can be deduced by multiplying the refuse gravimetric water content by the ratio of refuse dry bulk density to the density of water. The gravimetric water content is obtained in the laboratory through the conventional procedure of weighting a refuse sample (solids and water) and then drying the sample in an oven and weighting it. The dry bulk density is found by dividing the mass of an oven dried refuse sample by the total sample volume. The refuse field capacity and specific yield are more difficult parameters to assess due to its dependence on many factors, including refuse composition and age, degree of compaction, and depth location with a landfill. The refuse field capacity has been measured in the laboratory through large scale refuse liquid infiltration columns (e.g, Fungaroli 1971, Qasim and Burchinal 1970,

Walsh and Kinman 1979). The field capacity in refuse column experiments was assumed to occur when the rate of liquid collected from the column equaled the rate of liquid addition. The calculation of field capacity in this manner inherently assumes that the rate of liquid flow through the column is uniform. As discussed by Korfitias *et al.* (1984), this method does not account for the potential of non-uniform liquid movement and distribution in pore spaces that are unsaturated and are filled with both air and liquid. A more accurate procedure for calculating field capacity, and also the saturated water content, was adopted by Powrie and Beaven (1999) and Zeiss and Major (1993). The adopted procedure involved completely saturating a large refuse compression cell of a known volume and an initial refuse water content below field capacity. After the compression cell was fully saturated with liquid, the liquid was slowly drain out of the cell and the specific yield of the refuse was deduced from the volume of liquid drained per unit volume and the field capacity was calculated from the total mass of water retained by the sample when liquid drainage had stopped (Powrie and Beaven 1999).

Measurement of the in situ refuse field capacity and specific yield has generally been limited to test cells and pump tests. Yuen *et al.* (1999) constructed a large scale refuse test cell and equated the amount of water that was drained from a saturated zone at the base of the test cell as the refuse field capacity. Large scale pumps tests conducted by Burrows *et al.* (1997) and Oweis *et al.* (1990) use conventional groundwater analytical solutions (Theis 1935, Boulton 1963) to deduce the specific yield of the refuse. Recently, Zeiss and Norstrom (2005) presented and compared a new instrumentation to measure in situ refuse water contents with laboratory techniques. The in situ instrumentation generally had good agreement with the laboratory techniques over the range tested.

2.2.3 Reported Values

Table 2.4 summarizes the reported values for the initial water content, field capacity, saturated water content, porosity and specific yield as measured in field and laboratory studies and Table 2.5 summarizes the reported values for initial water content, field capacity and porosity using alternative methods. The data indicates that there is a wide range of values, but generally, the range for initial water content is about 0.10 to 0.15, field capacity is about 0.30 to 0.35, saturated water content is about 0.40 to 0.55, and specific yield is about 0.15 to 0.20.

2.2.4 Unsaturated Characteristics of MSW

It is to be expected that movement of liquid within a landfill for liquid injection and extraction systems could occur in regions where the refuse is not completely saturated, and as such, unsaturated flow theory may have to be applied. Richard's equation (1931) has been commonly used to assess the movement of liquid movement through unsaturated refuse (Reinhardt and Townsend 1997). Richard's equation describes one phase transport of an incompressible fluid through a homogenous, non-deformable unsaturated porous medium and can be written in one-dimension as follows:

$$\frac{\partial \theta}{\partial t} + \frac{\partial K(\theta)}{\partial z} - \frac{\partial}{\partial z} \left[D(\theta) \frac{\partial \theta}{\partial z} \right] = 0 \quad [2.1]$$

where θ is the volumetric water content, t is time, k is the hydraulic conductivity, z is the coordinate direction, and $D(\theta)$ is the hydraulic diffusivity due to capillary force.

The $D(\theta)$ term in Richard's equation was defined by Klute (1952) as follows:

$$D(\theta) = K(\theta) \frac{d\psi}{d\theta} \quad [2.2]$$

where Ψ is the refuse suction

In order to solve Richard's equation, the relationship between the change in water content with refuse suction, as well as, refuse hydraulic conductivity with change in refuse water content are required. For refuse, the following power law equations of Clapp and Hornberger (1978) have often been used.

$$\Psi = \Psi_s \left[\frac{\theta}{\theta_s} \right]^b \quad [2.3]$$

$$K = K_s \left[\frac{\theta}{\theta_s} \right]^B \quad [2.4]$$

where θ_s is fluid saturated volumetric water content, Ψ_s is the suction at the saturated water content, K_s is the saturated hydraulic conductivity, and b and B are empirical fitting parameters

Straub and Lynch (1982) conducted numerical simulations to fit the power law empirical coefficients to laboratory infiltration tests. Korifitias *et al.* (1984) also conducted numerical simulations with the power law equations on a large-scale column (0.56 m diameter) and small cylindrical cells (0.12 m diameter) to back-calculate the best fit empirical coefficients. The reported range of values for the empirical coefficients b and B in the power law equations is 4 to 7 and 8 to 11, respectively. Table 2.6 provides a complete summary of the literature reported values for the power law empirical parameters. Generally, laboratory techniques to measure the unsaturated hydraulic conductivity of soils has been considered a costly and time consuming procedure and the unsaturated hydraulic conductivity is often estimated from soil parameters obtained from a water content versus suction relationship curve. Recently, Kazimoglu *et al.* (2006) conducted a comparative analysis of refuse unsaturated hydraulic conductivity using an

outflow laboratory testing method and the van Genuchten (1980) expression for unsaturated hydraulic conductivity. Outflow laboratory experiments consist of obtaining the change in water content with suction relationship and the deduction of the hydraulic diffusivity with suction behavior, the corresponding unsaturated hydraulic conductivity can be calculated from Klute's (1952) diffusivity equation. The van Genuchten (1980) equation for change in water content with suction is given as follows:

$$S_e(\psi) = \frac{\theta - \theta_r}{\theta_s - \theta_r} = \frac{1}{\left(1 + |\alpha\psi|^n\right)^m} \quad [2.5]$$

where S_e is the effective saturation, θ_r is the residual water content, α , n , and m are parameters that are fitted to a soil water content versus suction curve.

The unsaturated hydraulic conductivity in terms of effective saturation is calculated as follows:

$$K(\theta) = K_s S_e^{1/2} \left[1 - (1 - S_e^{(1/m)})^m\right]^2 \quad [2.6]$$

The outflow laboratory testing methodology of Kazimoglu *et al.* (2006) consisted of measuring the volume of expelled from a refuse sample (0.25 m diameter and 0.14 m height) at different refuse suctions that were induced by a pressure plate apparatus. The collected water content versus suction relationship in the laboratory outflow experiments was used to deduce the following van Genuchten parameters: saturated water content equal to 0.58, the residual water content 0.14, and the curve fitting parameters α , n , and m equal to 1.5 cm^{-1} , 1.60, and 0.38, respectively. The unsaturated hydraulic conductivity with water content relationship was predicted with equation [2.6] using the obtained van Genuchten parameters and an estimated range for the refuse saturated hydraulic conductivity. The authors found good agreement with the measured unsaturated hydraulic

values at low water content, which correspond to high suction values; however, at higher moisture contents, the agreement between measured and predicted values diverged. The authors hypothesized that the discrepancy between prediction and measured results at the higher water contents could be attributed to the presence of very large pores in the refuse, and as such, the suction values may be very small and not measurable with conventional testing equipment.

2.2.5 Role of Overburden Pressure and Compaction Efforts

During landfill operation, the void spaces in refuse are expected to decrease due to an overall increase in the vertical stress from additional waste placement and also from landfill compaction efforts. A decrease in the void spaces has a direct implication on the liquid movement within refuse, as the refuse hydraulic conductivity will decrease due to an overall decrease in the available flow paths for liquid flow. Additionally, a decrease in the refuse voids will result in a decrease the storage capabilities of refuse as the overall porosity of refuse will decrease. The potential decrease in hydraulic conductivity and porosity due to overburden pressures and compaction are important design considerations in the long performance of liquid injection and extraction systems.

2.2.5.1 Methods of Determination

There has been a limited amount of research conducted on the direct effects of overburden pressure and compaction on refuse hydraulic conductivity and porosity. Laboratory testing has mainly consisted of obtaining refuse samples from representative landfills and measuring the hydraulic conductivity, porosity, and density at various applied effective stresses using modified large scale laboratory testing apparatus. Beaven

and Powrie (1995) and Powrie and Beaven (1999) used hydraulic pistons to simulate the stress levels at different landfill depths in a refuse cell with a sample size of two meters in diameter and three meters high. Additionally, the authors measured the refuse hydraulic conductivity, density, porosity, and specific yield at various applied vertical stresses. Zeiss and Major (1993) used a series of perforated plates of 100 kg to simulate various compaction ratios in a refuse test cell 0.57 meters in diameter and 1.8 meters high. The authors measured the corresponding change in porosity, field capacity, and hydraulic conductivity as a function of the level of compaction.

2.2.5.2 Reported Values

A summary of literature reported refuse hydraulic conductivity as a function of vertical stress, refuse depth, and refuse unit weight are provided in Figures Figure 2.1 to Figure 2.3, respectively. Based on the summaries provided in Figure 2.1 and Figure 2.2, a decrease of hydraulic conductivity of refuse from 10^{-4} to 10^{-8} m/s may be expected from an increase in approximately of 1000 kPa of vertical stress within a landfill or from the placement of an additional about 50 m of refuse. Additionally, the refuse hydraulic conductivity can be expected to decrease from a range of 10^{-4} m/s to 10^{-7} m/s for an increase of unit weight of 6 kN/m^3 to 14 kN/m^3 .

Powrie and Beaven (1999) and Beaven and Powrie (1999) presented the following empirical equations to relate vertical hydraulic conductivity to vertical effective stress, and the density of waste at field capacity and saturation to vertical effective stress, as follows:

$$K_{m/s} = 17(\sigma'_{\text{kPa}})^{-3.26} \quad [2.7]$$

$$\rho_{\text{FC}} = 0.448(\sigma'_{\text{kPa}})^{0.1563} \quad [2.8]$$

$$\rho_{\text{sat}} = 0.669(\sigma'_{\text{kPa}})^{0.0899} \quad [2.9]$$

where K is the vertical hydraulic conductivity and σ' is the vertical effective stress, ρ_{FC} is the density at refuse field capacity in tonnes/m³, and ρ_{sat} is the saturated density in tonnes/m³.

Utilizing the same Pitsea apparatus as Powrie and Beaven (1999), Hudson *et al.* (1999) found the anisotropy ratio (K_H to K_V) to increase from approximately 2 at an applied vertical stress of 40 kPa to approximately 5 at an applied stress of 600 kPa. Figure 2.4 presents the field capacity, saturated water content and specific yield for a vertical stress range of 0 to 463 kPa as measured in the Pitsea compression cell by Powrie and Beaven (1999). Generally, the specific yield of refuse decreased with increase in vertical effective stress over the range tested. However, the volumetric field capacity did not change significantly with the applied vertical effective stress. In addition to the refuse porosity, it was suggested by Geosyntec and Todd (1995) hypothesised that the field capacity can also decrease with depth in a landfill and proposed the following empirical equations.

$$f_c (\%_{\text{vol}}) = -0.62z + 54 \quad [2.10]$$

$$n (\%_{\text{vol}}) = -0.046z + 55 \quad [2.11]$$

where f_c is the volumetric refuse field capacity, n is the refuse porosity, and z is the depth in feet bellow the landfill surface.

Rowe and VanGulck (2004) presented a summary of the influence of the compaction effort on the refuse unit weight, the results of which are presented in Table 2.7 along with other published values. Generally, a low compaction effort corresponded to a refuse unit weight of approximately 3 kN/m³ and a high compaction effort of about 9

kN/m^3 . One can deduce from the summarised relationship between hydraulic conductivity and density (**Figure 3.3**) that a difference in compactive effort could change the hydraulic conductivity by more than two orders of magnitude. Zeiss and Major (1993) in their large scale refuse cell reported a decrease of refuse hydraulic conductivity of $1.1 \times 10^{-4} \text{ m/s}$ to $1.2 \times 10^{-5} \text{ m/s}$ from a low compaction ratio of 1.6 to a high compaction ratio of 2.85. Additionally, the authors measured a decrease in the refuse porosity from 0.58 to 0.47 for the low and high compactive ratios, respectively.

2.3 CONCLUSIONS

The expected refuse hydraulic properties are important considerations in the design and operation of bioreactors that incorporate leachate recirculation or in retrofitted leachate extraction wells that are used to control a leachate mound. The refuse hydraulic conductivity and the refuse water contents (field capacity and specific yield) are critical in evaluating the rate of liquid movement and liquid storage capabilities of refuse, respectively. Compared to field scale studies, laboratory testing of the refuse hydraulic properties has an advantage in limiting some of the factors that influence the magnitude of the hydraulic properties; however, laboratory methods are limited in accounting for large scale waste heterogeneity. Field scale studies generally have an advantage over laboratory studies as they test a much larger sample size; however, data generated from field is most often influenced by many factors, which are difficult to characterize compared to laboratory data.

The saturated refuse hydraulic conductivity is normally analyzed in the laboratory through custom built large scale refuse columns or through the modification of conventional geotechnical laboratory testing methods. Field studies of the refuse

saturated hydraulic conductivity have generally consisted of pump tests or injection liquid into refuse while monitoring the pressure responses within the formation (i.e. refuse) and using conventional ground water analytical solutions to estimate the refuse hydraulic conductivity. Based on the literature reported values, the refuse hydraulic conductivity ranged from 10^{-4} m/s to 10^{-8} m/s and the waste anisotropy ratio ranged from $K_H = 8 K_V$. Refuse specific refuse water contents, such as the initial water content, field, saturated water content, field capacity, and specific yield are complicated parameters to assess and studies have relied extensively on large scale infiltration columns or refuse cells in the laboratory and pump tests in the field. The literature reported range of the initial water content is about 0.10 to 0.15, field capacity is about 0.30 to 0.35, saturated water content about 0.40 to 0.55, and specific yield about 0.15 to 0.20.

The power law equations of Clapp and Hornberger (1978) have been used for refuse to quantify the unsaturated relationships of the changes in refuse water content with suction and the refuse hydraulic conductivity with suction. The power law parameters have often been obtained from the fitting of data obtained from large scale refuse column experiments. The reported range for the power law empirical coefficients b and B is 4 to 7 and 8 to 11, respectively.

The refuse hydraulic conductivity and porosity has been reported to decrease as a result of increased vertical stresses and from refuse compaction efforts. A summary of field and laboratory studies indicate that one can expect a decrease of hydraulic conductivity from 10^{-4} to 10^{-8} m/s for an increase 1000 kPa of vertical stress in a landfill or from the placement of an additional 50 m of refuse depth. Additionally, refuse

hydraulic conductivity was reported to decrease from 10^{-4} m/s to 10^{-7} m/s for an increase of unit weight of 6 kN/m^3 to 14 kN/m^3 . Waste degradation processes have also been attributed to a decrease in refuse hydraulic conductivity due to an increase in the refuse density and a decrease in the porosity.

2.4 REFERENCES

- Ahmed, S., Khanbilvardi, R., Fillos, J., and Gleason P.J. (1992) Two-dimensional Leachate Estimate through Landfills, *Journal of Hydraulic Engineering*, 118(2):306306-322.
- Aran, C., Franck, S., Berroir, G. and Gisbert, T. (1999) Leachate Recirculation by Horizontal Trenches Instrumentation, *7th International Waste Management and Landfill Symposium*, S. Margherita di Pula, Cagliari, Italy.
- Beaven, R.P. and Powrie, W. (1999) Analysis of waste flushing and flow to wells using modflow and an effective stress dependent hydraulic conductivity, *Proceedings Sardinia 99, Seventh International Waste Management and Landfill Symposium*, S. Margherita di Pula, Cagliari, Italy.
- Beaven, R. P. and Powrie, W. (1995). Hydrogeological and geotechnical properties of refuse using a large scale compression cell, *Proceedings of the 5th International Sardinia Landfill Conference.*, S. Margherita de Pula, Cagliari, Italy. Vol II:745-760.
- Bendz, D. and Flyhammar, P. (1999) Channel flow and its effects on long term metals in MSW landfills, *Proceedings Sardinia 99, Sixth International Landfill Symposium*, S. Margherita di Pula, Cagliari, Italy.
- Bendz, D., Singh, V.P., and Berndtsson, R. (1997) The Flow Regime in Landfills – Implications for Modelling, *Proceedings Sardinia 97, Sixth International Landfill Symposium*, S. Margherita di Pula, Cagliari, Italy.
- Blengino, A.M., Manassero, M., Rossello, A., Spanna, C. and Beggi, S. (1996) Investigation, monitoring and stability analyses of an old canyon landfill, *Proc.*

2nd International Congress on Environmental analyses of an old canyon landfill,
Osaka, Japan.

Bleiker, D. E., McBean, E. & Farquhar, G. (1993) Refuse Sampling and Permeability Testing at the BrockWest and Keele Valley Landfills. *Proceedings of the sixteenth International Madison Waste Conference. Department of Engineering Professional Development, University of Wisconsin, Madison/Extension, Madison, U.S.A.*

Blight, G.E., Ball, J.M, and Blight, J.J. (1992) Moisture and Suction in Sanitary Landfills in Semiarid Areas, *Journal of Environmentl Engineering, ASCE*, 188(6):865-877.

Boulton, N.S. (1963). Analysis of data from non-equilibrium pumping tests allowing for delayed yield from storage, *Ins. Civil Engineers Proc.*, 26:469-482.

Bromwell, L.G. (1978) Properties, Behaviour and Treatment of Waste Fills, *Seminar Series on Methods of Soil Improvement, Metropolitan Section, ASCE, New York.*

Burrows, M.R., Joseph, J.B. and Mather, J.D. (1997) The hydraulics of in situ landfilled waste, *Proceedings Sardinia 97, Sixth International Landfill Symposium, S. Margherita di Pula, Cagliari, Italy.*

Canziani, R. and Cossu, R. (1989) Landfill Hydrology and Leachate Production, *In Sanitary Landfill: Process, Technolgy and Environmental Impact, Harcourt Brace Jovanovich, New York, USA.*

Clapp, R.B. and Hornberger, G.M (1978) Empirical Equations for Some Soil Hydraulic Properties, *Water Resources Research*, 14(4):601-604.

- Cooper, H.H. and Jacob, C.E. (1946) A Graphical method for Evaluating Formation Constants and Summarizing Well Field History, *Am. Geophys. Union Trans*, 27:526-534.
- Demetracopoulos, A.C., Korfiatis, G.F., Bourdinos E.L. & Nawy, E.G. (1986) Unsaturated flow through solid waste landfills: model and sensitivity analysis, *Water Resources Bulletin*, 22:601-609.
- Driscoll, F.G (1986) *Groundwater and Wells 2nd Edition*, Johnson Division, St Paul, Minn, USA.
- Dusseck, C., Long, R., Wu, V.Y.N. and Cheng, T.K. (1999) The hydrological response of landfilled wastes to site restoration: a case study, *Proceedings Sardinia 99, Sixth International Landfill Symposium*, S. Margherita di Pula, Cagliari, Italy.
- Ettala, M. (1987) Infiltration and hydraulic conductivity at a sanitary landfill. *Aqua Fennia* 17,231-237.
- Fang, H.Y. (1983) Physical Properties of Compacted Disposal Materials. Unpublished Report.
- Fassett, J., Leonards, G., and Reppeto, P. (1994) Geotechnical Properties of Municipal Solid Waste and Their Use in Landfill Design," *Proc. Waste Tech '94, Solid Waste Association of North America*, Silver Springs, Maryland, 1-31.
- Fiend, M.C. and Hock, J.E. (1998) A side by side evaluation of vertical and horizontal leachate extraction wells in an MSW landfill, *Proc 20th International Madison Waste Conference*, Madison, WC,USA.
- Fungaroli, A.A. (1971) Pollution of Subsurface Water by Sanitary Landfills, *U.S. EPA report SW-12rg*, Vols. I-II.

- Fungaroli, A. A. & Steiner, R. L. (1979) Investigation of Sanitary Landfill Behavior, Vols 1 & 2. EPA-600/2-79-053a.
- Gabr, M.A. and Valero, S.N. (1995) Geotechnical properties of municipal solid waste, *Geotechnical Testing Journal*, 18: 241-251.
- Gachet, C., Gotteland, Ph, Lemarchal, D. and Prudhomme, B. (1998) An in situ household refuse density measurement protocol, *Proc. 3rd International Congress on Environmental Geotechnics*, Lisbon, Portugal, 849-854.
- GeoSyntec and Todd. D.K. (1995) Geotechnical Waste Characterization, Document prepared by GeoSyntec Consultants and David Keith Todd Consulting Engineers for a landfill in Southern California.
- Golder. (2004) Appendix XI Project Description & Natural Hazards Impact Assessment, *Ashcroft Ranch Landfill Project*, Golder Associates Ltd., Burnaby, British Columbia,
- Hentges, G. T., Thies, F. and Lemar, T. S. (1993) Leachate Extraction Well Assessments Des Moines, Iowa Metropolitan Park East Sanitary Landfill, Hamilton County, Iowa Sanitary Landfill. Proceedings of the Sixteenth International Madison Waste Conference. Department of Engineering Professional Development, University of Wisconsin, Madison/Extension, Madison, U.S.A.
- Hudson, A.P., Beaven, R.P. and Powrie, W. (1999) Measurement of the horizontal K of household waste in a large scale compression cell, *Proceedings Sardinia 99, Sixth International Landfill Symposium*, S. Margherita di Pula, Cagliari, Italy.

- Jang, Y.S. (2000) Analysis of flow behaviour in a Landfill with cover soil of low hydraulic conductivity, *Environmental Geology*,39.
- Jain, P., Powell J., Townsend, T.G. and Reinhart, D.R. (2006) Estimating the Hydraulic Conductivity of Landfilled Municipal Solid Waste Using the Borehole Permeameter Test, *Journal of Environmental Engineering*, 132(6):645-652.
- Kazimoglu, Y.K., Mcdougal, J.R. and Pyrah I.C (2006) Unsaturated Hydraulic Conductivity of Landfilled Waste, *Unsaturated Soils*.
- Korifiatis G. P., Demetracopoulos A. C., Bourodimos E. L. and Nawy E. G. (1984) Moisture transport in a solid waste column. *J. Env. Eng.*, 110(4): 789-796.
- Klute, A. (1952) A Numerical Method for Solving of Water in Unsaturated Material, *Soil Science*, 73:105-116.
- Kruseman, G.P. and de Ridder, N.A (1994) *Analysis and Evaluation of Pumping Test Data, 2nd edition*, International Institute for Land Reclamation & Improvement, Wageningen, The Netherlands.
- Landva, A.O., Pelkey, S.A. and Valsangkar, A.J. (1998) Coefficient of Permeability of Municipal Refuse, *Proceedings, 3rd International Congress on Environmental Geotechnics*, Lisbon, Portugal, 1: 63-68
- Landva, A.O. and Clark, J.I. (1990) Geotechnics of Waste Fill,” Geotechnics of Waste Fills – Theory and Practice, *STP 1070*, ASTM, Philadelphia, Pennsylvania .
- Landva, A.O. and Clark (1984) Report on Foundations liquid storage and slopes in refuse landfills, *Report submitted by Golder Associates to the Department of Supply and Services*, Canada.

- Lee, K.K., Kim, Y.Y., Chang, H.W. and Chug, S.Y. (1997) Hydrogeological studies on the mechanical behaviour of landfill gases and leachate, *Environmental Geology*, 31.
- Manassero, M. (1990) Pumping tests in a municipal solid waste landfill, *Geotechnics Seminar*, ENEL-CRIS, Milano, Italy.
- Marques A.C.M., Villar, O.M. and Kaimoto, L.S.A (1998) Urban solid waste – Conception and design of a test fill, *Proc. 3rd International Congress on Environmental Geotechnics*, Lisbon, Portugal, 127-132.
- McBean, E.A, Rovers, F.A and Farquhar, G.K. (1995) *Solid Waste Landfill Engineering and Design*, Prentice Hall PTR, Englewood Cliffs, New Jersey, USA.
- Merz, R.C., and Stone, R. (1962) Landfill Settlement Rates, *Public*, 93(9).
- Neuman, S.P. (1972) Theory of Flow in Unconfined Aquifer Considering Delayed Response Of The Water Table, *Water Resource Research*, 8(4):1031-1045.
- Oweis, I.S., Smith, D.A., Ellwood, R.B. and Greene, D.S. (1990) Hydraulic Characteristics of Municipal Refuse, *Journal of Geotechnical Engineering*, 116(4):539-553
- Oweis, I.S. and Khera, R.P. (1990) *Geotechnolgy of Waste Management*, Butter-Worths, London.
- Oweis, I.S., and Khera, R. (1986) Criteria for geotechnical construction of sanitary landfills, *Proc. International Symposium on Environmental Geotechnolgy*.
- Passioura, J.B. (1976) Determining soil water diffusivities from one-step outflow experiments, *Australian Journal of Soil Research*, 15:1-8.

- Pohland, F. G. (1975) Accelerated solid waste stabilization and leachate treatment by leachate recycle through sanitary landfills, *Progress in Water Technology*, 7: 753–765.
- Powrie, W. and Beaven, R.P. (1999) Hydraulic properties of household waste and implications for liquid flow in landfills. *Proceedings of the Institution of Civil Engineers, Geotechnical Engineering*, 235-247.
- Qasim, S.R. and Burchinal, J.C. (1970) Leaching from Simulated Landfills, *Journal of the Water Pollution Control Federation*, 42(3).
- Qian, X.; Koerner, R. M. and Gray, D. H. (2002) *Geotechnical aspects of landfill design and construction*, Prentice Hall, Upper Saddle River, N.J, USA.
- Qian, X. (1994) Analysis of Allowable Reintroduction Rate for Landfill Leachate Recirculation, *Department of Environmental Quality Waste Management Division, Lansing, MI, USA*.
- Reinhart, D.R. and Townsend, T.G. (1997) *Landfill Bioreactor design and operation*, CRC Press LLC, FL, USA
- Richards, L.A. (1931) Capillary Conduction of Liquid through Porous Medium, *Physics*, 1:318-333.
- Rovers, R.A. and Farquhar, G.J. (1973) Infiltration and Landfill Behavior, *Journal of Environmental Engineering*, ASCE, 99(5):671-690.
- Rowe. R.K., and VanGulck, J.V. (2004) Chapter 10: Landfilling Geotechnolgy, In Print.
- Rowe, R.K., Quigley, R.M., Richard W. I. Brachman, R.W.I., and Booker J.R. (2004) *Barrier Systems for Waste Disposal*, 2nd ed., Spon Press, New York, NY, USA.

- Rowe, R.K. and Nadarajah, P. (1996) Estimating leachate drawdown due to pumping wells, *Can. Geotech J.*, 33:1-10.
- Schroeder, P.R., Morgan, J.M., Walksi, T.M. and Gibson, A.C., (1984a) The Hydrologic Evaluation of Landfill Performance (HELP) Model, Volume I User's Guide for Version I, *Technical Resource Document, EPA/530-SW-84-009*, U.S. Environmental Protection Agency, Cincinnati, OH, USA.
- Schroeder, P.R., Gibson, A.C. and Smolen, M.D. (1984b) The Hydrologic Evaluation of Landfill Performance (HELP) Model Volume II, Documentation for Version I, *Technical Resource Document*, U.S. Environmental Protection Agency, EPA/530-SW-84-010,, June, Cincinnati, OH.
- Schroeder, P.R., Lyod, C.M., Zappi, P.A. and Aziz. N.M. (1994a) The Hydrologic Evaluation of Landfill Performance (HELP) Model, Volume I User's Guide for Version 3, , *Risk Reduction Engineering Laboratory, Office of Research and Development, EPA/600/R-94/168a*, U.S Environmental Protection Agency, September, Cincinnati, OH, USA.
- Schroder, P.R., Dozier, T.S., Zappi, P.A. McEnore, B.M., Sjostrom, J.W. and Peyton, R.L. (1994b) The Hydrologic Evaluation of Landfill Performance (HELP) Model, Engineering Documentation for Version 3, *Risk Reduction Engineering Laboratory, Office of Research and Development, EPA/600/R-94/168b*, U.S Environmental Protection Agency, September, Cincinnati, OH, USA.
- Schumaker, M.B. (1972) Construction Technique for Sanitary Landfill, *Waste Age*, March/April.

- Sharma, H.D. and Lewis, S.P. (1994) *Waste Contaminant System,, Waste Stabilization and Landfills*, John Wiley & Sons, Somerset, NK,USA.
- Sowers, G.F. (1973) Settlement of Waste Disposal, *8th Intl. Conf. S.M.F.E.*, Moscow.
- Straub, W.A. and Lynch, D.R. (1982) Models of landfill leaching: moisture flow and inorganic strength, *Journal of the Environmental Engineering Division*, 108(2):231-250.
- Theis, C.V. (1935) The relation between the lowering of the piezometric surface and the rate and duration of discharge of a well using groundwater storage, *Am Geophys Un Trans*, 16: 519-524.
- Townsend, T.G., Miller, W.L. and Earle, J.F.K (1995) Leachate Recycle Infiltration Ponds, *J. of Env. Eng*, 121(6):465-471
- UMA. (1996) The City of Winnipeg Brady Road Landfill Performance Monitoring Program, Report Submitted by UMA Engineering Ltd, Winnipeg, Manitoba, Canada.
- van Genuchten, M.T.H (1980) A Closed Form Equation for Predicting the Hydraulic Conductivity of Unsaturated Soils, *Soil Sci Soc. Am. J.* ,44.
- Van Impe, W.F. (1994) Municipal and industrial improvement by heavy tamping, *Proc. Meeting of Geotechnical Engineering, Geotechnics in the Design and Construction of Controlled Waste Landfills*, Millazzo, ME, Associazione Poligeotecnici Riuniti.
- Walsh, J.J. and Kinman, R.N. (1981) Leachate and Gas from Municipal Solid Waste Landfill Simulators , *In Land Disposal: Municipal Waste 7th Annual Research*

- Symposium*, U.S. Environmental Protection Agency, EPA-600/9-81/002a, Cincinnati, OH, USA.
- Walsh, J.K and Kinman, R.N. (1979) Leachate and Gas Production under Controlled Moisture Conditions, *Proceedings of the Fifth Annual Research Symposium*, EPA-600/9-79-023a.
- Wehran Engineering, P.C. and Dynatech Scientific Inc. (1987) Enhancement of Landfill Gas Production, Nanticoke Landfill Binghamton, Report 87-19 New York State Energy Research and Development Authority, New York, NY, USA.
- Wigh, R.J. (1979) Boone County Field Site Interim Report, *U.S. Environmental Protection Agency*, Cincinnati, OH, EPA-600/2-79/580.
- Yildiz, E.B., Unlu, K. and Rowe, R.K. (2004) Modelling leachate quality and quantity in municipal solid waste landfills, *Waste Management Res.*, 22(2): 78–92.
- Yuen, S.T.S, Styles, J.R., Wang, Q.J. and McMahon, T.A. (1999) Findings From a Full-Scale bioreactor Landfill Study in Australia, *Proceedings Sardinia 99, Sixth International Landfill Symposium*, S. Margherita di Pula, Cagliari, Italy.
- Zeiss, C. and Norstrom, J. (2005) Bioreactor Landfills – In-Situ Instrumentation Systems, Interpretations and New Directions, *Journal of Solid Waste Technology and Management*, 31(1).
- Zeiss, C. and Ugucioni, M. (1995) Mechanisms and Patterns of Leachate Flow in Municipal Solid Waste Landfills, *Journal of Environmental Systems*, 23(3): 247-270.
- Zeiss, C. and Major, W. (1993) Flow through municipal solid waste: pattern and characteristics, *Journal of Environmental Systems*, 22(3):211-232.

Zornberg, J.G., Jernigan, B.L., Sanglerat, T.R. and Coolery, B.H. (1999) Retention of free liquids in landfills undergoing vertical expansion, *Journal of Geotechnical and Geoenvironmental Engineering*, July.

Table 2.1: Summary of refuse hydraulic conductivity measurements conducted in the laboratory

Hydraulic Conductivity (m/s)		Laboratory Testing Method		Source
1.5 x 10 ⁻⁴	to	3.7 x 10 ⁻⁸	Pittesea Compression Cell, (2m diameter, 3m high)	Powrie and Beaven (1999) Beaven and Powrie (1995)
2.0 x 10 ⁻⁴	to	3.5 x 10 ⁻⁹		
6.1 x 10 ⁻⁷	to	6.1 x 10 ⁻⁸	Experimental Column, (0.56 m diameter, 1.8 m high)	Zeiss and Ugucioni (1995) Zeiss and Major (1993)
2.1 x 10 ⁻⁴	to	1.1 x 10 ⁻⁵		
4.5 x 10 ⁻⁵	to	4.1 x 10 ⁻⁹	Constant Head Vertical Consolidometer, (0.45 m diameter, 0.54 deep)	Landva and Clark (1984)
2.1 x 10 ⁻⁴	to	5.6 x 10 ⁻⁷	Constant Head Horizontal Consolidometer, (0.76 m diameter, 0.45 deep)	
1.0 x 10 ⁻⁵	to	1.0 x 10 ⁻⁷	Constant and Falling Head Consolidometer, (0.06 m diameter, 0.02 m deep)	Gabr and Valero (1995)
1.4 x 10 ⁻⁶	to	4.1 x 10 ⁻⁹	Fixed Ring Permeater (0.06 m diameter, 0.02 m deep)	Bleiker <i>et al.</i> (1993)
1.0 x 10 ⁻⁷	to	6.6 x 10 ⁻⁸	Constant Head Permeater with Flexible Membrane	
2.0 x 10 ⁻⁵	to	3.5 x 10 ⁻¹¹	Unsaturated Pressure Plate Apparatus, (0.25 diameter 0.140 m height)	Kazimoglu <i>et al.</i> (2005)
1.3 x 10 ⁻⁴	to	8.0 x 10 ⁻⁵	Constant Head Permeater	Korifitias <i>et al.</i> (1984)
9.9 x 10 ⁻⁷	to	3.5 x 10 ⁻¹⁰	Constant Head Test	Hentges <i>et al.</i> (1993)
1.6 x 10 ⁻⁵	to	6.3 x 10 ⁻⁵	Permeater	Wehran Engineering (1987)

Table 2.2: Summary of refuse hydraulic conductivity measurements conducted in the field

Hydraulic Conductivity (m/s)		Field Testing Method	Source	
6.7×10^{-5}	to	3.9×10^{-7}	Pumping Tests	Burrows <i>et al.</i> (1997)
1.0×10^{-5}			Pumping Test	Oweis <i>et al.</i> (1990)
1.5×10^{-6}			Falling Head	
1.1×10^{-5}			Test Pit	
2.2×10^{-5}			Pumping Test	Jang (2000)
3.4×10^{-5}			Slug Test	
1.0×10^{-4}	to	5.0×10^{-7}	Pumping Test	Dussek <i>et al.</i> (1999)
1.0×10^{-5}	to	5.0×10^{-5}	Slug Test	
2.6×10^{-4}	to	1.5×10^{-5}	Pumping Test	Manassero (1990)
6.1×10^{-7}	to	5.4×10^{-8}	Borehole Permeameter Test	Jain <i>et al.</i> (2006)
2.5×10^{-6}	to	2.0×10^{-7}	Slug Test	Hentges <i>et al.</i> (1993)
1.0×10^{-7}			Slug Test	Fiend & Hock (1998)
2.2×10^{-6}			Rising Head Slug Test	UMA (1996)
3.9×10^{-4}	to	1.0×10^{-5}	Test Pit	Landva <i>et al.</i> (1998)
3.0×10^{-6}	to	3.0×10^{-7}	Falling Head Test	Blengino <i>et al.</i> (1996)
1.1×10^{-5}	to	9.5×10^{-7}	Tension Infiltrometer	Lee <i>et al.</i> (1997)

Table 2.3: Summary of reported refuse hydraulic conductivity using alternative methods

Hydraulic Conductivity (m/s)	Description	Source
2.0×10^{-6}	HELP Version I and Version II	Schroder <i>et al.</i> (1984a,b)
1.0×10^{-5}	HELP Version III	Schroder <i>et al.</i> (1994a,b)
6.0×10^{-4} to 2.0×10^{-7}	Literature Reported Range	Yildiz <i>et al.</i> (2004)
1.1×10^{-3} to 9.2×10^{-6}	Estimated from Field Data	Qian (1994)
1.0×10^{-8}	Analytical Wetting Front Equation	Townsend <i>et al.</i> (1995)
1.0×10^{-9} to 1.6×10^{-11}	Mass Balance Calculation	Bleiker <i>et al.</i> (1993)
2.0×10^{-4}	Unknown Method	Ahmed <i>et al.</i> (1992)
1.5×10^{-4} to 7.1×10^{-6}	Unknown Method (Compacted Waste)	Fang (1983)
2.0×10^{-3} to 6.3×10^{-5}	Unknown Method (Light and High Compacted Waste)	Ettala <i>et al.</i> (1987)
1.0×10^{-3} to 1.7×10^{-7}	Unknown Method	Aran <i>et al.</i> (1999)
$3.5 \times 10^{-}$	$1.8 \times 10^{-}$ Unknown Method	Rowe and Nadarajah (1996)

Table 2.4: Summary of refuse initial water content, field capacity, porosity and specific yield using field and laboratory methods

Initial Water Content θ_{vol}	Field Capacity θ_{fc}	Saturated Water Content θ_{sat}	Porosity n	Specific Yield θ_{sy}	Testing Method	Source
	0.34				Full Scale Field Test Cell	Yuen <i>et al.</i> (1999)
				0.05	Field Scale Pumping Test	Oweis <i>et al.</i> (1990)
				0.09-0.16	Field Scale Pumping Test	Burrows <i>et al.</i> (1997)
	0.40-0.45	0.46-0.55*		0.02-.15	Pittessea Compression Cell, (2m diameter,3m high)	Powrie & Beaven (1999)
0.08	0.10		0.52	0.42	Experimental Column, (0.56 m diameter,1.8 m high)	Zeiss and Uguccion (1995)
0.02-0.05	0.12-0.14		0.47-0.58	0.32-0.44		Zeiss & Major (1993)
0.04	0.31				Landfill Lysimeter, (2.1 m depth)	Fungaroli (1971)
0.21	0.38				Refuse Column, (3.1 m depth)	Qasim and Burchinal (1970)
	0.37				Refuse Column, (2.4 m depth)	Walsh and Kinman (1979)
	0.20-.30	0.50-0.60			Cylindrical Refuse Cells, (0.12 m diamtr,0.30 m high)	Korifitias <i>et al.</i> (1984)
		0.58			Pressure Plate Apparatus, (0.25 m diamtr 0.140 m height)	
0.05	0.34				Mini - Lysimeter	Fungaroli and Steiner (1979)
	0.32		0.39		Percolation Test	Golder (2004)
			0.45		Constant Head Test	Hentges <i>et al.</i> (1993)
0.30	0.46		0.49		Core Samples	GeoSyntec and Todd (1995)

Table 2.5: Summary of refuse initial water content, and porosity using alternative methods

Initial Water Content θ_{vol}	Field Capacity θ_{fc}	Porosity n	Method	Source
0.28		0.52	HELP Version I and Version II	Schroder <i>et al.</i> (1984a,b)
0.29	0.29	0.67	HELP Version. III	Schroder <i>et al.</i> (1994a,b)
	0.12-0.14		Literature Reported Average	Bagchi (1993)
0.10-0.20	0.20-0.35	0.40-0.50	Literature Reported Average	Oweis <i>et al.</i> (1990)
0.04-0.21	0.28-0.40		Literature Reported Average	McBean <i>et al.</i> (1995)
0.04-0.19	0.29-0.39		Literature Reported Average	Canziani and Cossu (1989)
		0.40	Estimation	UMA (1996)
0.16	0.30		Unknown	Rovers and Farquhar (1973)
0.08	0.37		Unknown	Wigh (1979)
	0.22		Unknown	Sharma and Lewis (1994)
0.17	0.40		Unknown	Walsh and Kinman (1981)
0.30	0.47 - 0.53	0.49-0.62	Unknown	Zornberg <i>et al.</i> (1999)
		0.43	Unknown	Aran <i>et al.</i> (1999)
	0.05	0.42	Unknown	Ahmed <i>et al.</i> (1992)
	0.36		Unknown (Old Waste)	Blight <i>et al.</i> (1992)
	0.71		Unknown (Fresh Waste)	

Table 2.6: Summary of literature reported values of the power law empirical parameters for refuse.

Empirical Parameter		Methodology	Source
b	B		
7	8	Fitting of power law equations by Straub and Lynch (1982) on a experimental refuse column (0.31 m depth) tests conducted by Qasim and Burhchinal (1970)	Straub and Lynch (1982)
7	9	Fitting of power law equations by Straub and Lynch (1982) on a experimental refuse column (0.21 m depth) tests conducted by Fungaroli (1971)	
6	9	Fitting of power law equations by Straub and Lynch (1982) on a experimental refuse column (0.24 m depth) tests conducted by Walsh and Kinman (1979)	
1.5		Direct measurement of refuse water content and refuse suction in smaller cylindrical cells (0.15 m diameter)	Korifitias <i>et al.</i> (1984)
4	11	Fitting of power law equations on a experimental refuse column (0.56 m diameter and 1.83 m height)	
7	9	Numerical analysis on the sensitivity of the power law equations. Source of b and B empirical parameters unknown.	Demetracopulos <i>et al.</i> (1986)
4	11	Used a two dimensional model to compute the time variation of leachate flow in landfills due to infiltration. Source of b and B empirical parameters unknown	Ahmed <i>et al.</i> (1992)

Table 2.7: Summary of influence of compaction effort on the reported refuse unit weight. (modified from a summary compiled by Oweis and Khera (1986) and Rowe and VanGulck (2004).

Unit Weight (kN/m ³)	Level of Compaction	Source
2.8 - 4.7	Poor	Oweis and Khera (1990)
4.7 - 7.1	Moderate	
7.1 - 9.4	Good to Excellent	
5.5 - 10.5	Balled Waste	
6.4 - 10.5	Shredded	
10.0	Densified MSW (heavy tamping)	Van Impe (1994)
3-9	Poor	Fasset <i>et al...</i> (1994)
5-8	Moderate	
9 -10.5	Good	
1-8	Zero	Gachet <i>et al...</i> (1998)
2.4-6.5	Slight	
3.5-7.7	Mean	
2.5-12	Extreme	
3.6-6.6	Loose (pre-compaction)	Marques <i>et al.</i> (1998)
3.1	Poor	Bromwell (1978)
6.3	Good	
8.6	Best	
2.9	Poorly	Schumaker (1972)
4.6-5.8	Moderate	
8.7	Well-Constructed	
1.2-2.9	As Delivered	Sowers (1973)
2.4-2.7	As Delivered	Merz and Stone (1962)
4.9	Standard	
5.6	Maximum	
4.1	Standard	
3.2	Minimal	

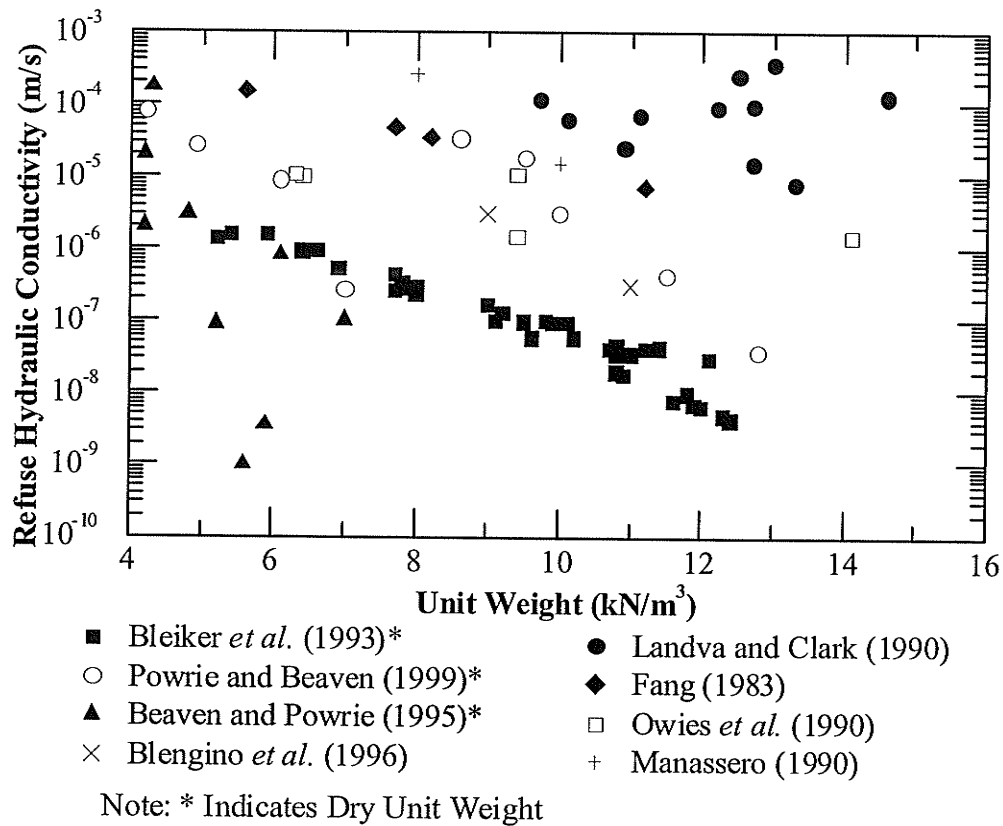


Figure 2.3: Hydraulic conductivity as a function of the refuse unit weight.

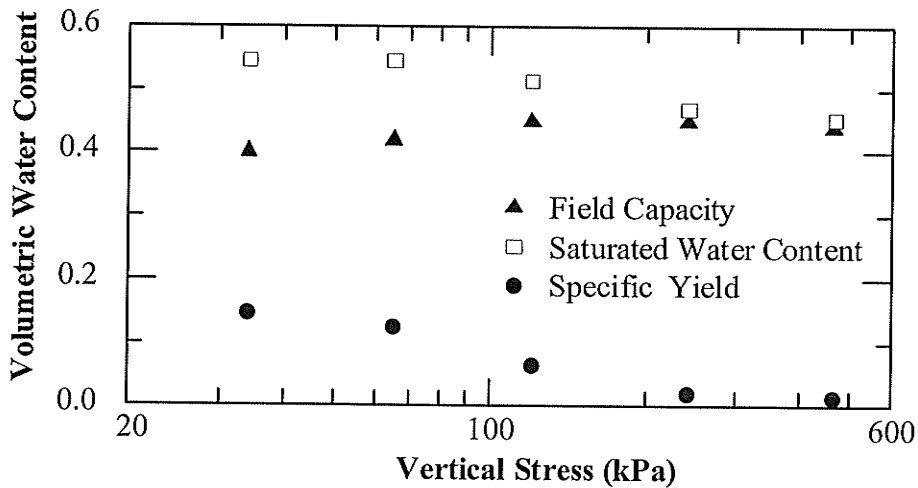


Figure 2.4: Change in field capacity, saturated water content and specific yield with induced vertical stress as measured by Powrie and Beaven (1999).

CHAPTER 3: HLIS NUMERICAL SIMULATIONS

3.1 INTRODUCTION

Bioreactor landfills are an emerging management strategy to enhance microbial processes within the landfill and accelerate waste degradation by increasing the moisture content of the refuse by injecting water or leachate into the refuse (Pohland 1975, Reinhart and Townsend 1997). Bioreactor landfills that incorporate moisture addition provide an increased benefit to the environment by reducing the overall contaminant lifespan of the landfill (Reinhart and Townsend 1997). Bioreactors additionally provided several economical advantages to conventional landfill such as an increase in landfill space due to an increase landfill settlement, reduction in leachate disposal costs from in situ leachate treatment, and energy recovery potential from enhanced landfill gas production and collection (Reinhart and Townsend, 1997). Methods employed to increase refuse moisture content include prewetting of waste shortly after placement, surface irrigation, vertical injection wells, and horizontal injection trenches (Reinhart and Townsend, 1997). Of these methods, horizontal trench injection systems provide the advantage of being able to inject large volumes of liquid (e.g., leachate or water), a relative low material cost, easy integration into landfill operations, and reduced odor and aesthetic problems (Reinhart and Townsend, 1997, Warzinski *et al.* 2000). Horizontal injection trenches are installed during landfill operation by digging a trench into the refuse at select vertical waste lift heights and horizontal spacings and backfilling the trench with a high permeability material (e.g. gravel or tire chips). Within the backfill material a perforated plastic pipe is placed to convey liquid from the landfill surface into the waste body. A uniform waste wetting from the horizontal liquid injection system (HLIS) is essential for uniform waste wetting and therefore degradation.

The design of HLIS involves the selection of appropriate pipe hydraulic parameters for designated vertical and horizontal spacing configurations within the landfill. VanGulck and Lozecznik (2004a) discussed the selection of pipe diameter, perforation size, delivery head, and inlet flow rate required to achieve uniform discharge along the length of a HLIS pipe; however, their study did not consider the liquid movement into the surrounding refuse. The hydraulic interactions for fluid movement between the perforated pipe, trench backfill material, and the surrounding refuse can influence the selection of trench spacing, liquid discharge rate from the perforated pipe, and liquid injection times. A field study consisting of eleven HLIS injection lines was conducted by Townsend and Miller (1998) at a landfill in North Central Florida. The results from the field study documented a decrease in system performance (e.g. decrease in injection rate) during a typical liquid injection run. Due to the heterogeneous nature of refuse, the effect of a broad range of spatial and temporal hydraulic conductivity and porosity within refuse requires consideration in the design and operation of HLIS. Maier (1998) developed an analytical technique to deduce the rate of liquid infiltration into refuse from a HLIS. The technique is based on the assumption of a constant refuse hydraulic conductivity during infiltration and an assumed zone of refuse wetting around the trench. McCreanor and Reinhart (2000) modeled liquid injection into refuse from a HLIS and also assumed a constant hydraulic conductivity with degree of refuse saturation. Additionally, McCreanor and Reinhart (2000) applied a specified flux of liquid infiltration into the refuse from the trench; thus, hydraulic interactions between liquid injection rate and refuse drainage were not considered in their analysis. Khire and Haydar (2003) modeled liquid injection into refuse with a varying hydraulic conductivity based on the degree of refuse saturation and specified a constant pressure of liquid

infiltration into the refuse from the trench. The constant pressure boundary condition does not consider the interaction between the liquid injection and movement in the refuse.

The objectives of this chapter are to demonstrate that the performance level, system operation, and design of HLIS are influenced by: the spatially and temporally variable hydraulic properties of the refuse, pipe hydraulic characteristics, and the liquid injection boundary condition applied at pipe perforation. The HLIS performance and operation will be assessed through modeling transient unsaturated-saturated fluid flow of liquid leaving the perforated pipe and transported through the surrounding refuse.

3.2 FIELD CASE STUDY

Townsend and Miller (1998) reported on the hydraulic performance of a horizontal injection trench at a landfill in North Central Florida. A series of eleven injection lines consisted of a 0.08 m external diameter PVC pipe, and various perforation size and perforation spacing configurations. Nine of the eleven injection lines were placed in a trench that was about 0.9 m wide and 0.9 m high and backfilled with tire shreds. Two of the injection lines were not placed in a trench and therefore were directly in contact with surrounding refuse. The influent flow rate and pressure head for each injection line were deduced by measuring the flow rate and pressure within the main header line using a paddle-wheel flow meter and an analog output pressure transducer, respectively. An example of a typical liquid influent flow rate and pressure head recorded during a single injection cycle are provided in **Figure 3.1**. Generally, all injection lines showed a decrease in flow rate and increase in pipe inlet pressure during liquid injection, until a near steady value were achieved (Townsend and Miller 1998).

Townsend and Miller (1998) reported that the observed changes in flow rate and pressure during injection were a function of the refuse water content and storage volume of the trench. The observed response could also be a result of: clogging within the pipe and pipe perforations (VanGulck and Lozecznik 2004b), non-ideal pipe hydraulic characteristics, and development of back pressure (discussed below) at the pipe perforation. If the rate at which liquid enters the trench is greater than the infiltration into refuse, the trench will saturate with liquid. A schematic representation of fluid discharge from a perforated pipe and pressure head increase in the trench during injection is provided in Figure 3.2. When the liquid level in the trench is below the elevation of the perforation, the perforation discharge at a specific pipe location will be constant for a constant pipe inlet flow rate and pressure head. A uniform perforation discharge along the length of the pipe can be designed and is a function of the influent flow rate and pressure head; pipe material, diameter, and length; and perforation size, spacing, and shape (see VanGulck and Lozecznik 2004a for details). During this stage of liquid injection, if the refuse is unsaturated, gas pressure acts at the perforation on the outlet side of the perforation. Once the liquid level in the trench reaches the perforation level, a liquid back pressure will act against the perforation. As the back pressure increases the perforation discharge will decrease and will induce a reduction in the flow rate and increase in pressure head at the influent end of the pipe.

A common operation strategy for HLIS is to inject liquid into the trench to elevate the pressure of liquid in the trench. Generally, the higher the pressure developed in the trench, the greater zone of refuse wetting around the trench (Al-Yousfi and Pohland 1998). However, as the pressure in the trench approaches the pressure within the perforated pipe, the perforation discharge approaches zero. This occurs when the injection pump approaches its operational

limits for flow rate and delivery head. The above explanation may be one of the reasons for the temporal changes in HLIS flow rate and pressure observed by Townsend and Miller (1998) and highlights the importance of considering the hydraulic interactions between the perforated pipe and the refuse hydraulic properties in HLIS design and operation.

3.2.1 Methodology

A cross section consisting of an injection pipe placed inside in granular backfilled trench buried in surrounding refuse was selected to represent a HLIS in a numerical domain. Transient unsaturated-saturated modeling of liquid movement from an injection pipe into the refuse via the trench was conducted using SEEP/W to investigate the influence of refuse hydraulic properties and pipe hydraulic characteristics on liquid injection system performance. SEEP/W is a two-dimensional finite element groundwater model based on Richard's equation which does not consider the influence of gas pressure changes on liquid migration. The model trench dimensions and a baseline case of the pipe hydraulic parameters (discussed below), were selected to resemble the physical study conducted by Townsend and Miller (1998). Two additional pipe hydraulic scenarios were selected as a comparative analysis to the baseline hydraulic case, one with a higher perforation flux and one with a higher perforation pressure. Three different boundary conditions (constant pressure, constant flux and head dependent flux) were applied to the pipe perforation to assess the influence on the performance of the HLIS.

3.2.2 Model Domain and Boundary Conditions

A 2-D cross-section of the HLIS and surrounding refuse was modeled. The pipe characteristics (described in pipe hydraulics section) were selected to obtain a uniform perforation discharge along the length of the line (<9% difference in perforation discharged between the inlet and end of the line). Thus, the increase in fluid pressure head acting at the base of the trench during injection and liquid infiltration into the refuse will be fairly uniform along the length of the line and 3-D effects can be considered negligible.

The problem domain and boundary conditions are depicted in Figure 3.3a. An artificial no flow ground water divide occurs along the center of the pipe and the gravel trench, and therefore a no flow boundary is implemented at the middle of the trench and the refuse. In order to isolate the leachate movement through the refuse due to liquid injection only from the pipe, a no flow boundary condition at the top of the refuse was assumed, thus neglecting water infiltration due to precipitation. The bottom of the problem domain was simulated to be a leachate collection system (LCS) at a position about 10 m below the bottom of the trench with a constant hydraulic head value of 0.3 m acting on the base of the landfill. A no flow boundary condition exists at a 10 m distance from the centre line of the trench. The 10 m distance was sufficient large that liquid infiltration from the trench was impacted by this boundary condition. A burial depth of 8 m from the trench bottom to the upper no flow boundary, and a 10 m spacing from the landfill base to the trench bottom was chosen to be representative of the full scale study conducted by Townsend and Miller (1998) and a numerical study conducted by McCreanor and Reinhart (2000). Additional details with regards to the trench configuration and boundary conditions are depicted in Figure 3.3b. The modeled trench has dimensions 0.9 m x 0.9 m and

contains a 38 mm coarse gravel backfill material with the base of the perforated pipe located 0.29 m from the bottom of the trench.

The standard numerical model setup used in all numerical simulations consisted of an unstructured automatic generated mesh with 1698 total elements, ,adaptive time stepping features of a maximum percentage change in head of 0.1% and minimum increment size of 0.1 seconds, and simulated data was saved at a constant time step interval of 360 seconds.

3.2.3 *Pipe Hydraulic Configurations*

In order to analyse the effect pipe hydraulic characteristics on HLIS performance and operation, three different pipe configurations were analyzed, see Table 3.1 for details. A baseline case was chosen to represent a perforated pipe design and operation that corresponded closely with the field study of Townsend and Miller (1998). The baseline case consisted of a specific injection line with a pipe internal diameter of 0.08 m which corresponds to an SDR 11 with outer pipe diameter of 0.10 m, and a and 0.0048 m perforation diameter (circular perforation) spaced at 1.5 m length for a pipe length of 75 m. Using Bernoulli equation for a clean HDPE pipe with no backpressure at the pipe perforation, the baseline case requires an inlet pipe pressure head of 3.75 m for a specified inlet flow rate of 0.295 m³/min. For the baseline configuration scenario, the difference in perforation discharge between the first and last perforation would be 9% with an average value of 6.01x10⁻³ m³/min. The normalised magnitude of perforation flux used in the numerical model for the baseline case was deduced to be equal to 2.00x10⁻³ m³/min per meter length of trench. The magnitude of the normalised perforation flux represents the average perforation discharge per meter length of trench divided by a factor of two to account for discharge into only half of the trench.

To compare the influence of pipe hydraulic configuration on HLIS performance and operation, two additional configurations were analyzed (see Table 3.1 for details). For each pipe configuration, the difference in discharge between the first and last perforation was less than 10% variation along the length of the line. The selected pipe in configuration two resulted in an inlet pressure head of 18.5 m, which is about 4.9 times larger than configuration one (3.75 m); however the inlet flow rate and normalised perforation flux were similar for each configuration. Pipe configurations one and three had a similar inlet flow rate and pressure head, but configuration three had a normalised flux $5.87 \times 10^{-3} \text{ m}^3/\text{min}/\text{m}$ which was about 2.9 times larger than configuration one ($2.00 \times 10^{-3} \text{ m}^3/\text{min}/\text{m}$).

3.2.4 Pipe Hydraulic Boundary Conditions

Three different boundary conditions were applied to the pipe perforation to simulate liquid injection and assess the impact of the boundary condition on HLIS performance. The three boundary conditions used in the numerical model were a constant perforation pressure of 3.75 m, constant perforation flux of $2.00 \times 10^{-3} \text{ m}^3/\text{min}/\text{m}$, and a pressure head dependent perforation flux. The use of constant perforation pressure and constant flux boundary conditions to simulate HLIS has been reported by McReanor and Reinhart (2000) and Khire and Haydar (2003), respectively; however both of these boundary conditions do not account for the reduction in perforation flux that occurs when a back pressure develops at the perforation. The reduction in perforation flux through a circular orifice in response to backpressure can be deduced through the application of Rawn's equation for discharge along a pipe manifold. The perforation discharge can be deduced through

$$q = ka\sqrt{2g\Delta h} \quad [3.1]$$

where q is the perforation discharge, k is a flow coefficient, a is the cross-sectional area of the orifice, g is the gravitational constant and Δh the change in hydraulic head on each side of the orifice (i.e., hydraulic head inside the pipe minus the hydraulic head in the fluid in the trench adjacent to the orifice).

The flow coefficient k for a circular orifice, is calculated from the following relationship (Subramanya and Awasthy 1970)

$$k = 0.675 \sqrt{1 - \frac{v^2}{2g\Delta h}} \quad [3.2]$$

where v is the mean velocity inside the pipe

Figure 3.4 displays the calculated decrease in the normalised perforation flux (q_{seep}) with an increase in backpressure development at the pipe perforation for the described three hydraulic pipe configurations. When the perforation backpressure approaches the inlet pressure head, the perforation discharge approaches a value of zero.

Liquid injection from the perforated pipe into refuse for each case and perforation boundary condition was simulated over 24 hour duration to assess HLIS performance. Additionally, drainage of the injected fluid away from the trench after only 4, 8, and 12 hours of liquid injection was analyzed. The selection of 8 hour liquid injection duration was obtained from HLIS numerical simulations conducted by McCreanor and Reinhart (2000), additionally the 4 and 12 hour injection durations were chosen to be representative of a single workday at an operational landfill (Maier and Vasuki 1996)

3.2.5 Refuse and Backfill Hydraulic Properties

The saturated hydraulic conductivity of refuse has been reported to range 10^{-4} to 10^{-8} m/s (Rowe *et al.* 2004) and may be influenced by, but not limited to, overburden load, refuse type and age, and landfilling operations. Powrie and Beaven (1999) experimentally showed that the refuse hydraulic conductivity can decrease by approximately two orders of magnitude due to increases in effective stress. Numerical simulations were conducted with a saturated refuse hydraulic conductivity of 10^{-4} , 10^{-6} , and 10^{-8} m/s to investigate the potential range reported in literature. Landva *et al.* (1998) and Hudson *et al.* (1999) reported refuse to be anisotropic with horizontal to vertical saturated hydraulic conductivity ratios of 8 and 2 to 5, respectively. Model simulations were completed with an anisotropic ratio of 4 horizontal to 1 vertical with respect to saturated hydraulic conductivity. To model liquid injection into and drainage through unsaturated refuse, a relationship between change in water content and hydraulic conductivity with change in suction was represented through the following empirical power law equations of Clapp and Hornberger (1978).

$$\psi = \psi_s \left[\frac{\theta}{\theta_s} \right]^b \quad [3.3]$$

$$K = K_s \left[\frac{\theta}{\theta_s} \right]^B \quad [3.4]$$

where ψ is waste suction, K is hydraulic conductivity, θ is volumetric water content, θ_s is fluid saturated volumetric water content, ψ_s is the suction of at the saturated water content, K_s is the saturated hydraulic conductivity, and b and B are empirical fitting parameters

A series of laboratory column infiltration tests conducted by Qasim and Burchinal (1970), Fungaroli (1971), Walsh and Kinman (1979) Korifitias *et al.* (1984) on refuse deduced values of 7 and 9 for the empirical fitting parameters b and B , respectively. The saturated volumetric water content was chosen to be 0.54, which is representative of the range 0.45 -0.60 measured by Powrie and Beaven (1999), Zeiss and Uguccon (1995), Zeiss and Major (1993), Hentges *et al.* (1993), and Korifitias *et al.* (1984). The suction value at the saturated volumetric water content was deduced from the power law equation equations to be equal to 2.1 cm (of water). All liquid injection simulations were conducted such that the initial minimum water content of was equal to a representative value for the refuse field capacity. The field capacity was chosen as the minim initial water content because it is anticipated that the field capacity in the surrounding refuse will be reached fairly quickly after operation of HLIS. The chosen volumetric refuse field capacity of 0.35 is within the literature reported range of 0.20 – 0.40 as reported by (Powrie and Beaven (1999), Yuen *et al.* (1995), Oweis *et al.* (1990), Korifitias *et al.* (1984), Fungaroli and Steiner (1979), Walsh and Kinman (1979)).

The trench backfill material was simulated to be representative of a 38 mm nominal size coarse gravel with a saturated hydraulic conductivity of 0.78 m/s and porosity of 0.46 (Rowe and McIsaac 2005). Due to the uniformity and large pore size of the coarse gravel the relationship between the changes in hydraulic conductivity with changes in suction was assumed to be constant and equal to the saturated hydraulic conductivity. The variation in water content with suction for the backfill material was simulated using literature reported van Genutchen values (Morris and Stormont 1998, Stormont 1995, Fayer *et al.* 1992) for a uniform coarse grained

gravel material, the residual volumetric water content (θ_r) equal to 0.005, with the empirical fittings parameters $\alpha = 4.93 \text{ cm}^{-1}$, and $N = 2.19$.

3.3 HLIS NUMERICAL SIMULATIONS

The role of unsaturated refuse hydraulic properties, pipe hydraulic configurations, and pipe perforation hydraulic boundary condition were analysed through a series of six HLIS numerical simulations (see Table 3.2 for summary). Each series consisted of three model runs that simulated injection into refuse with a saturated hydraulic conductivity of 10^{-4} , 10^{-6} , and 10^{-8} m/s for a total injection time of 24 hours. In order to investigate the transient behaviour and performance of a HLIS, simulated pressure head at the bottom of the trench, liquid injection flux, and the total volume of liquid injected was analyzed for all the numerical simulations. Table 3.3 summarizes the duration time to fill the injection trench, the pressure head at the bottom of the trench, the volume of liquid injected, and the (x) horizontal (Z_{up}) vertical upward, and (Z_{down}) vertical downward distances of 95% liquid saturation after 4, 8 and 24 hours of liquid injection, respectively

3.3.1 *Effect Of Refuse Properties on Liquid Injection*

The role of refuse hydraulic properties was investigated by simulating liquid injection into two specific refuse hydraulic conditions. The first case assumed a constant hydraulic conductivity with suction relationship and the second case employed a variable hydraulic conductivity with suction relationship, herein thereafter referred to as variable refuse hydraulic conductivity.

The pressure head acting on the base of the trench, for injection into constant and variable refuse hydraulic conductivities of 10^{-4} , 10^{-6} and 10^{-8} m/s are displayed in Figure 3.5 for the baseline configuration. For both cases examined, the lower the magnitude of refuse hydraulic conductivity, the slower rate of liquid infiltration into the refuse, and the larger increase in pressure head acting on the base of the trench (see Figure 3.5 and Figure 3.6). For liquid injection into a variable and constant refuse hydraulic conductivity of 10^{-8} m/s, the pressure head within the trench reached 0.9 m after about 99 minutes signifying that the trench was completely filled with liquid. Once the trench completely filled with liquid the pressure increased very rapidly and approached a steady state pressure of 4.04 m which was maintained for the remainder of the injection time. A steady state pressure value near 4.04 at the base of the trench indicates that the maximum pump delivery head of 3.75 m (since pipe perforation is located 0.29 m above the trench) for the baseline configuration

The representative liquid injection flux from the pipe perforation and the volume of liquid injected with time for a full size trench per meter length for constant and unsaturated refuse hydraulic conductivities of are presented in Figure 3.6, respectively. A large increase in backpressure at the perforation (due to low magnitude refuse hydraulic conductivity) at the pipe perforation will result in a decreased perforation flux and the volume of liquid that can be injected. For liquid injection into a saturated refuse hydraulic conductivity of 10^{-8} m/s, once the trench filled with liquid a rapid increase in backpressure resulted in the perforation flux to decrease very rapidly and once the pump limit was reached the volume of liquid injected to approach a value of zero.

A very high liquid infiltration rate for a saturated refuse hydraulic conductivity of 10^{-4} m/s caused the pressure within the trench never exceeded a value of 0.29 m, therefore the trench never completely filled with liquid and no backpressure occurred at the pipe perforation. The occurrence of no backpressure resulted in no decrease in the perforation flux and the total volume liquid injected after 24 hours represents the theoretical maximum value that could be injected for the baseline configuration (see Table 3.3 for additional details).

A difference in trench filling and pressure head development for a variable hydraulic conductivity with suction relationship in comparison to a constant hydraulic conductivity was most evident for a waste hydraulic conductivity of 10^{-4} m/s. Liquid injection into a constant hydraulic conductivity of 10^{-4} m/s resulted in the trench pressure head to decrease with time and eventually become negative indicating refuse suction. The difference in pressure head responses between the variable and constant hydraulic conductivity cases is due to the greater resistance to fluid flow through the refuse for the variable case. For example in the variable hydraulic conductivity case of 10^{-4} m/s, the unsaturated hydraulic conductivity prior to liquid injection was 10^{-8} m/s. The occurrence of refuse suction in the constant hydraulic conductivity case is most likely due to the high value of refuse hydraulic conductivity enabling a quick redistribution of the refuse field capacity throughout the problem domain.

3.3.2 Influence of Pipe Hydraulic Configurations

The influence of pipe hydraulic configurations was analysed by comparing the high perforation pressure and high perforation flux configurations to the baseline configuration, respectively. The pressure head increases at the base of the trench, and the perforation flux and

cumulative volume of liquid injected for the high perforation pressure and flux configurations are provided in Figure 3.7 and Figure 3.8, respectively.

For a refuse hydraulic conductivity of 10^{-4} m/s, the high flux configuration induced higher pressures within the trench but also resulted in a larger volume of liquid injected when compared to the baseline configuration. Conversely, due to the similar values of perforation flux injection into a hydraulic conductivity of 10^{-4} m/s using the high pressure configuration resulted in the similar pressure development and volume of liquid injected as the baseline configuration.

Injection into a refuse hydraulic conductivity of 10^{-6} m/s and a high pressure configuration resulted in larger pressure head development within the trench, and unlike the baseline configuration, the pump limit (equal to 18.5 m) was not reached after 24 hours of liquid injection. The higher pressure configuration enabled a much slower decrease in perforation flux compared to the baseline case, which corresponded to an overall larger volume of liquid that could be injected (see Table 3.3 and Figure 3.8 for more information). Injection into a refuse hydraulic conductivity of 10^{-6} m/s and the high perforation flux configuration resulted in the trench filling more quickly than the baseline case. Since the pump limit values were both equal to 3.75 m for the high perforation flux and baseline configurations, the pressure head development at the base of the trench and amount of liquid injected was very similar for both configurations.

3.3.3 Validity of Pipe Perforation Boundary Conditions

The pressure head increase acting on the base of the trench for a constant perforation pressure (3.75 m), a constant perforation flux (2.00×10^{-3} m³/min/m), and a head dependent flux perforation boundary for variable saturated refuse hydraulic conductivities of 10^{-4} , 10^{-6} and 10^{-8}

m/s are displayed in Table 3.3 and Figure 3.9. A constant perforation pressure boundary condition resulted in a constant pressure of 4.04 m at the base of the trench for all three refuse hydraulic conductivities. Injection into a refuse hydraulic conductivity of 10^{-8} m/s using a constant perforation flux caused the development of very large pressures (magnitude of 10^3 m) at the base of the trench. The high pressures developed at the base of the trench significantly exceeded the maximum pump capabilities of both the baseline and high pressure configurations.

The influence of the described pipe perforation boundary conditions on the cumulative injected volume was simulated for refuse hydraulic conductivities of 10^{-4} , 10^{-6} , and 10^{-8} m/s and displayed Figure 3.10. Due to the nature of the constant flux boundary condition, the injected volumes were equal to $5.77 \text{ m}^3/\text{m}$ after 24 hours for all three refuse hydraulic conductivities. The constant perforation pressure boundary condition simulated a significant increase in the volume of liquid that could be injected when compared to head dependent flux. The large volume injected for the constant pressure boundary condition is most evident for the 10^{-4} m/s refuse hydraulic, where the volume injected (see Table 3.3) compared to the baseline hydraulic configuration was exceeded by a factor of 9.

3.3.4 HLIS Zones of Liquid Saturation

It has been reported that waste degradation in full scale HLIS has been limited by an inability to uniformly apply liquid throughout the refuse (McCreanor and Reinhart 2000). Quantifying the zones of saturation that developed around a HLIS during liquid injection can provide guidance on reasonable vertical and horizontal trench spacing intervals for uniform waste wetting throughout the landfill.

Figure 3.12 displays the developed zones of saturation after 8 hours of injection using the baseline pipe configuration for variable saturated refuse hydraulic conductivities of 10^{-4} , 10^{-6} and 10^{-8} m/s. The zones of saturation of that developed around a HLIS is greatly influenced by the refuse hydraulic conductivity and for all other conditions being equal, the higher the hydraulic conductivity the more volume that can be injected and a larger zone of saturation around the trench. Table 3.3 summarizes the deduced 95% liquid saturation maximum distances horizontally from the edge of the injection trench (x), vertically upward (z_{up}) and downward (z_{down}) from the injection trench. Table 3.3 summarises the cumulative injected volume the deduced 95 % liquid saturation maximum distances horizontally from the edge of the injection trench (x), vertically upward from the top of the injection trench (z_{up}) and vertically downward from the bottom of the trench (z_{down}) after 4, 8 and 24 hours respectively of injection for all six series of HLIS simulations. A liquid saturation criterion of 95% water was chosen to be as a sufficient amount of water saturation for which to asses the saturated zones of influence around the trench. The zones of saturation of that developed around a HLIS is greatly influenced by the refuse hydraulic conductivity and for all other conditions being equal, the higher the hydraulic conductivity the more volume that can be injected and a larger zone of saturation around the trench.

A non pressurised HLIS at a refuse hydraulic conductivity of 10^{-4} m/s HLIS will correspond to a large volume of that can injected (as discussed) and as a result a large zone of saturation below the trench will develop (see Table 3.3 for additional information). A pressurised trench in a refuse hydraulic conductivity of 10^{-6} and 10^{-8} m/s creates zones of saturation above the injection trench unlike the 10^{-4} m/s case, however due to the backpressure development at the

perforation, lower volumes can be expected volume of liquid will be injected, and as such, lower zones of saturation can be expected (see Table 3.3 for additional information). As discussed earlier, the constant perforation flux and perforation boundary conditions can overestimate the pressure head and injected volumes within a HLIS for various refuse hydraulic conductivities resulting in a large zone of saturation around an injection trench (Table 3.3).

3.3.5 Liquid Injection Schedule Analysis

The time to completely drain an injection trench is an important parameter that can provide guidance on the selection of an appropriate liquid injection schedule. The role of refuse hydraulic conductivity and its impact on the time to completely drain a liquid injection trench was analysed and the simulated pressure head decrease at the base of an injection trench after an 8 hour liquid injection schedule (base line pipe configuration) into variable refuse hydraulic conductivities of 10^{-6} and 10^{-8} m/s are displayed in Figure 3.11. For both cases the trench depressurised fairly rapidly after drainage to a value of near 0.9 m at the base of the trench, which is equal to the height of the trench. Subsequently, a long duration of time was required to drain the trench (i.e., pressure head of 0 m on the base of the trench). The time to completely drain a trench was greatly influenced by the magnitude of refuse hydraulic conductivity and equaled about 20 and 507 days for refuse hydraulic conductivities of 10^{-6} and 10^{-8} m/s, respectively. Additional drainage simulations using the baseline pipe configuration were conducted to investigate the sensitivity of liquid injection duration (4, 8, and 12 hours) on the trench drainage time. A summary of the drainage time durations and reference values for the pressure head at the base of the trench and volume of liquid injected at the end of liquid injection are provided in Table 3.4 due to the similar pressure conditions within the trench at the end of

injection for each injection duration, the time to drain the trench only increased marginally with longer injection duration for the same hydraulic conductivity refuse. However, for a given injection duration, the time to drain a trench increased significantly with lower refuse hydraulic conductivity.

3.4 DESIGN IMPLICATIONS

A pressure head at the base of the trench equal to 0.29 m signifies that the liquid level in the trench has reached the pipe elevation and a perforation backpressure will occur until the pump is turned off and liquid drains into the surrounding refuse. The head dependent perforation flux boundary condition should be imposed to accurately simulate the rate of pressure head increase acting on the base of the trench and decrease in perforation flux and injected volumes.

The injection time to pressurize a trench is a function of the refuse hydraulic conductivity and the physical capabilities of the pump. For optimal overall performance, the operation and design of the injection system needs to carefully consider the decrease in the refuse hydraulic conductivity with depth in a landfill (Powrie and Beaven, 1999). For example, liquid injection into a deep landfill location that is representative of low refuse hydraulic conductivity and therefore low liquid infiltration rate may require short injection times and longer trench drainage durations. Additionally, injection in a deep landfill could result in low injected volumes due to the physical limits of the injection pump being reached quickly after filling. Low injected volumes also result in small zone of wettings and may require small vertical and horizontal trench spacing intervals if uniform liquid application is desired. Low injected volumes with short injection duration along with long drainage durations could also compromise planned leachate management strategies. Additionally liquid injection into refuse which has experienced a large

decrease in the refuse hydraulic conductivity from increased over burden pressures and waste degradation processes could become impractical due to a need for very short liquid injection schedules and spacing intervals. The volume of liquid injected could be increased in the design phase by the choosing a pipe configuration with a higher delivery hydraulic head, or by increasing the trench size which would increase the liquid storage capabilities of the trench. Compared to a low refuse hydraulic conductivity, liquid injection into a high refuse hydraulic conductivity, representative of a shallow landfill depth, may require long injection times and a large volume of liquid, due to a high rate of liquid infiltration into the refuse. Long injection times will require injection pumps to operate for extended periods of time which may increase operating costs. Consideration is also required to ensure liquid availability if large volumes require injection. If there is a high infiltration rate into the waste compared to the rate of liquid injection, this may result in ineffective wetting of the refuse above the injection trench since the injection trench will not reach a pressurized state. Assuming there is a sufficient liquid supply, a possible design solution is to choose a pipe configuration that generates a higher pipe flow rate to pressurize the trench in a short duration of time.

3.4.1 Empirical Correlations

A set of empirical equations were created to simulate the pressure rate development and the volume of liquid injected for a pressurized trench with a range of possible pipe hydraulic conditions and refuse hydraulic properties. The empirical correlations provide landfill engineering designers with a quick and efficient tool to evaluate the potential performance level of various design scenarios for a range of refuse hydraulic conductivity before full

implementation. Additionally the correlations can offer guidance on the planning of an efficient leachate management strategies and liquid injection schedule.

The empirical correlations were generated from numerical simulations into refuse with a constant saturated hydraulic conductivity value of 10^{-6} and 10^{-8} m/s. All numerical simulations were conducted for a pipe with an internal pipe diameter of 0.08 m (external diameter 0.1 m, SDR 11). The selected inlet hydraulic head ranged from 2 to 50 m and the deduced normalized perforation flux range was equal to 1×10^{-5} to 5×10^{-5} m³/s/m. The selected pipe configurations ranges were obtained from summary of literature reported injection system design parameters conducted by Lozecznik (2006) Results from the numerous numerical simulations that examine a range of injection conditions were normalized to produce empirical relationships to predict pressure head development within a trench and the cumulative volume of liquid injected with time. The empirical relationships and fitting parameters can be used by a designer to establish a first approximation of injection system performance to aid in directing efforts for more detailed design.

From each injection simulation, the injected volume after trench pressurization was fitted to a power law equation and the volume of liquid injected can be calculated as follows:

$$V = a_v (t_p)^{b_v} \quad [3.5]$$

where V is the cumulative volume injected after pressurization in m³/m, t_p is the time after pressurization in hours, a_v and b_v are derived empirical coefficients.

The simulated pressure head at the bottom of the trench was normalized to the trench pressurization time to produce an approximately-linear relationship with time. Rearrangement of

the approximately linear relationship provides a means to deduce the pressure head at the bottom of the trench with time as follows:

$$h_p = \frac{t_p}{((t_p \times a_{hp}) + b_{hp})} \quad [3.6]$$

where h_p is the pressure head at the bottom of the trench after pressurization in meters, a_{hp} and b_{hp} are derived empirical coefficients.

Figure 3.13 and Figure 3.14 display the empirical coefficient values for the pressure head development (a_{hp} and b_{hp}) and liquid injected volume (a_v and b_v), respectively, for liquid injection using a range of inlet hydraulic head and normalised perforation flux for a saturated refuse hydraulic conductivity of 10^{-4} and 10^{-6} m/s.

3.4.1.1 Empirical Design Methodology

The application of the empirical equations to estimate the expected pressure development and injected volume in an injection trench is best illustrated in the following two design examples. Example 1 consists of injection into a saturated refuse hydraulic conductivity of 10^{-8} m/s, a normalized perforation flux of $0.0027 \text{ m}^3/\text{min}/\text{min}$, and an inlet hydraulic head of 50 m. Example 2 considers liquid injection into a saturated refuse hydraulic conductivity of 10^{-6} m/s, a normalized before flux value of $0.0018 \text{ m}^3/\text{min}/\text{min}$, and an inlet hydraulic of 8 m. From Figure 3.13 it is seen that the pressure development empirical coefficients equal 0.020 and 0.141 (a_{hp}) and 0.000 and 0.101 (b_{hp}) for Example 1 and Example 2 respectively. The injected volume coefficients (Figure 3.14) were found to equal 0.080 and 0.163 (a_v) and 0.531 and 0.817 for Example 1 and Example 2 respectively. Once the empirical coefficients for pressure and volume are deduced Equation 5 and Equation 6 can be used to estimate the trench bottom pressure and

injected volume that could occur at any time after trench pressurization. For example after 12 hours of trench pressurization the trench bottom pressure was estimated (Equation 5) to be at the maximum pump delivery head of 50 m for Example 1, however in Example 2 a slower rate of pressure increase resulted in a bottom pressure estimate (6.0 m) that had not approached its maximum delivery head value of 8.0 m. With a quicker rate of pressure development in Example 1 than Example 2 one would expect as discussed earlier a lower overall injected volume for Example 1. The empirical estimation for injected volume (Equation 6) reflected the above stated assumption as the estimated injected volume equaled $0.3 \text{ m}^3/\text{m}$ and $1.2 \text{ m}^3/\text{m}$ for a Example 1 and Example 2 respectively.

3.5 CONCLUSIONS

Field observations of decrease in injection flow rate and increase in the pipe pressure head can be partially explained by the development of a back pressure within the injection trench acting against the pipe perforations. The hydraulic interactions during liquid injection from a HLIS and subsequent drainage into refuse were numerically simulated using a two-dimensional unsaturated-saturated fluid flow model. The numerical simulations suggest that the rate of pressure increase at the inlet of the perforated pipe and subsequent decrease in flow rate is inversely proportional to refuse hydraulic conductivity. HLIS positioned within a refuse with a relatively low hydraulic conductivity (based on literature reported values) resulted in rapid filling and pressurizing of the injection trench and a decrease in the injection flux and injected volume compared to a high hydraulic conductivity.

A relatively high refuse hydraulic conductivity (based on literature reported values) resulted in a large rate of liquid infiltration into the surrounding refuse compared to a low

hydraulic conductivity refuse. A high liquid infiltration rate can result in long injection time to fill and pressurize the trench, large volumes of liquid injected, and short durations to drain the liquid in the trench. Thus, the design, operation, and performance of a HLIS should take into consideration the surrounding in situ refuse hydraulic properties and the potential for a decrease in refuse hydraulic properties with depth and time in the landfill. A set of empirical equations on the transient pressure development and injected volume were developed from numerous numerical simulations. The empirical correlations can be used a design tool to predict the pressure development within a trench and the injected volume for a range of pipe hydraulic configurations and refuse hydraulic properties.

3.6 REFERENCES

- Al-Yousfi, A.B. and Pohland, F.G. (1998) Strategies for Simulation, Design and Management of Solid Waste Disposal Sites as Landfill Bioreactors, *Practice Periodical of Hazardous Toxic and Radioactive Waste Management*, 2(1):13-21.
- Clapp, R.B and Hornberger (1978) Empirical Equations for Some Soil Hydraulic Properties, *Water Resources Research*, 14(4).
- Demetracopoulos, A.C., Korfiatis, G.F., Bourodimos E.L. & Nawy, E.G. (1986) Unsaturated flow through solid waste landfills: model and sensitivity analysis, *Water Resources Bulletin*, 22:601-609.
- Fayer, M. J., Rockhold, M. L. and Campbell, M. D. (1992) Hydrologic Modeling of Protective Barriers: Comparison of Field Data and Simulation Results, *Soil Science Society of America Journal*, 56:690-700.
- Fungaroli, A.A. (1971) Pollution of Subsurface Water by Sanitary Landfills, *U.S. EPA report SW-12rg*, Vols. I-II.
- Fungaroli, A. A. & Steiner, R. L. (1979) Investigation of Sanitary Landfill Behavior, Vols 1 & 2. EPA-600/2-79-053a.
- Hentges, G. T., Thies, F. & Lemar, T. S. (1993) Leachate Extraction Well Assessments Des Moines, Iowa Metropolitan Park East Sanitary Landfill, Hamilton County, Iowa Sanitary Landfill. Proceedings of the Sixteenth International Madison Waste Conference. Department of Engineering Professional Development, University of Wisconsin, Madison/Extension, Madison, U.S.A.
- Hudson, A.P., Beaven, R.P. and Powrie, W. (1999) Measurement of the horizontal K of

- household waste in a large scale compression cell, *Proceedings Sardinia 99, Sixth International Landfill Symposium*, S. Margherita di Pula, Cagliari, Italy.
- Khire, M.V. and Haydar, M.M. (2003) Numerical evaluation of granular blankets for leachate recirculation in msw landfills, *Proceedings of Sardinia 2003 Ninth International Waste Management and Landfill Symposium*, S. Margherita di Pula, Cagliari, Italy.
- Korifiatis G. P., Demetracopoulos A. C., Bourodimos E. L. and Nawy E. G. (1984) Moisture transport in a solid waste column. *J. Env. Eng.*, 110(4): 789-796.
- Landva, A.O., Pelkey, S.A. and Valsangkar, A.J. (1998) Coefficient of Permeability of Municipal Refuse, *Proceedings, 3rd International Congress on Environmental Geotechnics*, Lisbon, Portugal, 1: 63-68
- Lozcznik (2006) Hydraulic Design, Operation and Clogging of Leachate Injection Pipes, *University of Manitoba MSc Thesis*.
- Maier, T. B. (1998) Analysis Procedures for Design of Leachate Recirculation Systems, *Proceedings from the SWANA 3rd Annual Landfill Symposium*, Palm Beach Gardens, FL, USA.
- Maier, T. B, and Vasuki, N.C. (1996) Expected benefits of a full-scale bioreactor landfill, *Proceedings of Wastecon*.
- McCreanor, P. T. and Reinhart, D. R. (2000) Mathematical Modeling of Leachate Routing in a Leachate Recirculating Landfill, *Wat. Res.*, 34(4): 1285-1295.
- Morris, C.E. and Stormont J.C. (1998) Evaluation of numerical simulations of capillary barrier field tests, *Geotechnical and Geological Engineering*, 16:201-213.

- Powrie, W. and Beaven, R.P. (1999) Hydraulic properties of household waste and implications for liquid flow in landfills. *Proceedings of the Institution of Civil Engineers, Geotechnical Engineering*, 235-247.
- Qasim, S.R. and Buurchinal, J.C. (1970) Leaching from Simulated Landfills, *Journal of the Water Pollution Control Federation*, 42(3).
- Rawn, A.M., Bowerman, F.R., and Chen, C.K. (1970) Diffusers for Disposal of Sewage in Sea Water, *Trans ASCE*, 126:344-388.
- Reinhart, D.R. and Townsend, T.G. (1997) *Landfill Bioreactor design and operation*, CRC Press LLC, FL, USA
- Reinhart, D.R. and Townsend, T.G. (1997) *Landfill Bioreactor design and operation*, CRC Press LLC, FL, USA.
- Rowe, R.K. and McIsaac, R. (2005) Changes in leachate chemistry and porosity as leachate permeates through tire shreds and gravel. *Can Geotech J.*, 42: 1173-1188.
- Rowe, R.K., Quigley, R.M., Richard W. I. Brachman, R.W.I., and Booker J.R. (2004) *Barrier Systems for Waste Disposal*, 2nd ed., Spon Press, New York, NY, USA.
- Stormont, J. C. (1995) The effect of constant anisotropy on capillary barrier performance, *Water Resources Research*, 31(3):783-785.
- Subramanya, K. and Awasthy, S.C. (1970) Discussion of the Paper by Vigander, *Jour. Hydraulics Div.*, Proc. Of ASCE, 96, no.HY12.
- Townsend, T.G. and Miller, W.L. (1998) Leachate Recycling Using Horizontal Injection, *Advances in Environmental Research*, 2(2):129-138.
- VanGulck, J.F. and Lozecznik, S. (2004) Hydraulic considerations of landfill leachate

injections systems. *Proceedings 1st Canadian Young Geotechnical Engineers and Geoscientists Conference*, Quebec City, Quebec, Canada.

VanGulck, J.F. and Lozecznik, S. (2004b). Predicting clog development in leachate transmission pipes- theoretical considerations, *Proceedings, 32nd Annual General Conference of the Canadian Society for Civil Engineering*, Saskatoon, Saskatchewan, Canada.

Walsh, J.K and Kinman, R.N. (1979) Leachate and Gas Production under Controlled Moisture Conditions, *Proceedings of the Fifth Annual Research Symposium*, EPA-600/9-79-023a.

Warzinski, J., Watermolen, B.T., Torresani, M.K.,and Genthe, D.R. (200) A Superior Approach To Recirculation, *Waste Age*, 31(2):

Zeiss, C. and Major, W. (1993) Flow through municipal solid waste: pattern and characteristics, *Journal of Environmental Systems*, 22(3):211-232

Table 3.1: Summary of the three selected pipe hydraulic configurations.

Configuration	Pipe				Perforation			
	Internal ϕ (m)	Length L (m)	Flow Rate Q (m ³ /min)	Head h _p (m)	Size (m)	Spacing (m)	Difference Discharge Δ_q %	Normalised Discharge* q _{seep} (m ³ /min/m)
1-Baseline	0.08	75	0.295	3.75	0.0048	1.5	9	2.00x 10 ⁻³
2-High Pressure	0.08	75	0.301	18.50	0.0032	1.5	2	2.01x 10 ⁻³
3-High Flux	0.08	35	0.411	3.75	0.0048	0.5	8	5.87x 10 ⁻³

* Normalised discharge is for ½ of the numerical problem domain.

Table 3.2: Summary of designated, saturated refuse hydraulic conductivities, pipe hydraulic configurations, and pipe perforation boundary conditions for a series of six HLIS numerical simulations.

Series #	Saturated Refuse Hydraulic Conductivity	Pipe Hydraulic Config.	Perforation Boundary Condition
-1	10 ⁻⁴ , 10 ⁻⁶ , 10 ⁻⁸ (Variable Suction)	1-Baseline	Constant Flux = 2.00 x 10 ⁻³ m ³ /min/m
-2	10 ⁻⁴ , 10 ⁻⁶ , 10 ⁻⁸ (Variable Suction)	1-Baseline	Constant Pressure = 3.75 m
-3	10 ⁻⁴ , 10 ⁻⁶ , 10 ⁻⁸ (Variable Suction)	1-Baseline	Head Dependent Flux
-4	10 ⁻⁴ , 10 ⁻⁶ , 10 ⁻⁸ (Constant Suction)	1-Baseline	Head Dependent Flux
-5	10 ⁻⁴ , 10 ⁻⁶ , 10 ⁻⁸ (Variable Suction)	2-High Pressure	Head Dependent Flux
-6	10 ⁻⁴ , 10 ⁻⁶ , 10 ⁻⁸ (Variable Suction)	3-High Flux	Head Dependent Flux

Table 3.3: Summary of the time required to fill a HLIS, the pressure head at the bottom of the trench (h_p) volume of liquid injected (V), and the deduced maximum horizontal (x), upward vertical (z_{up}), and downward vertical (z_{down}) distances for 4, 8 and 24 hours of liquid injection simulation respectively.

#	K_{sat} Refuse (m/s)	Fill Time (hr)	4 hours			8 hours			24 hours		
			h_p (m)	V (m ³ /m)	x, z_{up}, z_{down} (m)	h_p (m)	V (m ³ /m)	x, z_{up}, z_{down} (m)	h_p (m)	V (m ³ /m)	x, z_{up}, z_{down} (m)
-1	10^{-4}	no fill	0.19	0.95	1.4, 0.0, 1.5	0.19	1.91	1.6, 0.0, 2.9	0.19	5.77	1.8, 0.0, 6.4
	10^{-6}	1.75	14.1	0.95	1.4, 0.5, 0.5	22.4	1.91	2.1, 0.9, 1.0	36.4	5.77	4.3, 1.9, 1.9
	10^{-8}	1.65	914	0.95	1.2, 0.5, 0.3	1714	1.91	1.9, 0.8, 0.7	2870	5.77	3.7, 1.7, 1.6
-2	10^{-4}	N/A	4.04	11.41	5.7, 1.6, 3.6	4.04	19.83	7.2, 1.8, 5.6	4.04	51.35	8.1, 2.0, 10.0
	10^{-6}	N/A	4.04	0.86	1.2, 0.3, 0.4	4.04	1.10	1.5, 0.5, 0.6	4.04	1.85	2.1, 0.7, 0.8
	10^{-8}	N/A	4.04	0.43	0.6, 0.1, 0.1	4.04	0.44	0.6, 0.1, 0.2	4.04	0.48	0.7, 0.1, 0.2
-3	10^{-4}	no fill	0.19	0.95	1.3, 0.0, 1.5	0.19	1.91	1.6, 0.0, 2.9	0.19	5.77	1.8, 0.0, 8.1
	10^{-6}	1.77	3.60	0.67	1.0, 0.2, 0.3	3.82	0.96	1.3, 0.4, 0.5	3.91	1.72	2.0, 0.6, 0.8
	10^{-8}	1.65	4.05	0.42	0.6, 0.1, 0.1	4.05	0.44	0.6, 0.1, 0.2	4.06	0.48	0.7, 0.2, 0.2
-4	10^{-4}	no fill	0.26	0.95	0.0, 0.0, 0.0	0.02	1.91	0.0, 0.0, 0.0	-5.31	5.77	0.0, 0.0, 0.0
	10^{-6}	1.87	3.56	0.69	1.0, 0.3, 0.3	3.80	0.98	1.4, 0.4, 0.5	3.89	1.78	2.0, 0.7, 0.8
	10^{-8}	1.65	4.02	0.45	0.6, 0.2, 0.2	4.03	0.49	0.6, 0.3, 0.2	4.04	0.59	0.7, 0.4, 0.5
-5	10^{-4}	no fill	0.19	0.95	1.4, 0.0, 1.5	0.19	1.91	1.6, 0.0, 2.9	0.19	5.78	1.8, 0.0, 8.1
	10^{-6}	1.75	9.21	0.85	1.2, 0.4, 0.4	12.13	1.48	1.8, 0.7, 0.7	14.76	3.54	3.2, 1.4, 1.5
	10^{-8}	1.65	19.01	0.46	0.6, 0.2, 0.1	19.04	0.50	0.7, 0.2, 0.1	19.08	0.62	1.0, 0.3, 0.3
-6	10^{-4}	5.75	0.86	2.63	2.3, 0.0, 2.0	0.91	5.19	3.2, 0.1, 3.6	0.92	15.43	3.9, 0.2, 10.0
	10^{-6}	0.56	3.93	0.80	1.1, 0.3, 0.4	3.96	1.05	1.5, 0.5, 0.5	3.97	1.80	2.0, 0.7, 0.9
	10^{-8}	0.55	4.01	0.43	0.6, 0.1, 0.1	4.02	0.44	0.6, 0.2, 0.1	4.01	0.48	0.7, 0.2, 0.2

Table 3.4: Summary of the selected variable saturated refuse hydraulic conductivity, the initial drainage trench bottom pressure (h_p) and volume injected (V), and the time duration to drain a trench for each series of liquid drainage simulation.

Series #		K_{sat} Refuse (m/s)	h_p (m)	V (m ³ /m)	Drainage Time (days)
-1	4hr Injection	10^{-6}	3.61	0.68	18
		10^{-8}	4.04	0.42	491
-2	8hr Injection	10^{-6}	3.82	0.96	20
		10^{-8}	4.05	0.44	507
-3	12 hr Injection	10^{-6}	3.86	1.18	21
		10^{-8}	4.06	0.45	519

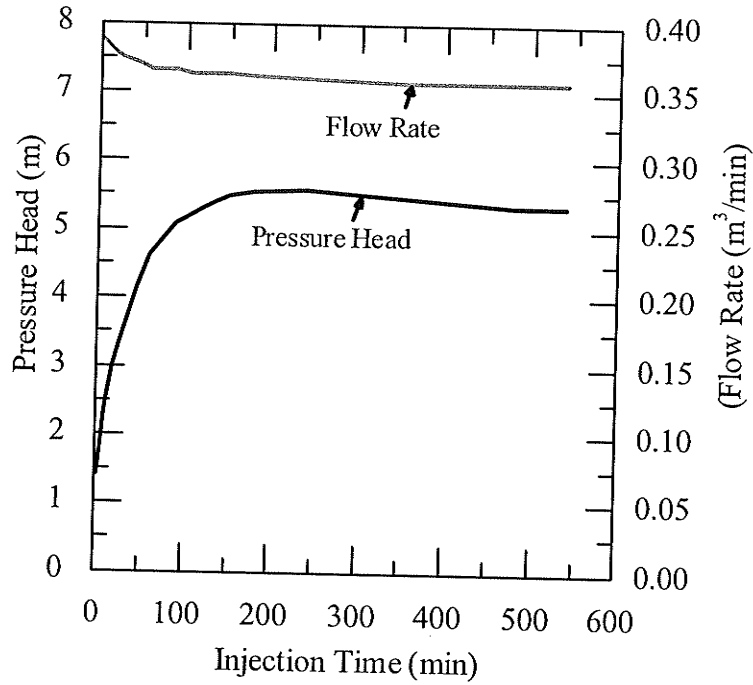
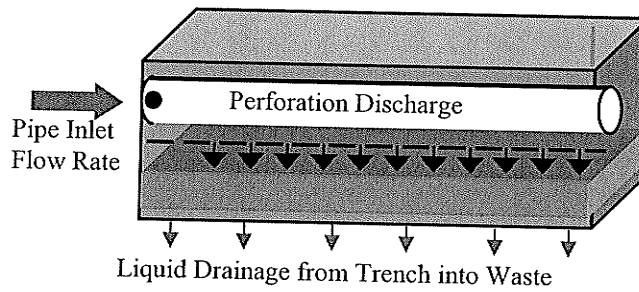


Figure 3.1: Typical injection flow and pressure head response (modified from Townsend and Miller 1998).

(a)



(b)

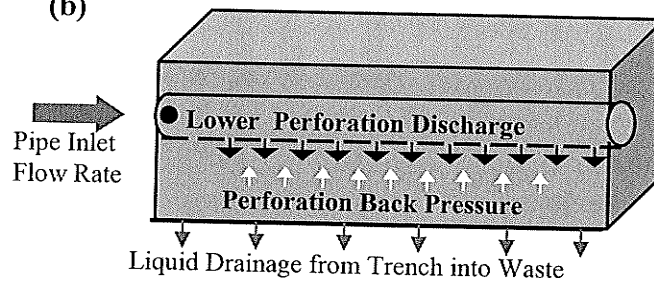


Figure 3.2: Schematic representation of uniform pipe perforation discharge, backpressure, and liquid drainage into surrounding refuse for: (a) partially filled trench and (b) completely filled trench.

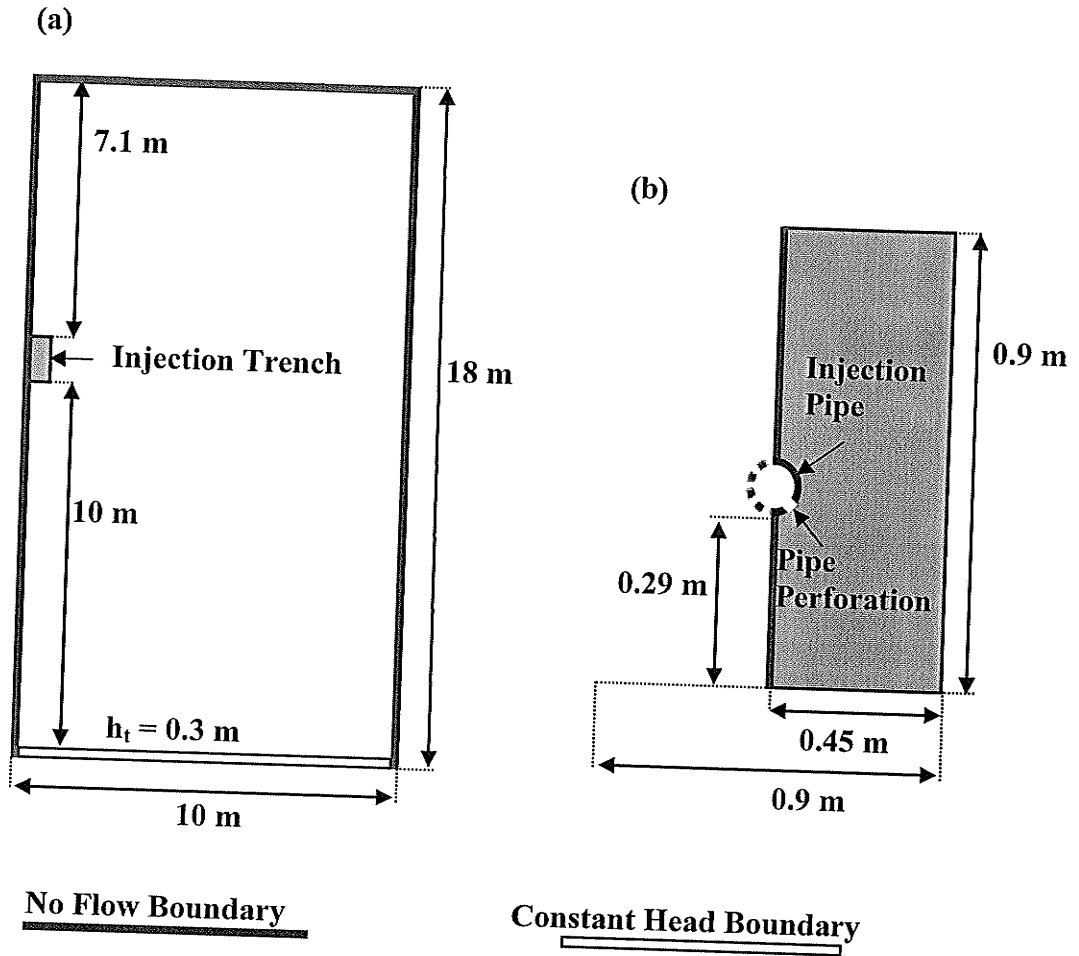


Figure 3.3:(a) Numerical model boundary conditions and problem domain, (b) detailed trench configuration and numerical model boundary conditions.

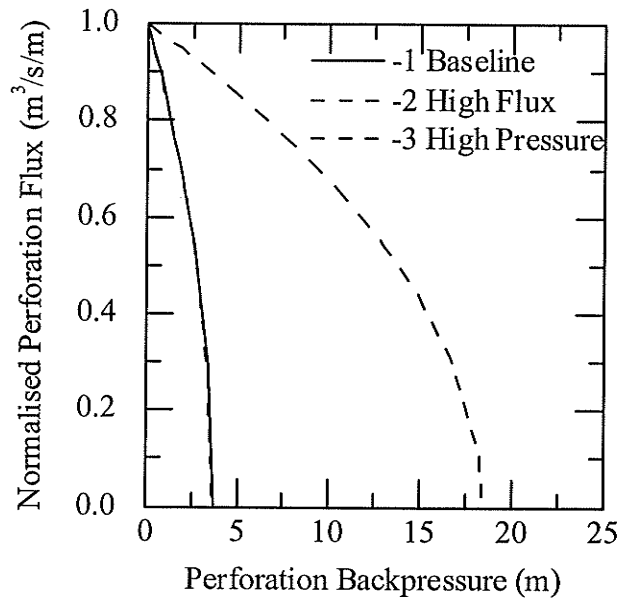


Figure 3.4: Perforation backpressure and model perforation flux relationship for the described three hydraulic pipe scenarios.

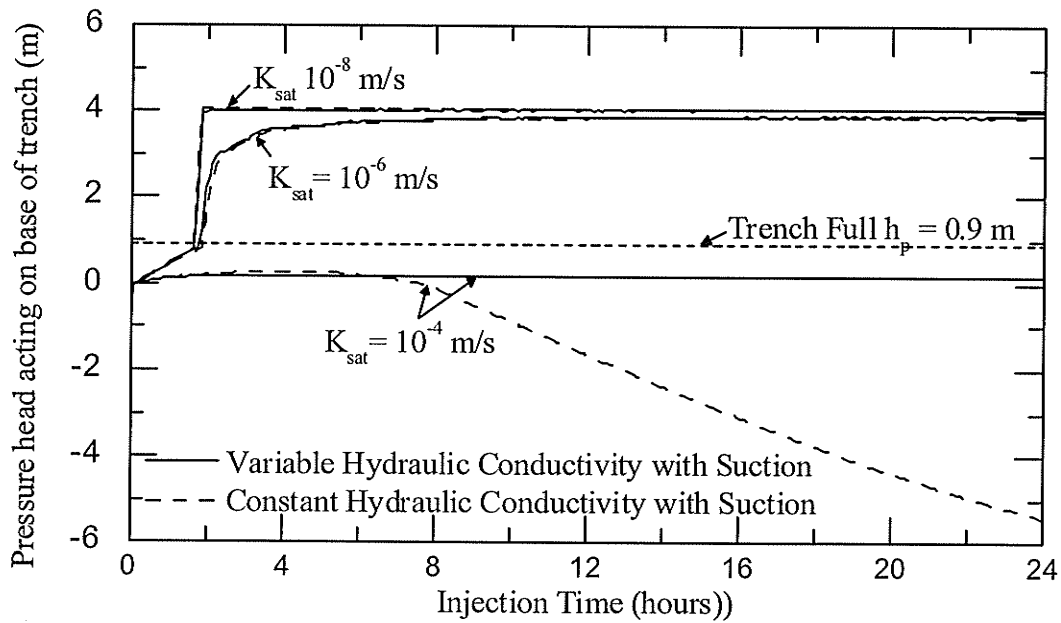


Figure 3.5: Baseline configuration pressure head increase at the trench base during liquid injection for refuse saturated hydraulic conductivities of 10^{-4} m/s, 10^{-6} m/s and 10^{-8} m/s with variable and constant hydraulic conductivity with suction.

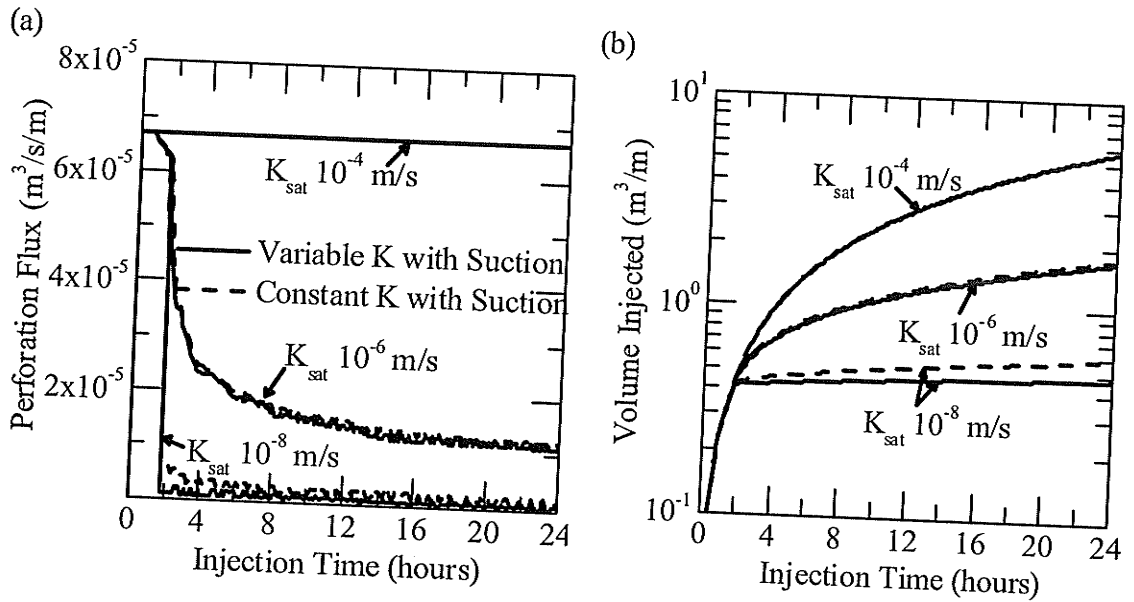


Figure 3.6: Deduced perforation liquid injection flux for baseline configuration (a) and cumulative volume of liquid (b) for simulated liquid injection for refuse saturated hydraulic conductivities of $10^{-4} m/s$, $10^{-6} m/s$ and $10^{-8} m/s$ with variable and constant hydraulic conductivity with suction.

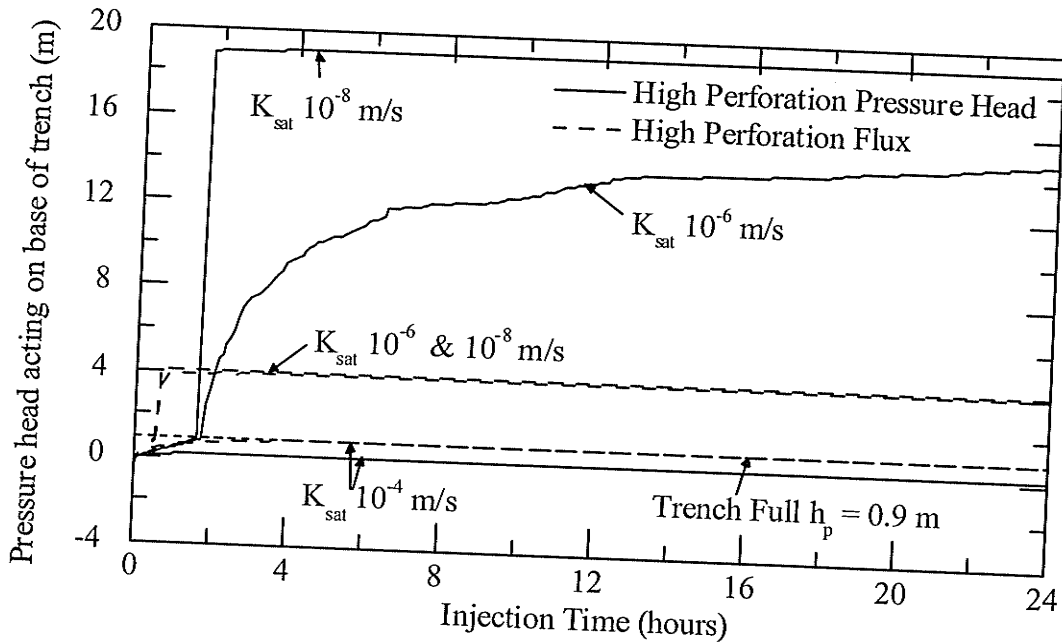


Figure 3.7: Pressure head deduced at the trench base during liquid injection for refuse saturated hydraulic conductivities of $10^{-4} m/s$, $10^{-6} m/s$ and $10^{-8} m/s$ with a high perforation flux and high perforation pressure head pipe configuration.

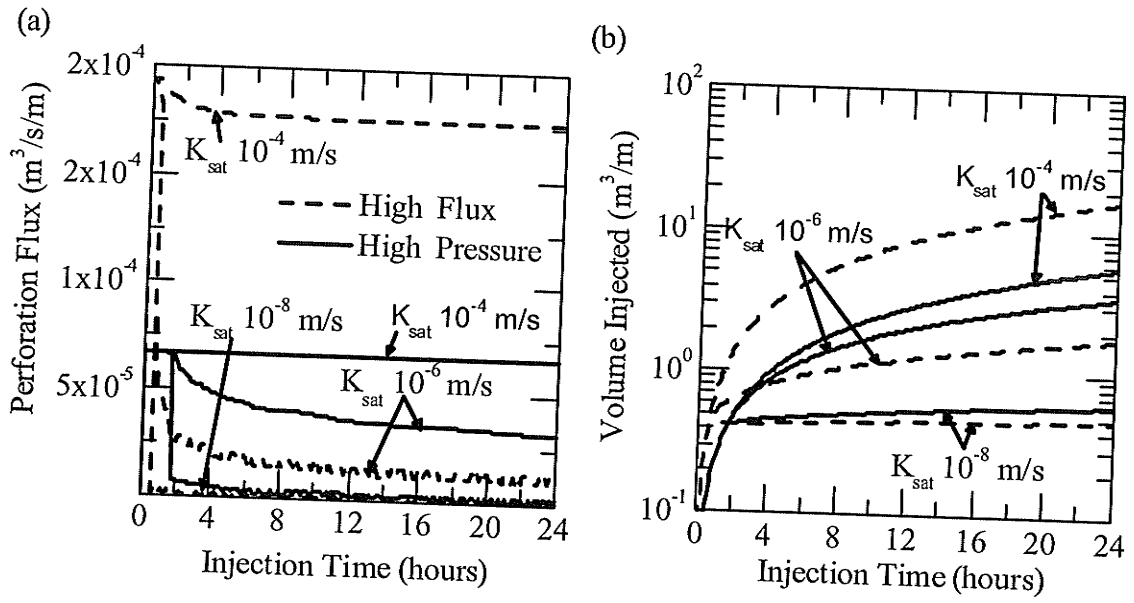


Figure 3.8: Deduced perforation liquid injection flux (a) and cumulative volume of liquid (b) for simulated liquid injection for refuse saturated hydraulic conductivities of 10^{-4} m/s , 10^{-6} m/s and 10^{-8} m/s for the high perforation flux and high perforation pressure head hydraulic scenarios.

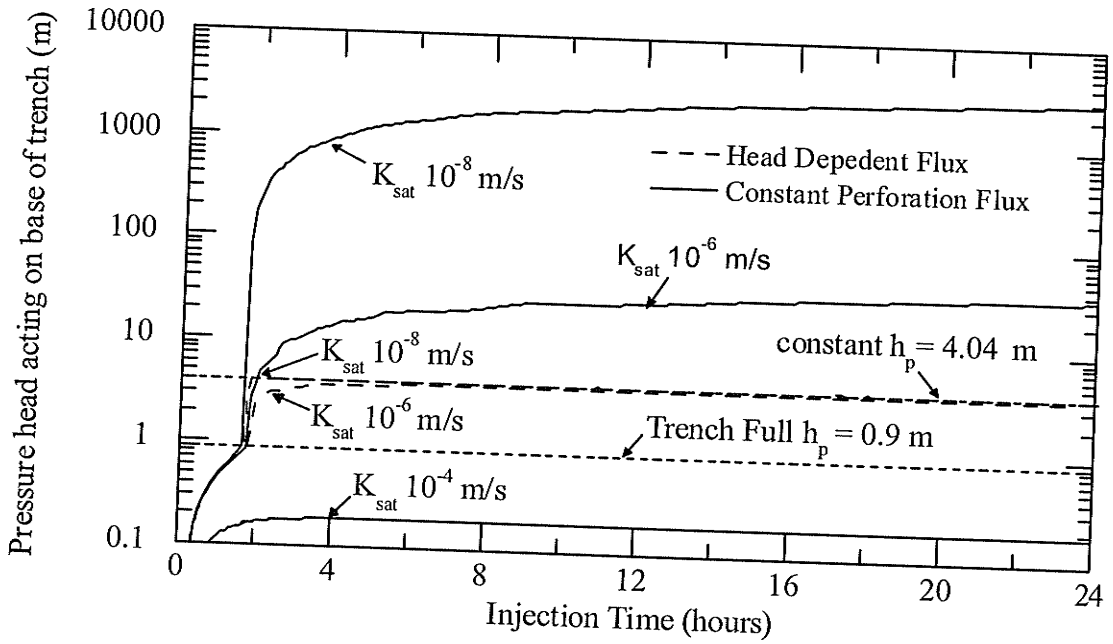


Figure 3.9: Pressure head deduced at the trench base during liquid injection for variable refuse saturated hydraulic conductivities of 10^{-4} m/s , 10^{-6} m/s and 10^{-8} m/s with a head dependent flux, constant flux, and constant pressure perforation hydraulic boundary condition.

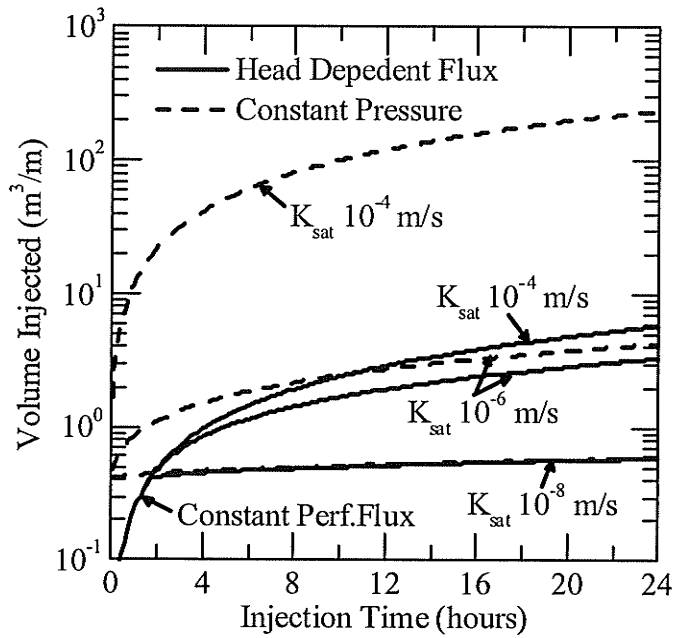


Figure 3.10: Cumulative volume of liquid for simulated liquid injection for refuse saturated hydraulic conductivities of 10^{-4} m/s, 10^{-6} m/s and 10^{-8} m/s for a head dependent flux, constant flux, and constant pressure perforation hydraulic boundary condition

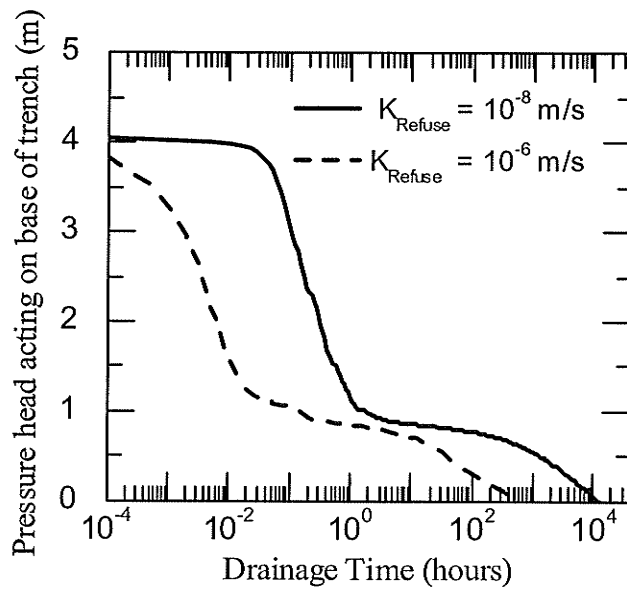


Figure 3.11: Deduced pressure head decrease at the trench base from liquid drainage into variable refuse hydraulic conductivities of 10^{-6} and 10^{-8} m/s for an 8 hour liquid injection schedule using the baseline pipe hydraulic configuration.

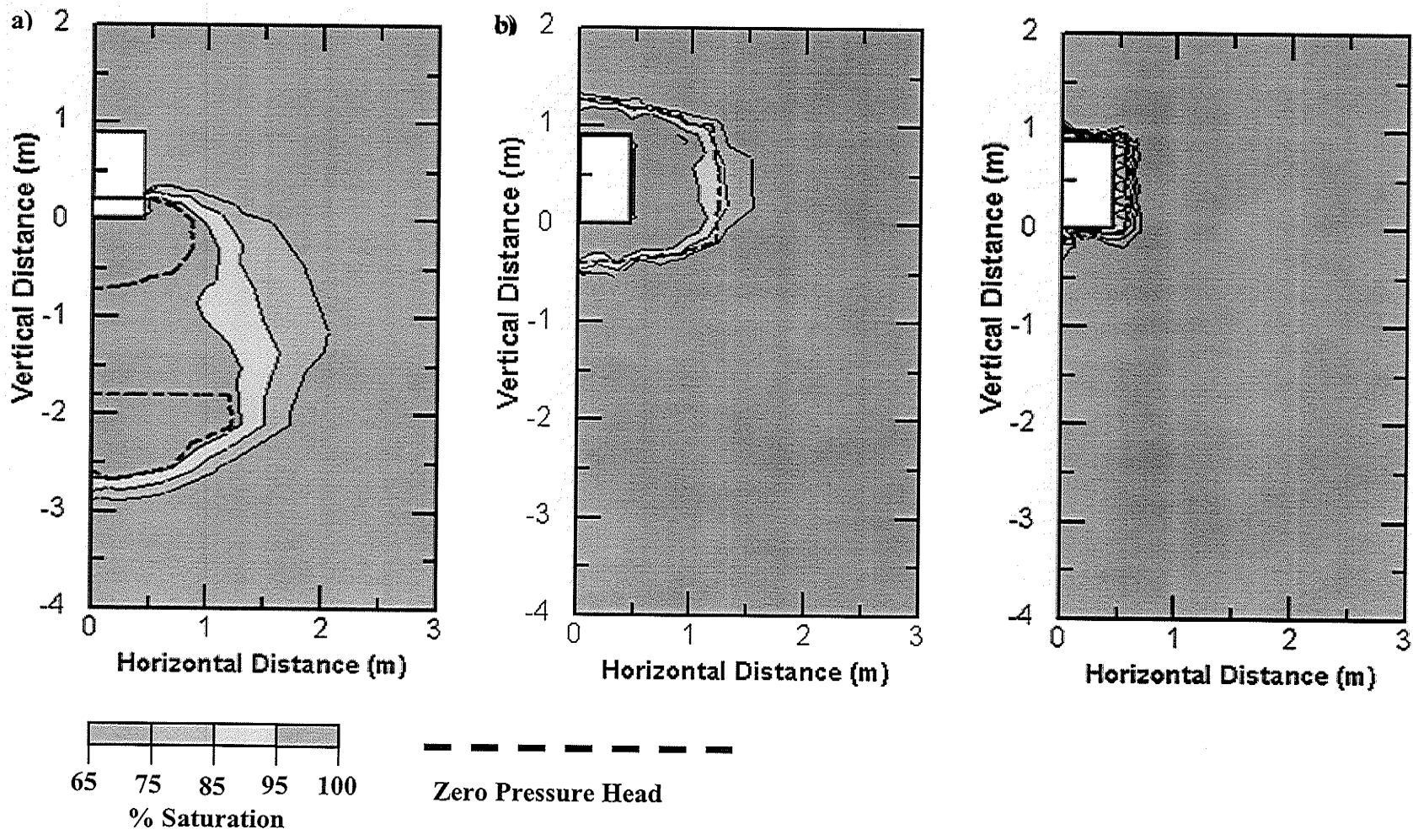


Figure 3.12: Developed zones of saturation after 8 hrs of liquid injection into a variable refuse hydraulic conductivity of a) 10^{-4} , b) 10^{-6} and c) 10^{-8} m/s hydraulic conductivity using the baseline pipe configuration.

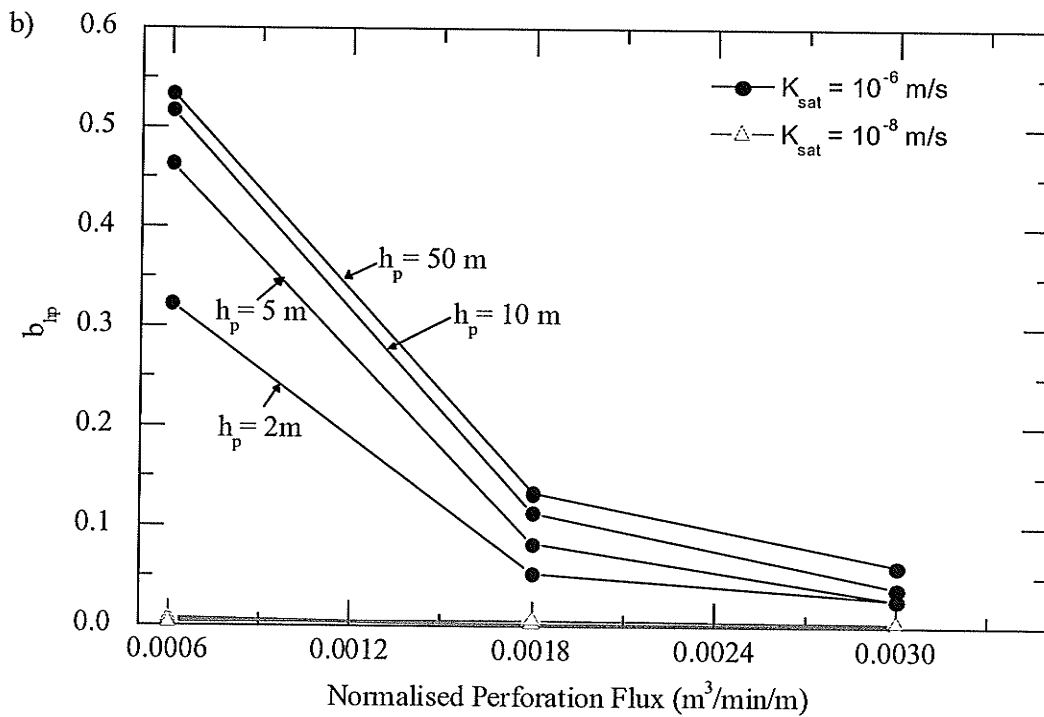
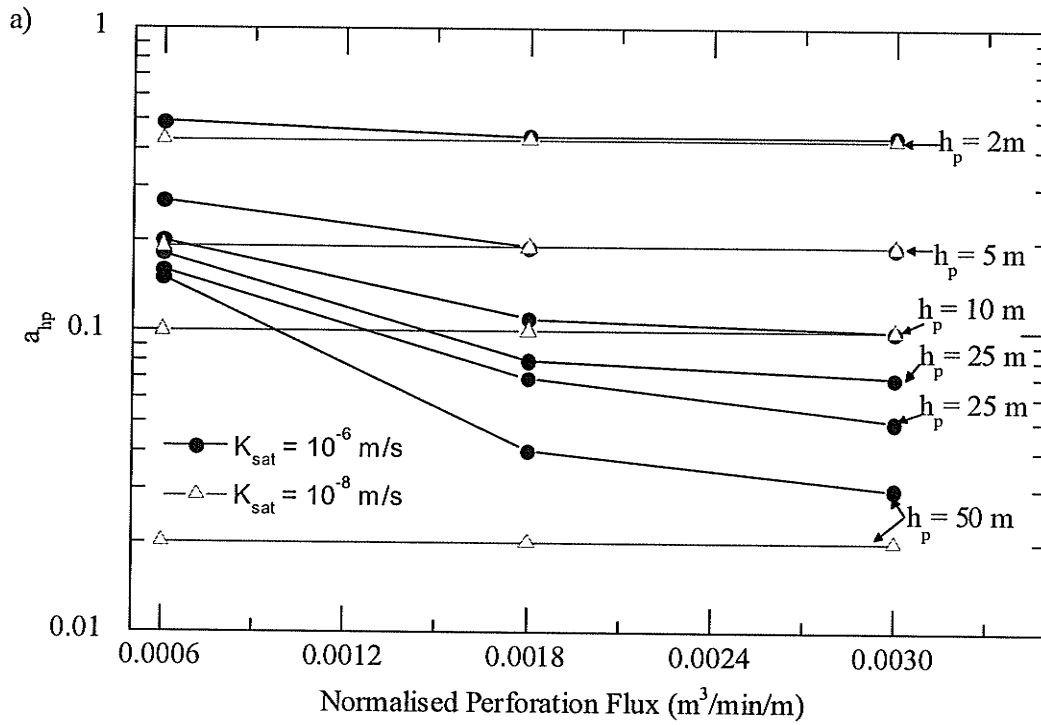


Figure 3.13: a_{hp} and b_{hp} pressure head development coefficients for liquid injection using range of inlet hydraulic head and normalised perforation flux with saturated refuse hydraulic conductivity of 10^{-6} and 10^{-8} m/s.

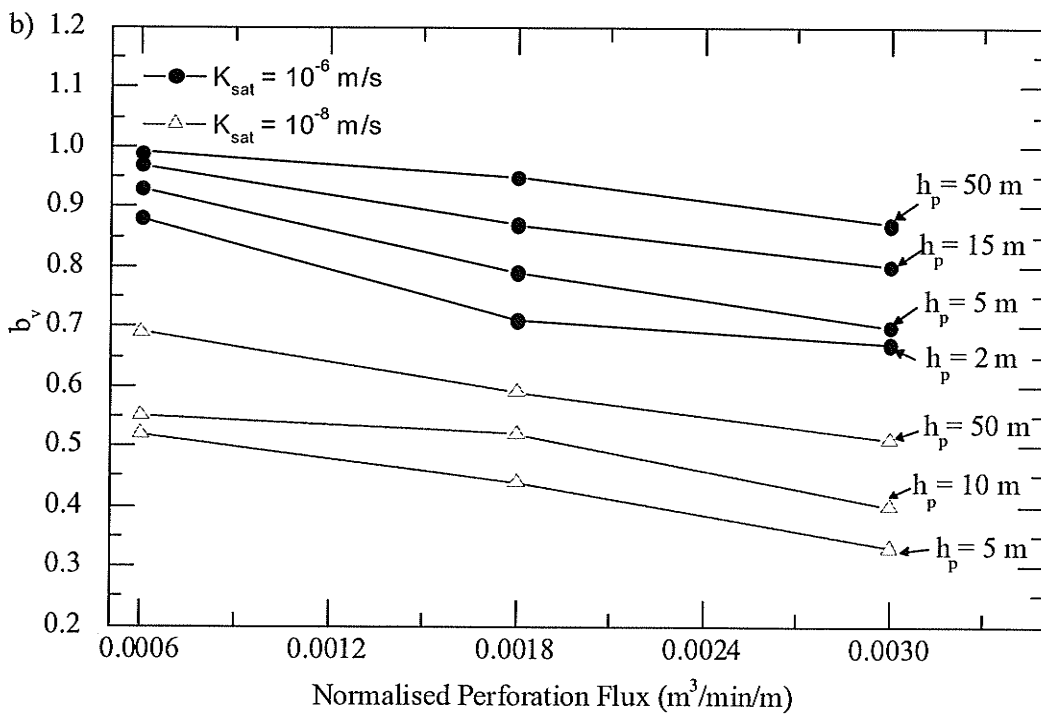
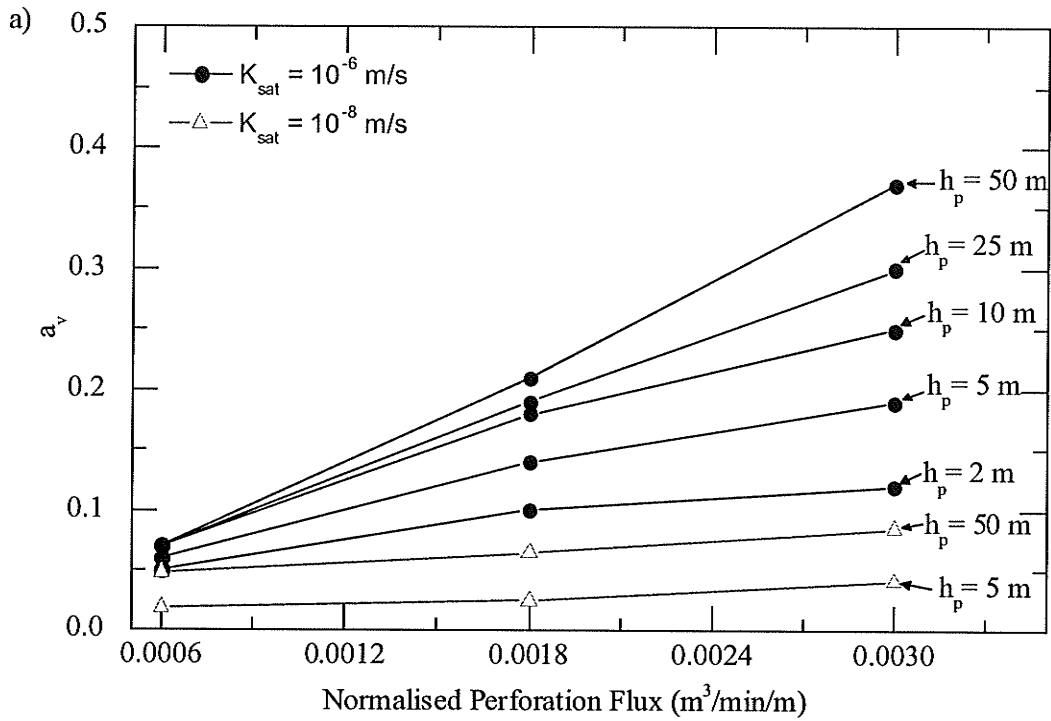


Figure 3.14: a_v and b_v liquid volume coefficients for liquid injection using range of inlet hydraulic head and normalised perforation flux with saturated refuse hydraulic conductivity of 10^{-6} and 10^{-8} m/s.

CHAPTER 4: BRADY ROAD LANDFILL WELL EXTRACTION TESTS

4.1 INTRODUCTION

In older dumps and landfills with no or clogged leachate collection systems a leachate mound will develop with time over any liners underlying the refuse. Additionally, soils with high silt or clay content that may be used as daily and intermediate cover for refuse can create low permeability horizontal layers upon which leachate can become perched and mound within the landfill cell. A high leachate mound poses several environmental dangers that include contamination of any underlying ground and surface water due to seepage through the landfill liner system and seep breakouts through landfill cover, respectively (Rowe and Nadarajah 1996). A high leachate mound can also compromise planned landfill gas extraction strategies and the overall slope stability of the landfill (Qian *et al.* 2002).

In order to safeguard the environment and maintain efficient and safe landfill operation, retrofitted leachate extraction wells may be installed to decrease and control the leachate mound height within a landfill cell (Rowe and Nadarajah 1996). Leachate extraction wells are constructed and operated similar to groundwater-extraction wells that aim to draw water out of an aquifer for drinking water or industrial purposes. Critical for effective well layout, design and operation is the selection of the well depth, screen length, extraction rate of leachate, and specific capacity (ratio of extraction rate to drawdown in the well). The hydraulic properties of the refuse, specifically, the refuse transmissivity, storativity and specific yield, are critical inputs to assess the performance (i.e., the ability to reduce leachate mound) of a specific extraction well design.

Laboratory test measurements to obtain refuse transmissivity and storage characteristics (i.e., storativity and specific yield) which rely on small sample sizes and idealized test conditions may yield results that are not representative of conditions within a landfill (Rowe and VanGulck, 2004). In situ measurements of refuse transmissivity and storage properties have been achieved by completing pump, slug, and falling head tests and applying analytical well hydraulic equations (e.g. Theis 1935, Boulton 1963, Cooper and Jacob 1946, Neuman 1972, Driscoll 1986). The use of pump and injection tests to measure hydraulic properties of a porous media and is an effective and commonly employed method for geological formations (Kruseman and de Ridder, 1994); however, the applicability of these methods to obtain refuse hydraulic properties may be limited due to the spatial and temporal heterogeneous composition of refuse (Fasset *et al.* 1994).

The first objective of this chapter is to investigate the movement of liquid and pressure drawdown responses with time in refuse through a large scale field pump and recovery test conducted at the Brady Road Landfill in Winnipeg, Canada. The second objective of this chapter is to assess the ability of conventional aquifer ground water analytical formulas to capture the measured spatial changes in water pressure within refuse during a pump and recovery test and also a slug test to deduce the bulk hydraulic properties of the refuse.

4.2 LEACHATE EXTRACTION WELL FIELD STUDIES

Field studies that have involved vertical leachate extraction wells have primarily consisted of measuring the ability of the wells to extract leachate from the saturated zone and to monitor the pressure responses within an extraction well and at any nearby piezometer(s). The pressure response data is then applied to conventional well analytical

formulas to deduce transmissivity (or hydraulic conductivity) and storage properties of the refuse. Summarized below are the test methodologies of four literature reported leachate extraction field tests.

4.2.1 Iowa Sanitary Landfills, United States, Hentges et al. (1993)

Hentges et al. (1993) measured the time drawdown measurements due to pumping within multiple extraction wells and piezometers at two different landfill sites in Iowa, USA. Additionally, four slug tests were completed at the second landfill site. The authors reported well specific capacities in three pump tests where the drawdown response had reached an equilibrium value at a constant pumping rate, and they were equal to 2.15, 8.94 and 9.48 m³/day/m. The refuse hydraulic conductivity from the slug tests was analyzed using the Bouwer and Rice (1976) method and ranged in value from 2×10^{-6} to 2×10^{-7} m/s. The transmissivity and storativity of the two landfill sites was analyzed using equations developed for a confined aquifer as it was hypothesised that landfill gas would create confining layers with the landfill. The deduced transmissivity and storativity values for a landfill with ten extraction wells ranged from 0.05 to 3.50 m²/day and 0.002 to 0.418, respectively. For a different landfill with five extraction wells the transmissivity and storativity ranged 0.0037 to 1.11 m²/day and 0.005 to 0.228, respectively (see Table 4.1).

4.2.2 Buckinghamshire and Cambridgeshire, England, Burrows et al. (1997)

A total of 54 short and long pump and recovery tests were conducted by Burrows et al. (1997) on twenty full penetrating and full screened wells and at four landfill sites located in England. The long term drawdown/recovery tests were conducted on a

triangular arrangement of three pumping wells and three piezometers. Termination of all the pump tests occurred when a quasi steady state drawdown response was obtained in the piezometers for the applied extraction rate. The pump test analysis completed included the Theis (1935), Cooper and Jacob (1946), Rorabaugh (1953), Boulton (1963), and Neuman (1975) methods. The deduced transmissivity and specific yield for three of the four landfills range from 0.3 to 21.8 m²/day and 0.092 to 0.15, respectively. Well specific capacity data enabled the prediction of sustainable leachate extraction rates for the three landfills and ranged from 6.0 to 19.2 m³/day for wells penetrating on average 14.5 m of saturated waste. The deduced transmissivity values and specific yield values for Site D were generally higher than the other three sites (see Table 4.2). The authors attributed the higher value at site D due to the absence of low permeability cover material, a lower waste thickness reducing the waste loading and density, and a less advanced rate of waste degradation. Table 4.2 summarizes the saturated depth, deduced transmissivity, hydraulic conductivity, specific yield, and sustainable yield for the extraction wells from Burrows *et al.* (1997).

4.2.3 Chianni Landfill, Pisa, Italy, Giardi (1997)

Giardi (1997) conducted pump and recovery on single wells and on a field test site of five wells at a landfill located in Italy. Two step-type pump tests of 24 hour duration were carried on two separate wells in order to further investigate well specific capacity and extraction rates. Drawdown data from the pump test was hypothesised to show features similar to an unconfined aquifer, and as such, the refuse transmissivity values were calculated using the Cooper and Jacob (1946) method for an unconfined aquifer. The specific capacity for one extraction well ranged from 0.50 to 0.90 m³/day/m;

meanwhile the second well displayed slightly higher well specific capacities and ranged from 1.71 to 4.80 m³/day/m. The deduced transmissivity for the single well tests ranged from 0.10 to 0.24 m²/day for extraction rates of 2.9 to 17.3 m³/day. The conducted tests at the trial station produced slightly higher values than the single well tests for transmissivity and they ranged from 0.29 to 0.50 m²/day. Table 4.3 summarizes key characteristics of the pump tests conducted by Giardi (1997).

4.2.4 New Jersey, United States, Oweis et al. (1990)

A test well penetrating about 30 m of refuse was installed at landfill located in Northern New Jersey by Oweis et al. (1990). Drawdown measurements were made at the extraction well and at three observations wells located at distances of 9, 22, and 61 m away from the extraction well. The refuse transmissivity was analyzed by the non-equilibrium methods of Theis (1935) and Boulton (1963) and also the straight line solution of Jacob (1946). One pump test consisted of pump duration of one day at an extraction of 109 m³/day and the deduced transmissivity was equal to 19.6 m²/day. Another pump test was conducted for duration of two and a half days at an extraction rate of 65 m³/day and the deduced transmissivity was equal to 7.9 m²/day.

4.3 THEORETICAL BACKGROUND INFORMATION

If the refuse hydraulic properties are known, analytical and numerical modeling of fluid flow to an extraction well can be used to assess the performance of extraction wells. Rowe and Nadarajah (1996) presented the only analytical technique for estimating average leachate drawdown between two extraction wells within a landfill. Their method is useful in design to select required well spacings, but subject to the following

assumptions and limitations: assumed steady-state flow conditions; the horizontal and vertical hydraulic conductivity of the waste is spatially and temporally constant; and negligible influence of daily soil cover between waste lifts. Lack of the latter condition could provide preferential flow paths and barriers for fluid flow to an extraction well. Powrie and Beaven (1999) numerically modeled steady-state leachate flow to an extraction well, but considered spatial changes in waste hydraulic conductivity due to changes in effective stress using a laboratory-derived empirical correlation from tests completed on fresh waste with no daily cover. Al-Thani *et al.* (2004) extended Powrie and Beaven's (1999) work to numerically model transient leachate flow to an extraction well. The use of analytical and numerical methods to assess the potential performance of extraction wells is still highly dependent on the selection of the refuse hydraulic conductivity and it is advisable to obtain the in situ refuse hydraulic through field techniques.

4.4 BRADY ROAD FIELD STUDY

The hydraulic properties of refuse at the City of Winnipeg's Brady Road Landfill were deduced by completing a field pump test. The Brady Road Landfill is a 790- hectare Class 1 Solid Waste Disposal facility that opened in 1973 and currently holds 5 million metric tonnes of municipal solid waste (MSW) (City of Winnipeg 2007) Figure 4.1 provides a schematic of the extraction well and piezometer layout for the field test. Two leachate-extraction wells were installed into the waste two meters apart – one at a depth of 8.8 m and the other at a depth of 4.6 m below the ground surface. Polyvinyl chloride (PVC) well casing and well screen was used. The well bore had a diameter of 203 mm (8 inches) with a well casing diameter of 102 mm (4 inches). The screened portion of each

well were backfilled with pea gravel and the remainder of the bore was filled with bentonite pellets to act as an impermeable seal. The selected well casing and borehole diameters are within the range of reported values for field extraction wells studies conducted by Dussek *et al.* (1994), Oweis *et al.* (1990), and Giardi (1997). The well screen length was 2 m in length and had a screen size aperture size equal to 0.254 mm (0.01 inches). Three nested piezometers made from schedule 40 PVC pipe of diameter 50.8 mm (2 inches) with a screen length of 0.6 m (2 feet), each located one meter apart, was installed within the refuse to target depths of, 3.0 m, 6.1 m, and 9.1 m below ground surface (see Table 4.4: for a complete summary of the elevations and depths of the wells and piezometers). Nested piezometers were installed at radial distances of 1, 3, 10, 21, and 35 m from the extraction well along one transect, and at 1 and 3 m along a different transect (see Appendix C for the layout of the test site). A total of twenty one piezometers were installed, each completed within a 102 mm (4 inches) bore diameter. The well and piezometers bores were drilled using a spiral drill auger. The general landfill composition observed from auger drilling consisted of a 0.6 to 1 m clay cap material (Figure 4.3a) followed by a mixture of waste (plastic bags, paper, etc..) and clay materials. Once a liquid level was observed in the boreholes the waste composition was consisted of a grayish to black high moisture slurry material (Figure 4.3b). A high permeability geotextile sock was placed over the screened portion of all the piezometers in order to minimize the intrusion of fine sand particles into the well screen. In order to ensure hydraulic connectivity between the surrounding refuse and only the screened portion of piezometers, the borehole was backfilled with silica sand up to piezometer

screen and the remainder of the borehole was filled with bentonite pellets to act as an impermeable seal.

Liquid was removed from the extraction wells using a Grundfos Redi-Flo2[®] 0.051 m (2 inch) diameter stainless steel submersible pump. The pump intake area location was designated to be equal to 0.3 m above the bottom well elevation for all pump tests. The pump was powered by gasoline generator and the flow rate was regulated by a Baldor[®] Series 15H variable frequency controller capable of achieving an extraction rate range of 0.1 to 49.1 m³/day. The time-dependent changes in fluid pressure in the refuse during pumping were deduced by measuring the change in fluid level in each piezometer and extraction well. Pressure transducers (Diver[®] DI 243 by Van Essen Instruments) were used to monitor liquid level in the wells and nearby piezometers (depicted in Figure 4.1) and a water-meter tape at all locations. The pressure transducers automatically measure (range of +/- 3.0 cm of water) and register liquid levels within a piezometer and extraction well at a minimum sample rate of 0.5 seconds for up to a total of 24,000 data readings over the duration of the pump test.

4.4.1 Field Study Hydrogeology

Figure 4.2 displays the averaged static (not influenced by leachate extraction from pumping) liquid elevations from three piezometers depths in the landfill (3.0 m, 6.1 m and 9.1m) with transect radial distance away from the extraction wells for a monitoring period of approximately 109 days. The average liquid elevation near the extraction well indicate that there is a downward vertical gradient with depth within the landfill. A possible explanation for a vertical gradient with depth could be the presence of low

permeability horizontal layers that limit the vertical migration of liquid infiltration to greater depths in the landfill. Liquid recharge through the temporary landfill cover is likely the cause for the vertical gradient to be maintained at the test site location. The test site is located at an intermediate flat elevation with a gradual increase (approximately 10 m) in the landfill cell elevation at an approximate distance of 100 meters North of the field site (see Figure 4.4). Thus, liquid could be moving laterally from the higher elevation in the landfill cell to the well location through horizontal waste layers.

4.4.2 Leachate Extraction Pump and Slug Tests

Two pump tests were completed on well W1. Test 1 was conducted on May 26/06 for duration 135 minutes, and Test 2 was performed on June 21/06 for duration of 767 minutes. Full recovery of leachate levels was obtained before start of Test 2. For both tests the well extraction rate and well specific capacity (ratio of extraction rate to drawdown in the well) of the well decreased with time over the duration of the tests (see Figure 4.5a and b, respectively). A decrease in the well extraction rate with time can be attributed to an overall decrease in the pump driving hydraulic head. A decrease in the pump driving hydraulic head with time is a result of drawdown within the extraction well. The well extraction rate for Test 1 had an initial value of 4.9 m³/day and decreased to 3.8 m³/day at the end of pumping, and the well specific capacity had an initial value of 6.8 m³/day/m and decreased to 4.4 m³/day/m at the end of pumping. For Test 2 the well extraction rate had a higher initial value of 6.7 m³/day and decreased to 2.5 m³/day at the end of pumping, and the well specific capacity had an initial value of 4.4 m³/day/m and decreased to 1.1 m³/day/m at the end of pumping.

A pump test on W2 was attempted however the initial rate of drawdown in the extraction well resulted in the liquid elevation to go below the intake of the submersible pump within about 9 minutes after pumping. The quick rate of drawdown and the lack of a large driving head (1.4 m) resulted in an unsustainable extraction rate for the available pump and variable controller system employed.

In addition to pump tests conducted on the wells, fourteen slug removal tests were conducted on select piezometers. The submersible pump used for the pump test was also used to quickly remove liquid from piezometers located at 6.1 m and 9.1 m depths. Slug tests were not conducted on the 3.1 m depth piezometers since there was not a sufficient liquid level rise in the piezometers to conduct a slug test.

4.4.3 Pump and Recovery Test Pressure Behaviour

The drawdown pressure responses during pumping and recovery (Test 1 and Test 2) for 9.1 m deep piezometers at radial distances of 1 m (P1A), 1.4 m (P6A), 3 m (P2A), and 3.2 m (P7A) are displayed in Figure 4.6 and Figure 4.7, respectively. Table 4.5 summarizes the maximum drawdown response that occurred within the 3.0 m (PC), 6.1 m (PB), and 9.1 (PA) deep piezometers during pump duration for Test 1 and Test 2. The 9.1 m deep piezometers located at radial distances of 10 to 35 m did not experience any significant drawdown responses (less than 5 cm of drawdown) during pumping. As such, the pressure response measured from the 9.1 m deep piezometers located at radial distances of 1 to 3.2 m provided data that were used for analysis and discussion on the refuse hydraulic pressure behaviour due to pumping and recovery. Provided below is a summary of observed trends on the drawdown pressure responses within the 9.1 m deep piezometers e for each pump tests.

- The maximum measured drawdown responses for Test 1 of 0.3 m (in P1A) was significant lower than Test 2 which had a maximum drawdown response of 1.14 m (in PA). The larger drawdown responses for Test 2 than Test 1 is likely a result of the higher initial extraction rate (6.7 m³/day to 4.9 m³/day) and longer duration (767 minutes to 135 minutes) of pumping in Test 2 when compared to Test 1 respectively.
- Measured pressure responses located at a close radial distances (1.0 m (P1A) and 1.4 m (P6A)) from the extraction well experienced an immediate (i.e., within 1 to 3 minutes) drawdown response; meanwhile, the piezometers located further away (3.0 m (P2A) and 3.2 m (P7A)) from the extraction well averaged a lag time of 30 to 60 minutes for Test 1 and Test 2 respectively before a pressure response occurred.
- For Test 2, piezometers near the extraction well (P1A and P6A) experienced a very quick and large drawdown of approximately 0.30 m in the first 15 minutes of pumping. For piezometers located further away from the extraction well (P2A and P7A), a more gradual and constant pressure response was observed through out the duration of the pump.
- After the described quick and large drawdown response for Test 2, P1A and P6A the piezometers experienced minimal drawdown pressure responses for approximately 10 to 15 minutes. The lack of pressure response is observed as a flat segment on the pressure response with time graph.

The immediate pressure response and larger rate of initial drawdown in the piezometers located near the extraction well, and the lag response time and more constant drawdown increase in piezometers located further away from the well is analogous to the theoretical short term pressure of an aquifer response to pumping. Theoretically, a cone of depression from the extraction well will develop fairly rapidly after pumping begins since liquid is initially released from storage; however, as pumping continues the expansion and enlargement of the cone of depression decreases since a larger volume of stored liquid becomes available. The intermediate minimal pressure response that occurred during pumping and the subsequent increase in drawdown is commonly observed in unconfined aquifer systems. A minimal drawdown response during pumping in an unconfined aquifer generally occurs when the effects of gravity drainage from overlying pores becomes dominant, this process is often referred to as a delayed yield response. Eventually at later times the effects of gravity drainage will be minimized and the rate of drawdown will begin to increase. The described delayed yield response of unconfined aquifer has also been documented (Muldoon and Bradbury 2005, Horgan 1996) to be similar to a dual porosity soil system. A dual porosity systems is defined as where there are overlapping reservoirs which interact hydraulically

Once pumping had stopped, the recovery response in all the piezometers generally exhibited: a lag time (5 to 24 minutes) of little to no recovery, and then a fairly linear recovery response that approached its original static elevation. The liquid level recovery in the piezometers approached its original static levels in approximately 0.3 and 5,070 minutes for Test 1 and Test 2, respectively.

Unlike the piezometers installed at a greater depth of 9.0, the shallow piezometers of 3.0 and 6.1 m depth at close radial distances of 1 m and 1.2 m measured minimal drawdown response during pumping (see Table 4.5). The apparent lack of hydraulic connectivity between the 9.0 m and 6.0 m deep piezometers, as indicated by a minimal drawdown in the 6.0 m deep piezometers, could be caused by the presence of low permeability horizontal layers within the landfill created by daily and intermediate clay cover material commonly used at this landfill or a decrease in refuse hydraulic conductivity with depth in the landfill. It has been reported by McCreanor and Reinhart (2002) that low permeability layers within a landfill could limit the downward movement of liquid and cause perched liquid elevations to move laterally along the low permeability layers.

4.4.4 Refuse Hydraulic Properties Method of Analysis

The collected drawdown and recovery pressure responses from the pump and slug tests were used to deduce the refuse transmissivity and hydraulic conductivity, storativity, and anisotropy using conventional well hydraulic analytical equations. An analytical equation for an unconfined refuse aquifer system was selected for the pump tests since the drawdown pressure responses resembled the theoretical behaviour of an unconfined aquifer and is consistent with the method employed by Giardi (1997) and Burrows *et al.* (1997) to assess refuse hydraulic properties. Additionally, a dual porosity pressure analytical equation was also selected to analyze the pump test data as it was hypothesised that a dual pressure response could be possible. Two widely used analytical methods for recovery analysis and slug test removals were utilized to analyze the recovery and slug test data. AQTESOLV[®], an aquifer test analysis software program, was used to solve the

various selected analytical equations. Provided below is a summary of the methods utilized to analyze the drawdown/recovery data from the pump and slug tests.

4.4.4.1 Neuman (1974) Unconfined Aquifer Drawdown Pumping Response

The average water level readings (see Figure 4.2) and bottom elevation measurements (see Table 4.4) and a well screen length of 2 m indicate that both extraction wells can be considered as partial penetrating since each do not extended the full saturated thickness of the refuse. It is assumed that refuse could occur as a result of previous laboratory studies (Landva *et al.* 1998, Hudson *et al.* 1998, Hudson *et al.* 1999) have measured a refuse anisotropy ratio of a larger horizontal (K_H) to vertical (K_V) saturated hydraulic conductivity. Neuman's (1974) solution for an unconfined anisotropic aquifer was selected as it can incorporate the added complexity of partial well penetration and refuse anisotropy. This method of analysis requires an assessment of the refuse-saturated thickness, which can be a difficult parameter to evaluate when the extraction wells and piezometers screen lengths do not complete penetrate the aquifer. The chosen refuse saturated thickness of 2.9 m was deduced as the average of the difference between the average liquid elevations and the bottom 9.1 deep piezometer elevations at a close radial distances (1 to 10 m) near the extraction well. The approach of selecting the 9.1 m deep piezometer liquid elevation rather than the 6.1m deep piezometer was based the observed lack of hydraulic connectivity between the two piezometers during the pump test. Additionally it should be noted that the state approach for selecting the refuse saturated thickness does not account for the saturated thickness extending below the bottom of the piezometers.

4.4.4.2 Moench (1984) Dual Porosity Drawdown Pumping Response

Pump test analyses using dual porosity models are normally incorporated in situations where one aquifer is hydraulically connected to another water source or aquifer or in fractured rock aquifer systems. Zeiss and Major (1993) and Zeiss and Uguccioni (1995) suggested that liquid flow through refuse could be analyzed as a dual porosity model. They hypothesized that compacted refuse consists of large objects with large pore spaces that have an outer envelope (plastic bags, etc.), and that within the outer envelope there are smaller particles with smaller pore sizes. Additionally, Kazimoglu *et al.* (2006) stated that the presence of large pores in refuse may make the use of conventional flow models that were designed for soils with a particular pore structure and pore size distribution inappropriate. The Moench (1984) dual porosity equation with spherical shaped blocks was selected as another method to analyse the measured drawdown response. The Moench (1984) equation provides a solution for storativity and transmissivity for two geological media that could be representative of large and small refuse particle sizes. There has been a very limited amount of literature reported values on the average particle size of refuse (Zeiss and Major 1993, Nakamura *et al.* 2005) and as such a representative range of 0.1 m to 1 m for the diameter of the spherical blocks parameter was selected for the analysis. Moench (1984) does not account for anisotropy and assumes complete extraction well penetration. The saturated thickness was selected as 2.9 m (see previous section for explanation).

4.4.4.3 Theis (1935) Recovery Analysis

The Theis (1935) method which assumes an exponential recovery response has been commonly used to analyze recovery tests, and was also employed by Burrows *et al.*

(1997) and Giardi (1997) to deduce refuse hydraulic characteristics. The Theis (1935) recovery method is based on the principle of superposition that creates a solution for the residual drawdown from the summation of image wells. The Theis (1935) method is generally used for confined aquifer systems however it can be applied to unconfined aquifer systems and in partially penetrated extraction wells if a set of conditions on the pump and recovery times are satisfied. However, the Theis (1935) recovery method does not account for anisotropy. Kruseman and de Ridder (1994) stated that the Theis recovery method can be used for partial penetrating wells only if the pumping is of sufficient duration so that the following criterion by Uffink (1982) is achieved

$$t_p > 10D^2S/T \quad [4.1]$$

where t_p is the pumping time, D is the saturated aquifer thickness, S is the aquifer storativity and T is aquifer transmissivity.

Using the and reported ranges for refuse storativity, transmissivity, and saturated thickness by Hentges *et al.* (1993) Burrows *et al.* (1997), Giardi (1997) and Oweis *et al.* (1990) the suggested criterion for pumping time by Uffink (1982) was significantly violated for Test 1 and it was decided to analyze the recovery data for Test 2 only. Additionally, using the deduced values for refuse storativity and transmissivity values from the Neumann (1974) solution also resulted in a significant violation of Uffink (1982) criterion for pumping time for Test 1.

4.4.4.4 Bouwer and Rice (1976)

The Bouwer and Rice (1976) solution for a slug test was used to analyze the pressure response in an unconfined aquifer as a result of an instantaneous withdrawal of liquid from a piezometer. The Bouwer and Rice (1976) unconfined aquifer method was

selected because it could be directly compared to the conventional pump tests analysis using the unconfined method of Neuman (1974). Additionally, the pump study by Hentges *et al.* (1993) also utilized the unconfined method of Bouwer and Rice (1976). In order to maintain consistency with the other analysis, the saturated aquifer thickness of 2.9 m was selected (see Neuman (1974) section for previous explanation).

4.4.5 Deduced Refuse Hydraulic Properties

Figure 4.8 displays an example of the solution fit to the collected drawdown data for the a) Neuman (1974) and the b) Moench (1984) analytical equation, respectively. Both the Neuman (1974) and Moench (1984) methods fit the drawdown data very well for all the selected piezometers. Additionally, both solutions were able to reasonably simulate the observed early and long term pump response behaviour for piezometers located near the extraction well (see Appendix D for model fits for all piezometers).

Figure 4.9 and Figure 4.10 display an example of a solution fit to the collected pump and slug recovery data for the Theis (1935) and Bouwer and Rice (1976) analytical equations, respectively. Due to the inherit nature of the solution of the Theis (1935) recovery solution which assumes a logarithmic type recovery behaviour it was unable to simulate the observed initial lag recovery time or the recovery approach at or near the static elevation. The Bouwer and Rice (1976) method successfully reproduced the early and late time pressure response for all the slug tests; however, in certain circumstances the magnitude of the initial displacement (h_0) was underestimated.

The deduced values for refuse transmissivity, specific yield, storativity, and anisotropy ratio using the Neuman (1974) solution for an unconfined aquifer are

displayed in Table 4.6. The deduced values for refuse transmissivity and storativity using the Theis (1935) recovery method are displayed in Table 4.7. Table 4.8 displays the summary of deduced refuse transmissivity and storativity for two geological mediums using the Moench (1984) dual porosity solution and two-selected diameter of spherical blocks. Finally, Table 4.9 provides a summary of the deduced values for refuse transmissivity using the slug test method of Bouwer and Rice (1976) for an unconfined aquifer.

4.4.5.1 Transmissivity

Provided bellow is a summary of the deduced values and observations of the refuse transmissivity using the analytical methods of Neuman (1974), Moench (1984) Theis (1935) and Bouwer and Rice (1976):

- Neumann (1974) solution and Test 2 drawdown data deduced a transmissivity that ranged from 0.18 to 0.77 m²/day. The deduced transmissivity values lie within the range reported by Hentges *et al.* (1993), Giardi (1997), and in the lower end range reported by Burrows *et al.* (1997).
- Moench (1984) solution produced an overall transmissivity range of 0.21 to 0.96 m²/day for both geological media. One geological medium generally produced higher transmissivity values when compared to the other; the higher transmissivity medium could be representative of refuse with large particles sizes.
- Theis (1935) recovery method resulted in a higher transmissivity range of values (1.97 to 9.65 m²/day) than the Neuman and Moench pump test solutions. A possible explanation for the larger transmissivity values in the recovery tests could be due to effects of liquid recharge. The lateral movement of liquid from the higher

cell elevation to the extraction well and nearby piezometers could have resulted in a shorter recovery period than expected (without recharge effects) and also an overestimation of refuse transmissivity using the Theis (1935) solution.

- The Bouwer and Rice (1976) slug test method deduced a wide range of transmissivity (0.01 to 6.81 m²/day), a large deduced transmissivity range for the slug tests is most likely due to a combination of the heterogeneity of refuse and inherent limitation of the slug test method. A slug test removes a small volume of liquid instantaneously from a piezometer and therefore the hydraulic properties can be estimated in only the area immediately surrounding the piezometer.
- The transmissivity from piezometers at a depth of 9.1 m generally had a lower transmissivity value when directly compared to the 6.1 m depth piezometers (see Figure 4.11). The phenomena of a decreased transmissivity with depth at a landfill has been reported (Burrows *et al.* 1997, Jain *et al.* 2006) and investigated in the laboratory by (Zeiss and Major 1993, Beaven and Powrie 1995, Powrie and Beaven 1999). The decrease in transmissivity with depth is mostly likely due to a decrease in the refuse void spaces and hence available flow paths for liquid flow.

4.4.5.2 Storativity and Specific Yield

From the drawdown methods of Neuman (1974) and Moench (1984) and recovery method of Theis (1935), the majority of the storativity values were in the range of 10⁻¹ to 10⁻³, and the overall median was equal to 2 x 10⁻². The deduced storativity range encompass the range in values (4 x 10⁻¹ to 2 x 10⁻³) reported by Hentges *et al.* (1993). Freeze and Cherry (1979) discussed the overall difficulty in accurately estimating the storativity parameter, and using a range of values for storativity is acceptable practice.

Only two piezometers near the extraction well P1A and P6A for Pump Test 2 produced late drawdown behaviour analogous to an unconfined aquifer response, and the deduced values of specific yield using the Neuman (1974) unconfined aquifer method for the two piezometers was equal to 0.13 (for P1A) and 0.14 (for P6A). The two values of specific yield are within the range (0.09 to 0.16) reported by Burrows *et al.* (1997).

4.4.5.3 Anisotropy

The deduced anisotropy ratio of horizontal (K_H) to vertical (K_V) saturated hydraulic conductivity from Neuman (1974) ranged from $K_H = 0.03K_V$ to $K_H = 0.19K_V$. A higher vertical than horizontal hydraulic conductivity ratio differs from laboratory tests on refuse that have reported horizontal to vertical saturated hydraulic conductivity ratios of 8 (Landva *et al.*, 1998) and 2 to 5 (Hudson *et al.*, 1999). A possible explanation for the differences in refuse anisotropy is the presence of vertical flow components before and during the pump test. The Neuman (1974) analytical solution assumes that the liquid levels within the landfill are hydrostatic before pumping, however this is not the case at field study location where a vertical gradient has been observed. The Neuman (1974) solution is able to account for vertical flow components during pumping by generating individual type curves for each set of piezometer datasets; however, there is a possibility that the summation of vertical flow effects from the initial vertical gradient and partial penetration were so great that it resulted in a large underestimation of the horizontal to vertical hydraulic conductivity anisotropy ratio.

4.5 DESIGN IMPLICATIONS

The ability of a vertical well extraction system to successfully decrease and control a leachate mound requires careful selection of the well extraction rate, well depth location, and well screen length. For example, the selection of a large well extraction rate in a deep landfill representative of a low refuse transmissivity could result in a low volume of a leachate extracted and minimal leachate mound decrease due to a quick dewatering of the well. A large extraction rate is more appropriate at a well depth near the landfill surface where a larger refuse transmissivity can be expected. The selection of the well screen length should take into account the type of leachate mound that has developed. For example, a small well screen length may not be appropriate if numerous perched leachate mounds have developed with depth in a landfill. The selection of a small screen length may be preferable in situations where concentrated leachate outbreaks from preferential flow paths have been observed.

The measured drawdown pressure response at the Brady Road Landfill site was best simulated using the analytical unconfined aquifer method of Neuman (1974). The analytical technique of Neuman (1974) has potential to be used as a design aid in the selection of the well extraction rate, well size and screen length, well sizes and spacing intervals, however one must have an understanding of the expected refuse hydraulic properties specifically the refuse transmissivity. Additionally if the landfill hydrogeology consists of noticeable vertical gradients or liquid recharge processes the use of a numerical extraction flow model as a design tool could be more appropriate than using the analytical technique of Neuman (1974).

4.6 CONCLUSIONS

Large-scale pump tests and slug removal tests were conducted at the Brady Road Landfill, in Winnipeg, Manitoba. Leachate was extracted from two wells, the pressure responses were monitored in an array of piezometers. Additionally, the well extraction rate and well specific capacity were measured. A lack of pressure responses in piezometers located at shallower depths than the extraction well screen indicate the possible presence of low permeability layers that limit the vertical migration of fluid. Measured drawdown responses from pump tests were accurately simulated using the unconfined method of Neuman (1974) and the double porosity aquifer model of Moench (1984). The analytical methods of Theis (1935) and Bouwer and Rice (1976) simulated the general recovery behaviour trends however they were both unable to accurately simulate the measured pressure recovery responses that occurred after a pump test and slug test respectively. The deduced transmissivity and storativity from all the selected analytical methods ranged from 0.16 to 9.65 m²/day and the storativity ranged from 10⁻¹ to 10⁻³. Additionally the Neuman (1974) solution deduced two values (0.13 and 0.14) for refuse specific yield and horizontal to vertical hydraulic conductivity anisotropy ratios in the range of 0.04 to 0.19. The deduced anisotropy ratios differ from literature reported values possibly due to large vertical flow components.

4.7 REFERENCES

- Al-Thani, A.A., Beaven, R.P. and White, J.K. 2004. Modelling flow to leachate wells in landfills, *Waste Management*, 24:271–276.
- Boulton, N.S. (1963). Analysis of data from non-equilibrium pumping tests allowing for delayed yield from storage, *Ins. Civil Engineers Proc.*, 26:469-482.
- Bouwer, H. and R.C. Rice, (1976) A slug test method for determining hydraulic conductivity of unconfined aquifers with completely or partially penetrating wells, *Water Resources Research*, 12(3):423-428.
- Burrows, M.R., Joseph, J.B. and Mather, J.D. (1997) The hydraulics of in situ landfilled waste, *Proceedings Sardinia 97, Sixth International Landfill Symposium*, S. Margherita di Pula, Cagliari, Italy.
- City of Winnipeg (2007) Department of Water and Waste Website, <http://www.winnipeg.ca/waterandwaste/garbage/bradyroad.stm> ,updated May 18,2007.
- Cooper, H.H. and Jacob, C.E. (1946) A Graphical method for Evaluating Formation Constants and Summarizing Well Field History, *Am. Geophys. Union Trans*, 27:526-534.
- Driscoll, F.G. (1986) *Groundwater and Wells 2nd Edition*, Johnson Division, St Paul, Minn, USA.
- Dusseck, C., Long, R., Wu, V.Y.N. and Cheng, T.K. (1999) The hydrological response of landfilled wastes to site restoration: a case study, *Proceedings Sardinia 99, Sixth International Landfill Symposium*, S. Margherita di Pula, Cagliari, Italy.

- Fassett, J., Leonards, G., and Reppeto, P. (1994) Geotechnical Properties of Municipal Solid Waste and Their Use in Landfill Design," *Proc. Waste Tech '94, Solid Waste Association of North America*, Silver Springs, Maryland, 1-31.
- Freeze, R.A. and Cherry J.A. (1979), *Groundwater*, Prentice-Hall, Inc., Englewood Clifss, NJ.
- Giardi, M. (1997) Hydraulic behaviour of waste: Observations from Pumping Tests, *Proceedings Sardinia 97, Sixth International Landfill Symposium*, S. Margherita di Pula, Cagliari, Italy.
- Hentges, G. T., Thies, F. and Lemar, T. S. (1993) Leachate Extraction Well Assessments Des Moines, Iowa Metropolitan Park East Sanitary Landfill, Hamilton County, Iowa Sanitary Landfill. Proceedings of the Sixteenth International Madison Waste Conference. Department of Engineering Professional Development, University of Wisconsin, Madison/Extension, Madison, U.S.A.
- Hudson, A.P., Beaven, R.P. and Powrie, W. (1999) Measurement of the horizontal K of household waste in a large scale compression cell, *Proceedings Sardinia 99, Sixth International Landfill Symposium*, S. Margherita di Pula, Cagliari, Italy.
- Jacob, C.E. (1946) Radial Flow in a leaky artesian aquifer, *Am. Geophys. Union Trans.*, 27(2):198-205.
- Kazimoglu, Y.K., Mcdougal, J.R. and Pyrah I.C (2006) Unsaturated Hydraulic Conductivity of Landfilled Waste, *Unsaturated Soils*.
- Kruseman, G.P. and de Ridder, N.A. (1994) *Analysis and Evaluation of Pumping Test Data, 2nd edition*, International Institute for Land Reclamation & Improvement, Wageningen, The Netherlands.

- Landva, A.O., Pelkey, S.A. and Valsangkar, A.J. (1998) Coefficient of Permeability of Municipal Refuse, *Proceedings, 3rd International Congress on Environmental Geotechnics*, Lisbon, Portugal, 1: 63-68
- Nakamura, M, Castaldi, M.J and Themelis, N.J. (2005) Measurement of Particle Size and Shape of New York City Municipal Solid Waste and Combustion Residues Using Image Analysis," Proc. 16th Japan Society of Waste Management Experts (JSMWE) Fall Conference, pp. 1-3, Sendai, Japan.
- Neuman, S.P. (1972) Theory of Flow in Unconfined Aquifer Considering Delayed Response Of The Water Table, *Water Resource Research*, 8(4):1031-1045.
- Neuman, S.P. (1974) Effect of partial penetration on flow in unconfined aquifers considering delayed gravity response, *Water Resources Research*, 10(2): 303-312.
- Moench, A.F. (1984) Double-porosity model for a fissured groundwater reservoir with fracture skin, *Water Resources Research*, 20(7):831-846.
- Neuman, S.P. (1975) Analysis of Pumping Test Data From Anisotropic Unconfined Aquifers Considering Delayed Gravity Response, *Water Resources Research*, 11(2): 329-342.
- Oweis, I.S., Smith, D.A., Ellwood, R.B. and Greene, D.S. (1990) Hydraulic Characteristics of Municipal Refuse, *Journal of Geotechnical Engineering*, 116(4):539-553.
- Powrie, W. and Beaven, R.P. (1999) Hydraulic properties of household waste and implications for liquid flow in landfills. *Proceedings of the Institution of Civil Engineers*, Geotechnical Engineering, 235-247.

- Rorabaugh, M.I. (1913) Graphical and Theoretical Analysis of Step-Drawdown of Artesian Well, Proceedings of the American Society of Civil Engineers, 79(362):1-23.
- Rowe, R.K., and VanGulck, J.V. (2004) Chapter 10: Landfilling Geotechnolgy, In Print.
- Rowe, R.K. and Nadarajah, P. (1996) Estimating leachate drawdown due to pumping wells, *Can. Geotech J.*, 33:1-10.
- Qian, X.; Koerner, R. M. and Gray, D. H. (2002) *Geotechnical aspects of landfill design and construction*, Prentice Hall, Upper Saddle River, N.J, USA.
- Theis, C.V. (1935) The relation between the lowering of the piezometric surface and the rate and duration of discharge of a well using groundwater storage, *Am Geophys Un Trans*, 16:: 519–524.
- Uffink, G.J.M. (1982) Richtlijnen voor het uitvoeren van putproeven H₂O, 15:202-2005.
- Zeiss, C. and Uguccioni, M. (1995) Mechanims and Patters of Leachate Flow in Municipal Solid Waste Landfills, *Journal of Environmental Systems*, 23(3): 247-270.
- Zeiss, C. and Major, W. (1993) Flow through municipal solid waste: pattern and characteristics, *Journal of Environmental Systems*, 22(3):211-232.

Table 4.1: Summary of deduced transmissivity and storativity values for all extraction wells used by Hentges *et al.* (1993) (modified from Hentges *et al.* (1993)).

Well #	Saturated Thickness (m)	Transmissivity (m^2/day)	Storativity (-)	Measured/Predicted Extraction Rate	Recovery Period
Des Moines Sanitary Landfill Pump Tests					
EW-10	1.33	0.05	2.93×10^{-1}	5.45 m ³ /day dewatered in min/hours	About two days
EW-3	1.31			5.45 m ³ /day dewater in few min/hours	About two days
EW-1	0.45			5.45 m ³ /day dewater in few min/hours	About two days
EW-4	2.26	3.50	2.00×10^{-3}	1.89 to 3.79 m ³ /day	About two days
EW-2	2.93	2.74	5.30×10^{-2}	0.83 m ³ in 19 hours	Five day period
EW-9	3.62	1.49	2.06×10^{-1}	5.68 m ³ /day	Two day
EW-12	3.57			2.27 m ³ /day	About three days
EW-7	2.07	0.78	1.46×10^{-1}	1.89 to 3.79 m ³ /day	One to two days
EW-14	4.38	0.18	4.18×10^{-1}	5.45 m ³ /day for five to seven days	Five days
EW-11	9.42	0.38	1.52×10^{-1}	3.78 to 5.68 m ³ /day	
#1 LMEW-51.80		0.024		5.45 m ³ /day dewater in few min/hours	About two days
#2 LMEW-51.80		0.0037		5.45 m ³ /day dewater in few min/hours	About two days
#3 LMEW-51.80		0.16		5.45 m ³ /day dewater in few min/hours	About two days
#4 LMEW-51.80		1.11		5.45 m ³ /day dewater in few min/hours	About two days
LMEW-3	6.20	0.57			
LMEW-4	2.94	0.27			
LMEW-5	5.91	0.55			
LP -5	5.20	0.48			

Table 4.2: Saturated refuse depth, deduced values for refuse transmissivity, hydraulic conductivity, specific yield, and sustainable yield from Burrows *et al.* (1997) Buckinghamshire and Cambridgeshire, England (modified from Burrows *et al.* (1997).

Well #	Saturated Depth (m)	Transmissivity (m ² /day)	Hydraulic Conductivity (x 10 ⁻⁶ m/s)	Specific Yield (%)	Sustainable Yield (m ³ /day)
A1	12.02	2.42	2.33 x 10 ⁻⁶		9.6
A2	10.37	3.89	4.34		14.4
A3	11.75	21.8	21.47		19.2
A4	13.32	1.39	1.21		9.6
A5	14.01	5.12	4.23		12.0
A6 ob	14.00	8.79	7.27	9.2	
A7 ob	15.03	1.40	1.08	14.6	
B1	20.05	6.10	3.50		6.0
B2	20.00	13.68	7.92		13.7
C1	15.00	19.61	15.13		
C2	15.00	8.58	6.62		
C3	20.00	4.37	2.53		
C4	10.00	0.34	0.39		
C5	12.07	0.56	0.54		
D1	4.62	8.71	21.87	16.3	2.4
D2	4.60	15.83	39.83	14.2	14.4
D3	3.84	22.22	66.91		3.6
D4 ob	3.32	4.21	14.68		
D5 ob	4.00	4.74	13.72	9.1	
D6 ob	1.46	2.64	20.93	13.2	

Table 4.3: Summary of extraction well depth, ground elevation, piezometric surface, extraction rate, and deduced transmissivity for drawdown and recovery from Chianni Landfill, Italy (modified from Giardi (1997)).

Well#	Well Depth (m)	Well Ground Elevation (m a.s.l)	Well Piezometric Surface (m a.s.l)	Extraction Rate (m ³ /day)	Transmissivity	
					Drawdown (m ² /day)	Recovery
Pumping Tests on Single Wells						
PC5	25.0	132.4	123.1	2.9	0.13	0.10
PC5	25.0	132.4	123.1	3.6	0.14	0.11
PC8	33.0	132.4	121.3	17.3	0.24	0.13
PC8	33.0	132.4	121.3	5.8	0.12	0.10
PC9	26.0	132.2	123.0	4.5	0.16	0.16
Pumping Tests on Trail Station						
PC10	27.5			8.6	0.30	0.50
PC12	33.0			11.5	0.29	0.37

Table 4.4: Summary of the top casing elevation, bottom elevation, and depth for installed extractions wells and piezometers at the Brady Road Landfill.

Location	Top Casing Elevation (m a.s.l)	Bottom Elevation (m a.s.l)	* Depth (m)
Well#1	238.7	228.7	8.8
Well#2	238.7	233.0	4.6
P7A	238.6	228.7	8.8
P7B	238.5	231.8	5.7
P7C	238.3	234.9	2.6
P6A	238.5	228.5	9.0
P6B	238.5	231.6	5.9
P6C	238.3	234.7	2.8
P5A	238.3	228.4	9.1
P5B	238.3	231.4	6.2
P5C	238.2	234.5	3.1
P4A	238.3	228.4	9.1
P4B	238.3	231.4	6.1
P4C	238.4	234.7	2.9
P3A	238.3	228.4	9.1
P3B	238.2	231.4	6.2
P3C	238.1	234.4	3.2
P2A	238.3	228.4	9.1
P2B	238.2	231.4	6.2
P2C	238.1	234.4	3.1
P1A	238.3	228.4	9.1
P1B	238.3	230.5	7.1
P1C	238.3	234.6	3.0

* Depth of the piezometer and wells was deduced from the bottom measurement elevations and from two ground surface elevations.

Table 4.5: Summary of the maximum measured drawdown with radial distance from the extraction for the 9.1 m, 6.1 m and 3.0 m deep piezometers during pump Test 1 and Test 2.

Pump Test #	Piezometer Location	Radial Distance from Extraction Well (m)	Maximum Measured Drawdown (m)
Test #1	9.1 m Deep Well		
	P1A	1.0	0.30
	P6A	1.4	0.27
	P2A	3.0	0.03
	P7A	3.2	0.05
	6.1 m Deep Well		
	P1B	1.0	-0.02
	P6B	1.4	-0.04
	P2B	3.0	0.01
	P7B	3.2	0.00
	3.0 m Deep Well		
	P1C	1.0	0.00
	P6C	1.4	-0.08
	P2C	3.0	0.00
	P7C	3.2	-0.07
Test #2	9.1 m Deep Well		
	P1A	1.0	1.14
	P6A	1.4	0.90
	P2A	3.0	0.33
	P7A	3.2	0.59
	P3A	10.0	0.06
	P4A	21.0	0.01
	P5A	35.0	0.01
	6.1 m Deep Well		
	P1B	1.0	0.05
	P6B	1.4	0.05
	P2B	3.0	0.05
	P7B	3.2	0.05
	3.0 m Deep Well		
	P1C	1.0	0.05
P6C	1.4	0.05	
P2C	3.0	0.05	
P7C	3.2	0.03	

Note: Negative drawdown values indicated that the pressure response in the piezometer was increasing

Table 4.6: Summary of the deduced refuse transmissivity, specific yield and anisotropy from drawdown and extraction rate data collected from Pump Test 1 and Test 2 using the Neuman (1974) solution for an unconfined aquifer.

Pump Test	Piezometer Location	Transmissivity T (m ² /day)	Specific Yield	Storativity	Anisotropy Ratio
			S _y -----	S -----	K _{hor.} : K _{ver.}
Test 1	P1A	0.16	0.24	2.9 x 10 ⁻³	0.03
	P6A	2.17	0.03	1.5 x 10 ⁻²	0.09
Test 2	P1A	0.36	0.14	4.7 x 10 ⁻³	0.04
	P6A	0.18	0.13	2.4 x 10 ⁻³	0.06
	P2A	0.77	0.07	1.0 x 10 ⁻³	0.07
	P7A	0.38	0.03	7.6 x 10 ⁻³	0.19

Table 4.7: Summary of the deduced refuse transmissivity and storativity using the Theis (1935) recovery method.

Pump Test #	Piezometer Location	Transmissivity	Storativity
		T (m ² /day)	S -----
Test #2	P1A	1.97	3.9 x 10 ⁻²
	P6A	1.95	7.6 x 10 ⁻²
	P2A	9.65	3.0 x 10 ⁻⁴
	P7A	3.50	1.3 x 10 ⁻²

Table 4.8: Summary of selected spherical block diameter and deduced refuse transmissivity and storativity using the dual porosity spherical block model of Moench (1984).

Pump Test #	Piezometer		Geological Medium #1		Geological Medium #2	
	Location	Block Diameter-D (m)	Transmissivity T (m ² /day)	Storativity S -----	Transmissivity T (m ² /day)	Storativity S -----
Test #1	P1A	1.0	5.93	6.2×10^{-3}	2.86	5.3×10^{-4}
		0.1	5.93	6.2×10^{-3}	2.86	5.3×10^{-4}
	P6A	1.0	2.35	7.6×10^{-3}	2.04	3.1×10^{-2}
		0.1	2.35	7.6×10^{-3}	0.03	3.1×10^{-2}
Test #2	P1A	1.0	0.39	1.0×10^{-3}	1.58	1.3×10^{-1}
		0.1	0.39	1.0×10^{-3}	0.01	1.3×10^{-1}
	P6A	1.0	0.29	6.4×10^{-3}	0.01	2.2×10^{-2}
		0.1	0.21	8.2×10^{-3}	0.001	2.4×10^{-2}
	P2A	1.0	0.93	5.7×10^{-2}	0.98	1.5×10^{-2}
		0.1	0.97	5.8×10^{-2}	0.001	1.5×10^{-2}
	P7A	1.0	0.41	4.6×10^{-3}	0.05	2.8×10^{-2}
		0.1	0.41	5.0×10^{-3}	0.004	2.8×10^{-2}

Table 4.9: Summary of initial displacement after slug injection, and deduced refuse transmissivity using the slug tests method of Bouwer and Rice (1976).

Piezometer Location	Initial Displacement h_0 (m)	Transmissivity T (m²/day)
P1A	1.3	0.89
P2A	2.4	0.17
P3A	2.6	1.15
P4A	0.5	0.03
P5A	3.0	0.01
P6A	1.8	0.68
P7A	2.1	0.64
P1B	1.0	0.12
P2B	1.3	1.99
P3B	1.2	2.04
P4B	1.8	0.22
P5B	1.7	0.43
P6B	1.7	6.81
P7B	1.4	6.07

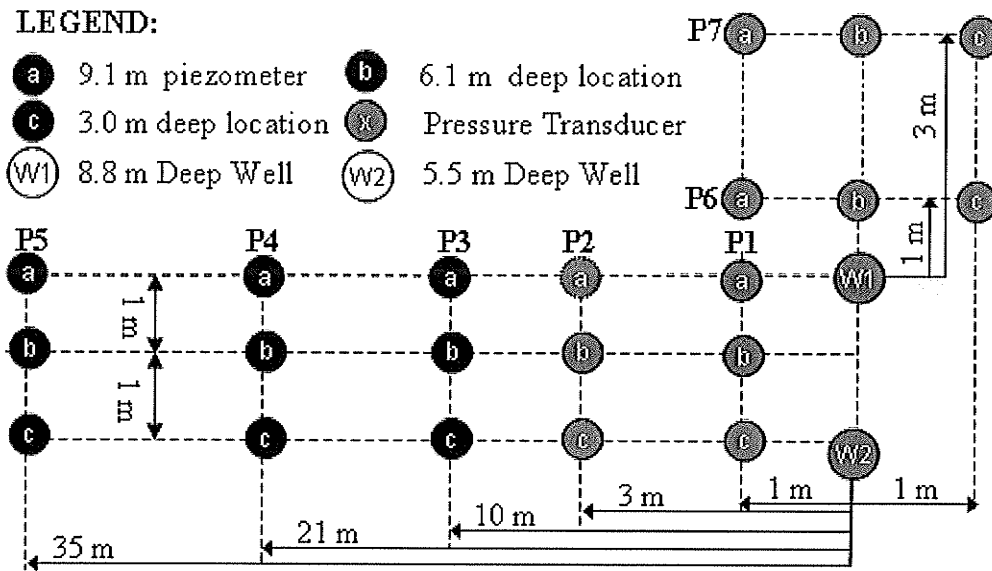


Figure 4.1: Plan view schematic of extraction well and piezometer layout (not to scale)

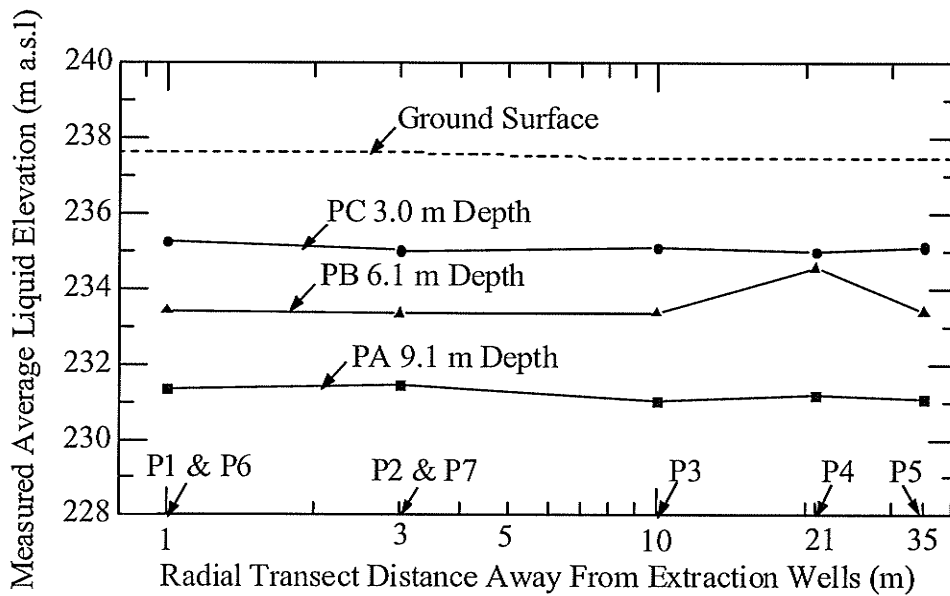


Figure 4.2: Measured average liquid elevations with radial distance from three piezometers located at depths of 3.0 m, 6.1 m and 9.1 m within the Brady Road Landfill.

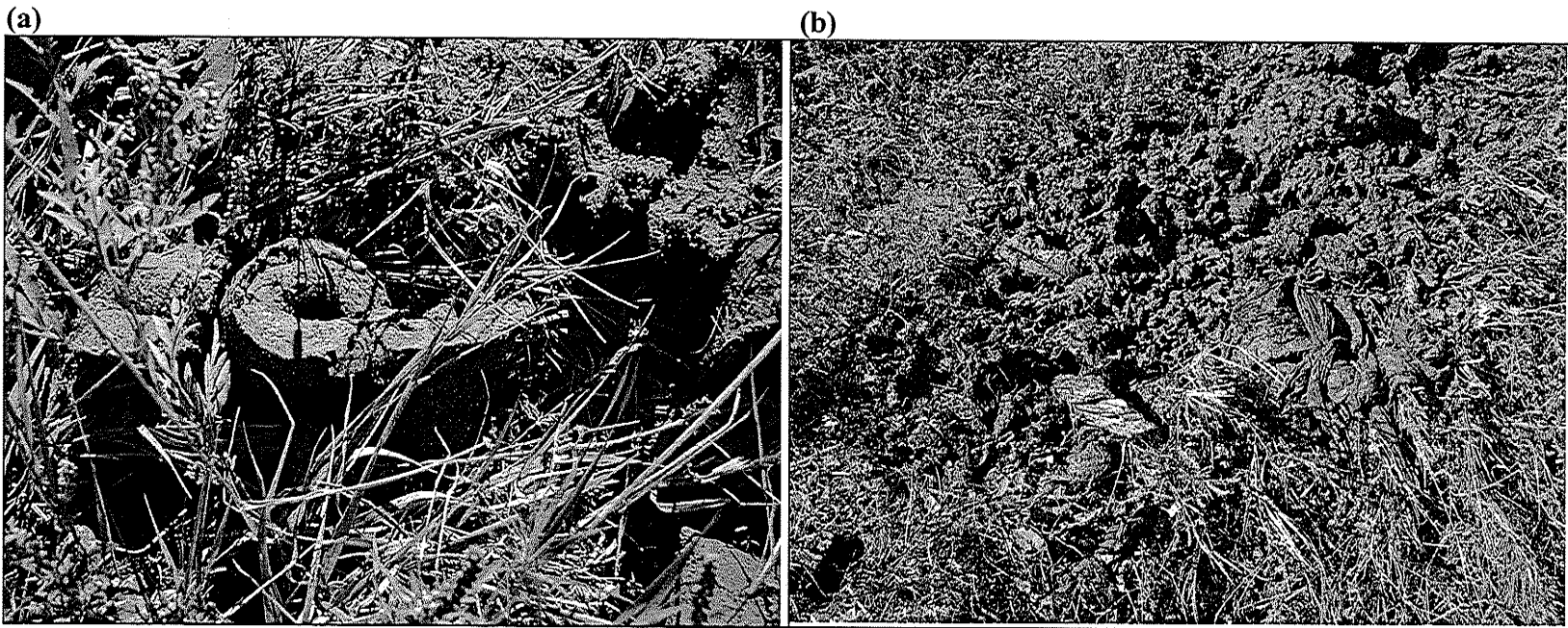


Figure 4.3: Observed landfill composition during drilling: (a) clay cap material and (b) grayish to black slurry waste material

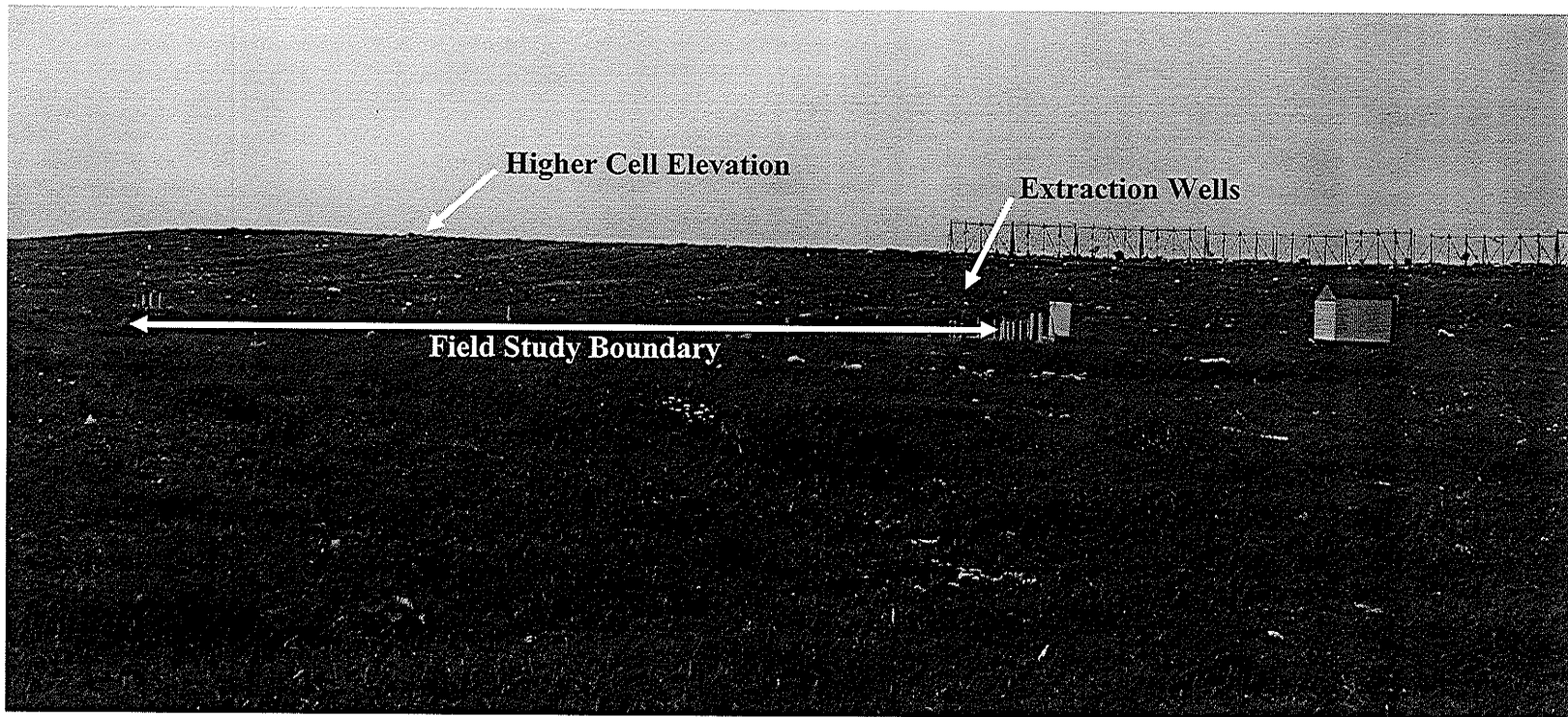


Figure 4.4: Field test location and the surrounding landfill cell at a higher elevation.

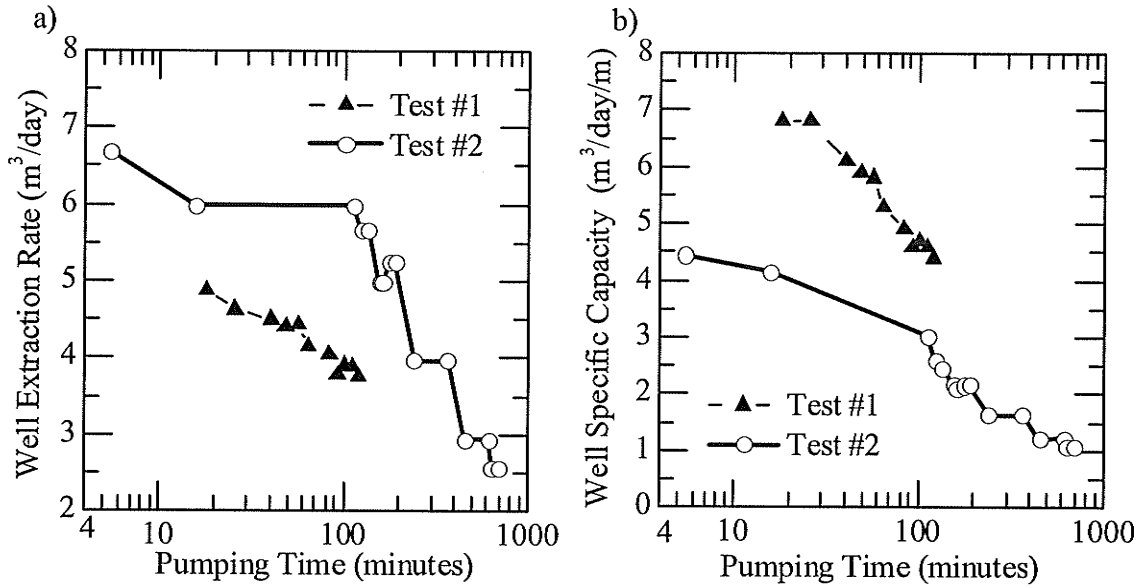


Figure 4.5: Measured a) well extraction rate and b) well specific capacity for two pump tests conducted at the Brady Road Landfill.

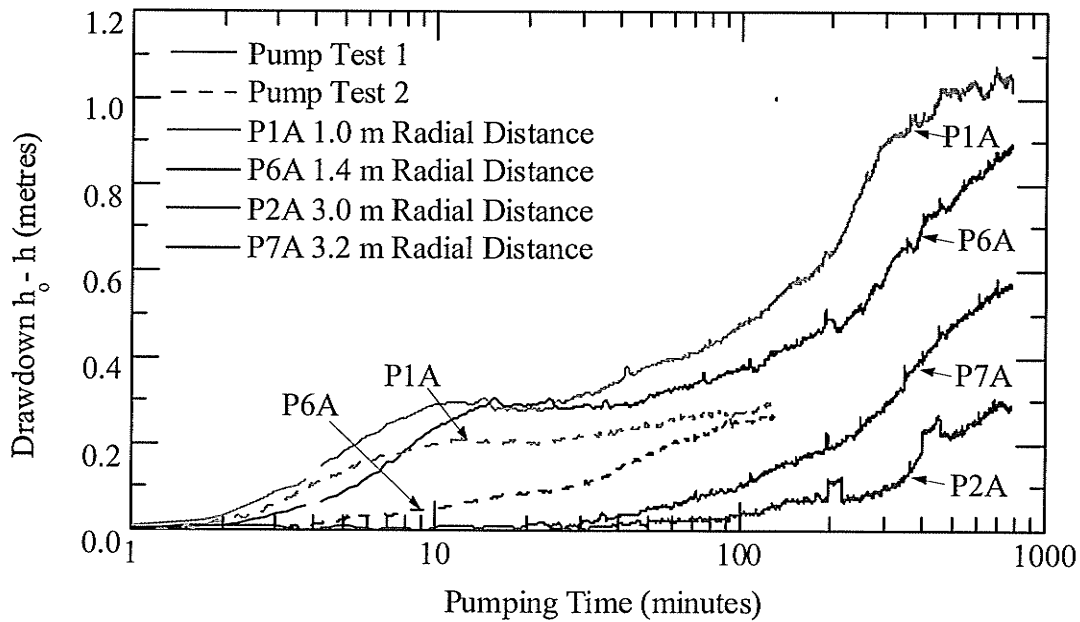


Figure 4.6: Pressure response in 9.1 m deep piezometers at radial distances of 1.0 m, 1.4 m, 3.0 m and 3.2 m away from the extraction for two pump tests.

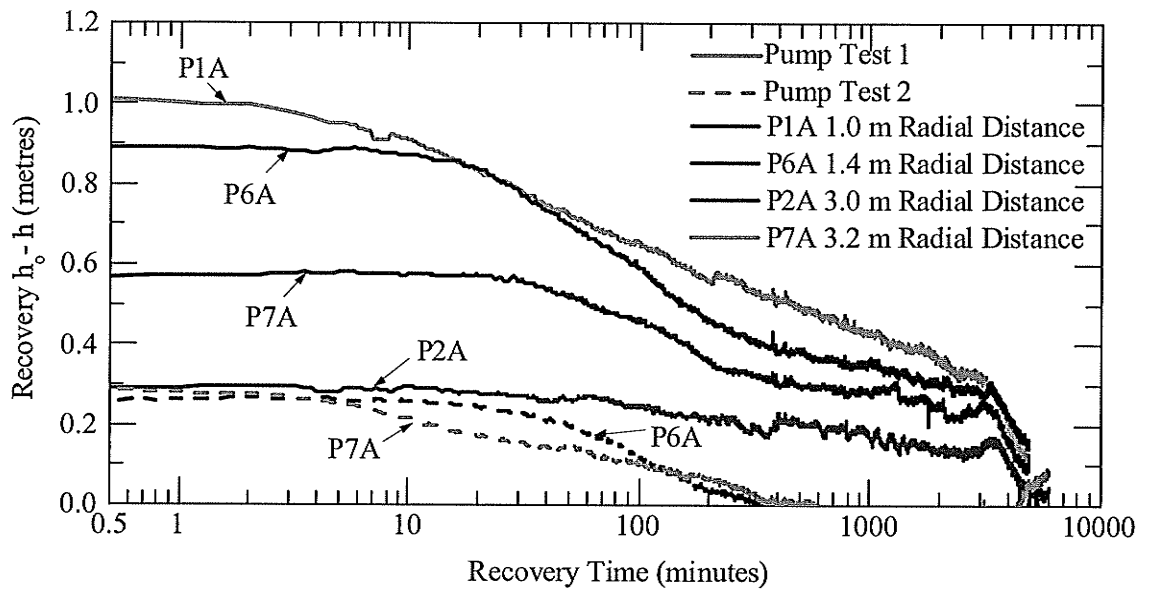


Figure 4.7: Recovery response for 9.1 m deep piezometers at radial distances of 1.0 m, 1.4 m, 3.0 m and 3.2 m away from the extraction for two pump tests.

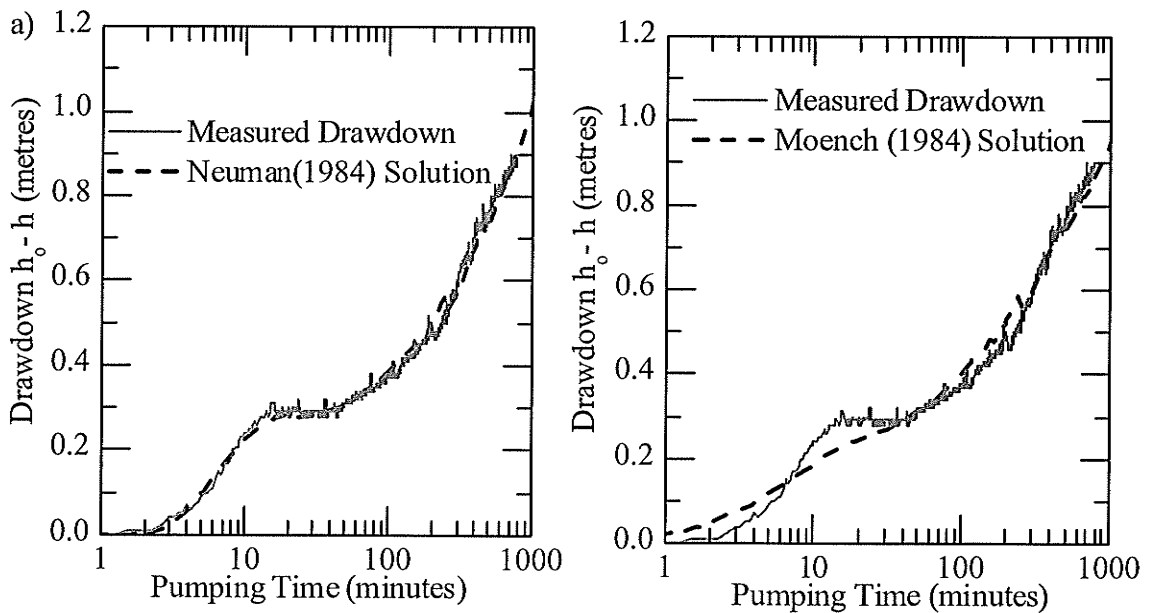


Figure 4.8: Example of a) Neuman (1974) and b) Moench (1984) solution fit to measured drawdown for Test 2 and P6A.

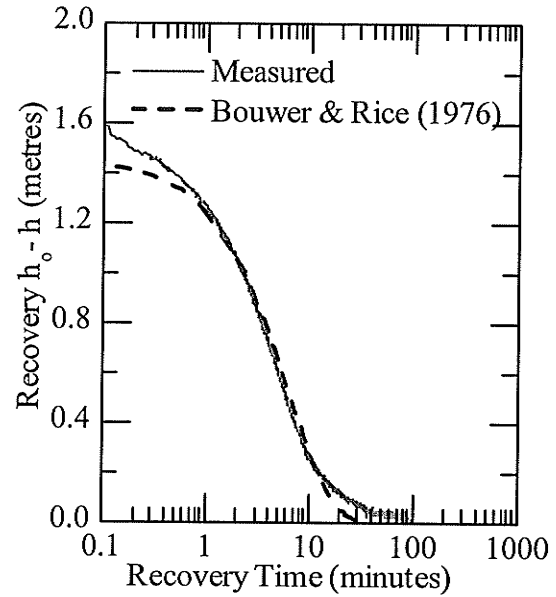
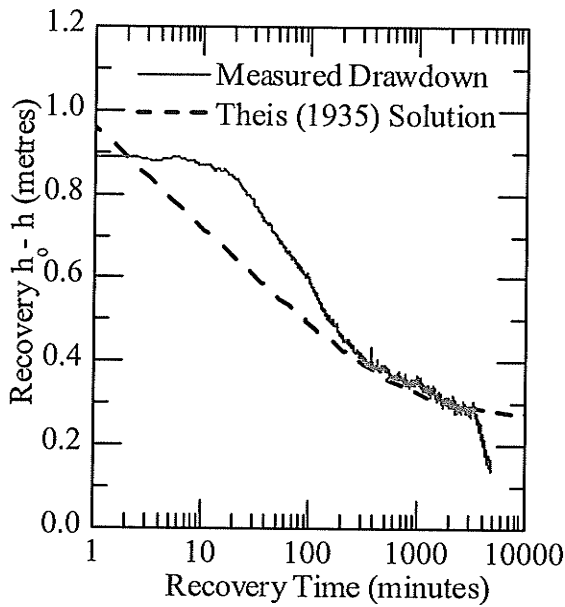


Figure 4.9: Example of Theis (1935) solution fit to measured recovery response at piezometer P6A after Pump Test 2.

Figure 4.10: Example of Bouwer and Rice (1976) solution fit to slug removal test at piezometer P6A.

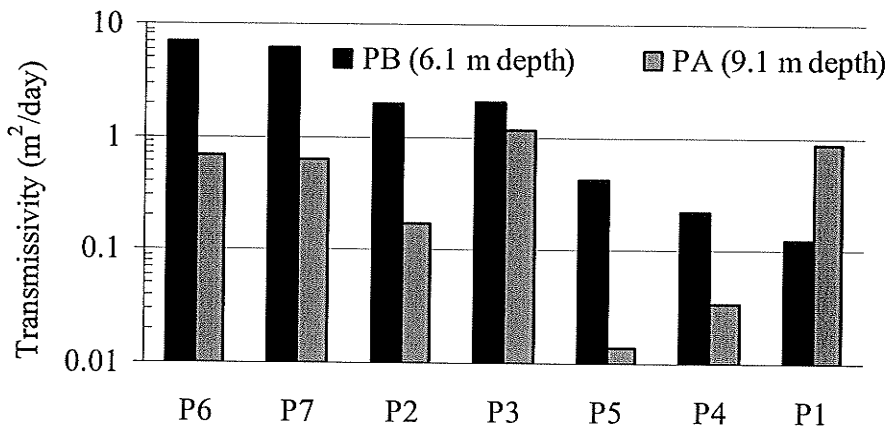


Figure 4.11: Deduced transmissivity for 6.1 m and 9.1 m depth piezometers using the slug method of Bouwer and Rice (1976).

CHAPTER 5: CONCLUSIONS AND RECOMENDATIONS

5.1 INTRODUCTION

The performance level of horizontal liquid injections systems and retrofitted leachate extraction wells that are installed in landfills are dependent on engineering design and operational management. The movement of liquid through the refuse is highly influenced by its spatial and temporal hydraulic properties. These characteristics typically control the effective design and operation of liquid injection and extraction systems in landfills. The first half of this thesis considered the implications of refuse hydraulic properties on the design and operation of a horizontal injection trench for use in bioreactor landfills. The second half of this thesis involved investigating the movement of liquid and pressure response through a field-scale pump and recovery test. This chapter provides a summary and the conclusions and recommendations of the research completed.

5.2 SUMMARY AND CONCLUSIONS

Chapter 2 presented a review of the field and laboratory studies that have been conducted to assess refuse hydraulic properties; specifically, the refuse hydraulic conductivity and the refuse water contents (field capacity and specific yield). Additionally, Chapter 2 included a summary of field and laboratory studies that have reported a decrease in refuse hydraulic conductivity and an increase of refuse unit weight in response to increased vertical stresses and refuse compaction efforts. A broad range of literature values for refuse hydraulic conductivity that range from 10^{-4} m/s to 10^{-8} m/s have been reported. Specific studies have indicated that a decrease in refuse hydraulic

conductivity from 10^{-4} m/s to 10^{-8} m/s can occur from an increase of 1000 kPa of vertical stress in a landfill or from the placement of an additional 50 m of refuse depth.

Chapter 3 investigated the influence refuse hydraulic properties and liquid injection boundary conditions on the performance level, system operation, and design of horizontal injection systems (HLIS). Chapter 3 also presented the results of a two-dimensional unsaturated fluid flow model that was used to simulate the hydraulic interactions that occur during liquid injection and drainage from a HLIS. The numerical simulations indicate that the rate of pressure increase and subsequent decrease in flow rate within a perforated pipe is inversely proportional to the refuse hydraulic conductivity. HLIS positioned within refuse with a relatively low hydraulic conductivity resulted in rapid saturation and pressurizing of the injection trench and a decrease in the injection flux and injected volume compared to a high hydraulic conductivity. Additionally, a set of empirical equations to predict the pressure development within a trench and injection volume for a range of refuse hydraulic properties and pipe hydraulic configurations were presented.

Chapter 4 presented the results of a field test conducted at the Brady Road Landfill, in Winnipeg Manitoba to assess refuse hydraulic properties. Leachate was extracted from two wells and the pressure responses were monitored in an array of piezometers. The well extraction rate and well specific capacity were measured. Pressure responses from the pump tests indicate that low permeability layers may limit the vertical migration of fluid in a landfill. Measured drawdown responses from the conducted pump tests were most accurately simulated using analytical methods for an unconfined aquifer and with a double aquifer analytical model. Additionally, collected recovery response

data and slug test data were analyzed with unconfined aquifers analytical methods . The deduced transmissivity from all the selected analytical methods ranged from 0.16 to 9.65 m²/day and the storativity ranged from 10⁻¹ to 10⁻³. A solution for an unconfined aquifer deduced a refuse specific yield that ranged from 0.13 to 0.14.

5.3 PRACTICAL FINDINGS AND RECOMMENDATIONS

Findings from Chapter 3 suggest that the refuse hydraulic properties, specifically, the refuse hydraulic conductivity can significantly affect the performance and operation of liquid injection systems which can compromise the potential for uniform waste degradation and its benefits.

The numerical simulations partially accounted for the presence of gas by considering unsaturated flow theory however, the numerical liquid injection simulations completed did not consider the transient creation and collection of landfill gas as a result of microbial activity within the refuse pores. In some bioreactor landfills, landfill gas collection systems are installed to control methane green house gas migrations into the surrounding environment provide economic gain, and energy Gas generation and migration coupled with liquid migration was not considered in Chapter 3 to isolate the impacts of liquid injection on design and operation. For coupled liquid injection and landfill gas extraction systems investigation into the creation of gas and gas migration to extraction wells is needed to assess the optimum spacing of gas extraction systems, and optimum liquid injection and gas extraction operation schedules.

Full scale pump tests were conducted to gain insight into the movement of liquid and drawdown responses at an operational landfill. The pump tests measured minimal pressure response due to pumping in the unscreened depths of the partially penetrating

well. The lack of pressure response in the unscreened portion of the extraction well may be attributed to the presence of distinct low permeability layers from clay cover material that limit vertical liquid migration. Previous numerical studies by Powrie and Beaven (1999) and Al-Thani *et al.* (2004) evaluated the influence of spatial changes in hydraulic conductivity on the movement of liquid to an extraction well however their research did not consider the influence of cover. Further in situ field testing research is needed to independently assess the influence of daily cover material and effective stress on the movement of liquid to an extraction well.

APPENDIX A NUMERICAL STABILITY ANALYSIS

A.1 NUMERICAL STABILITY ANALYSIS OF HLS MODEL

In order to ensure numerical model stability the standard model setup with the baseline configuration was compared to different numerical arrangements: a finer unstructured meshes arrangement and a more stringent adaptive time stepping criterion. Liquid injection into refuse hydraulic conductivity of 10^{-6} m/s and 10^{-8} m/s (see Figure A.1) using the above described cases produced the same results as the standard model setup and as such the standard case was deemed to be numerically stable.

A.2 NUMERICAL STABILITY ANALYSIS OF VERTICAL EXTRACTION WELL MODEL

In order to verify numerical stability a case of liquid extraction with an anisotropy ratio of 1, a refuse compressibility of 5.5×10^{-5} kPa⁻¹ and a hydraulic conductivity of 6.3×10^{-7} m/s was compared to the different numerical arrangements: a finer structured mesh arrangement and a more stringent adaptive time stepping criterion. Liquid extraction using the above described cases produced same pressure behaviour and responses (Figure A.2) as the original non modified simulations as such the flow model was deemed to be numerically stable for the intended purpose.

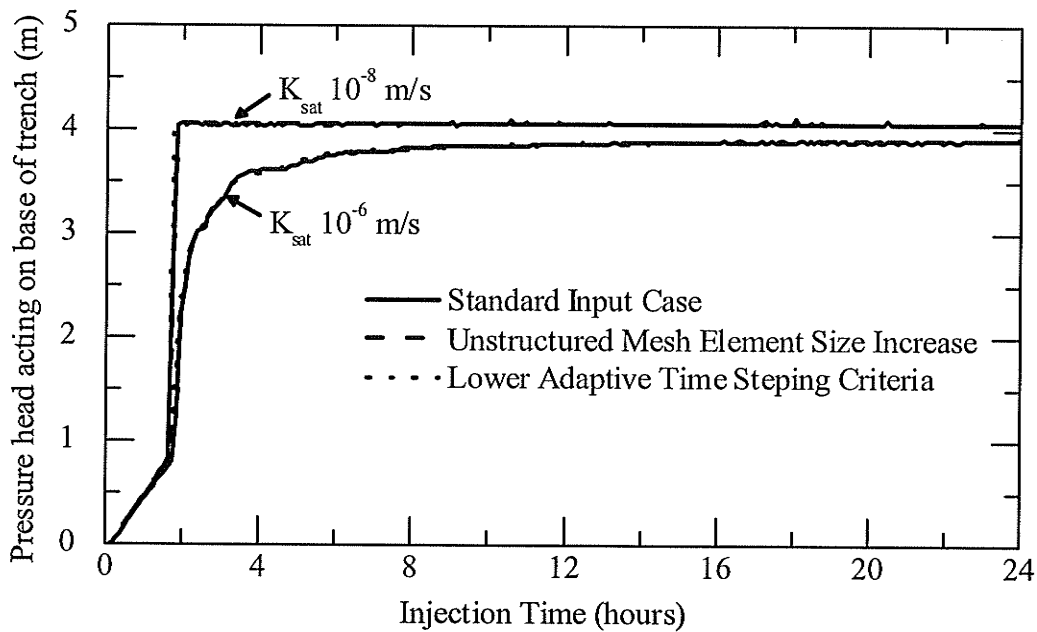


Figure A.1: Pressure head deduced at the trench base during liquid drainage injection for a refuse saturated hydraulic conductivities of 10^{-6} m/s the baseline pipe configuration and two specific model input scenarios.

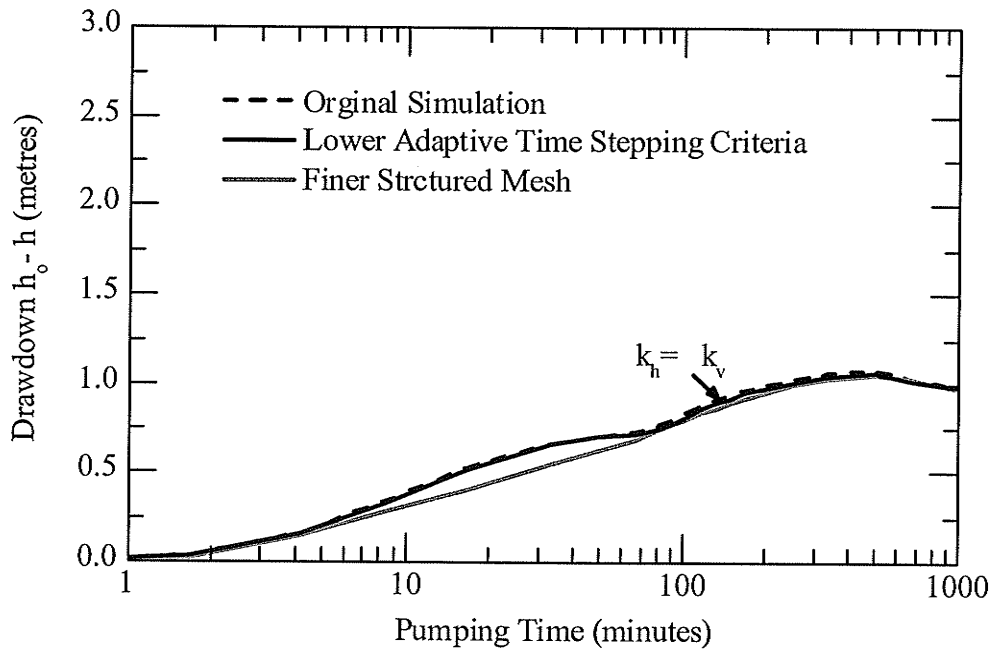


Figure A.2: Original simulated drawdown response at radial distance of 1 m and refuse depth of 8.8 m for a vertical to hydraulic anisotropy ratios of 1, refuse compressibility of $5.5 \times 10^{-5} \text{ kPa}^{-1}$, and refuse hydraulic of $6.3 \times 10^{-7} \text{ m/s}$, and for two specific model input scenarios.

APPENDIX B HLIS EMPIRICAL CORRELATIONS

Table B.1: Deduced values for the a_v and b_v and a_{hp} and b_{hp} derived coefficients for a refuse hydraulic conductivity of 10^{-8} m/s and selected model refuse inlet hydraulic head (h_p), and , normalised perforation flux (q_{seep}).

Head h_p (m)	Normalised Discharge q_{seep} ($m^3/min/m$)	Pressure Coefficient a_{hp} -----	Volume Coefficient b_{hp} -----	Pressure Coefficient b_{hp} -----	Volume Coefficient b_{hp} -----
2	3.0×10^{-3}	0.44	0.027	0.12	0.67
2	1.8×10^{-3}	0.44	0.054	0.10	0.71
2	6.0×10^{-4}	0.49	0.324	0.05	0.88
5	3.0×10^{-3}	0.19	0.027	0.19	0.70
5	1.8×10^{-3}	0.19	0.083	0.14	0.79
5	6.0×10^{-4}	0.27	0.464	0.06	0.93
10	3.0×10^{-3}	0.10	0.039	0.25	0.76
10	1.8×10^{-3}	0.11	0.114	0.18	0.84
10	6.0×10^{-4}	0.20	0.518	0.07	0.96
15	3.0×10^{-3}	0.07	0.048	0.27	0.80
15	1.8×10^{-3}	0.08	0.121	0.19	0.87
15	6.0×10^{-4}	0.18	0.522	0.07	0.97
25	3.0×10^{-3}	0.05	0.056	0.30	0.85
25*	1.8×10^{-3}	0.07	0.125	0.19	0.90
25	6.0×10^{-4}	0.16	0.530	0.07	0.98
50	3.0×10^{-3}	0.03	0.061	0.37	0.87
50	1.8×10^{-3}	0.04	0.134	0.21	0.95
50	6.0×10^{-4}	0.15	0.535	0.07	0.99

Table B.2: Deduced values for the a_v and b_v and a_{hp} and b_{hp} derived coefficients for a refuse hydraulic conductivity of 10^{-8} m/s and selected model refuse inlet hydraulic head (h_p), and , normalised perforation flux (q_{seep})..

Head h_p (m)	Normalised Discharge q_{seep} ($m^3/min/m$)	Pressure Coefficient		Volume Coefficient	
		a_{hp}	b_{hp}	a_v	b_v
2	3.0×10^{-3}	0.43	0.005	0.014	0.44
2	1.8×10^{-3}	0.43	0.007	0.020	0.35
2	6.0×10^{-4}	0.43	0.004	0.014	0.42
5	3.0×10^{-3}	0.19	0.002	0.041	0.33
5	1.8×10^{-3}	0.19	0.003	0.025	0.44
5	6.0×10^{-4}	0.19	0.009	0.019	0.52
10	3.0×10^{-3}	0.10	0.001	0.047	0.40
10	1.8×10^{-3}	0.10	0.002	0.030	0.52
10	6.0×10^{-4}	0.10	0.007	0.026	0.55
50	3.0×10^{-3}	0.02	0.001	0.085	0.51
50	1.8×10^{-3}	0.02	0.001	0.065	0.59
50	6.0×10^{-4}	0.02	0.009	0.048	0.69

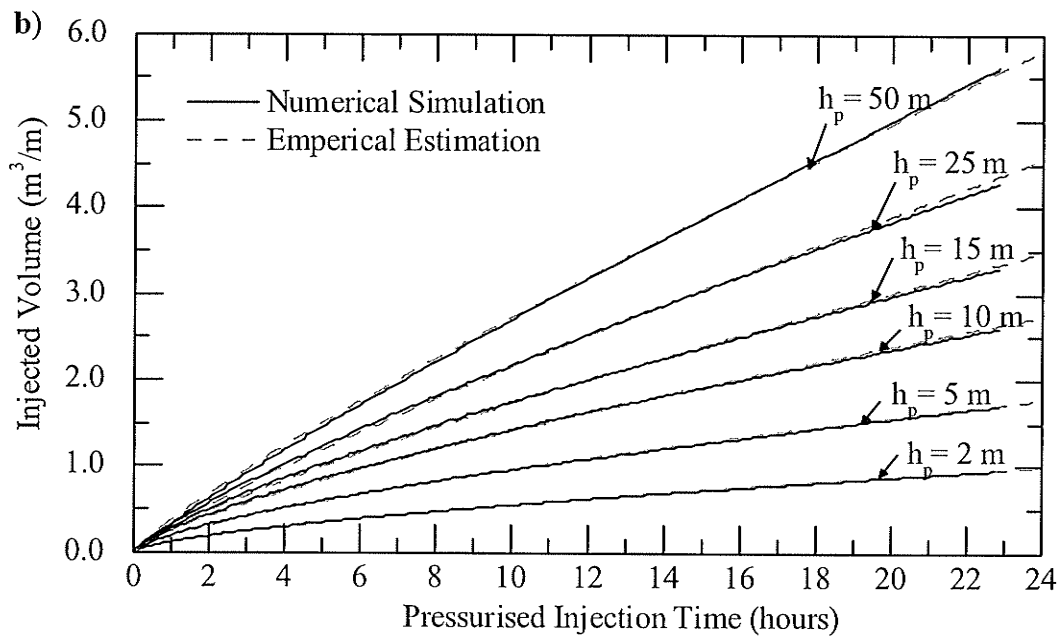
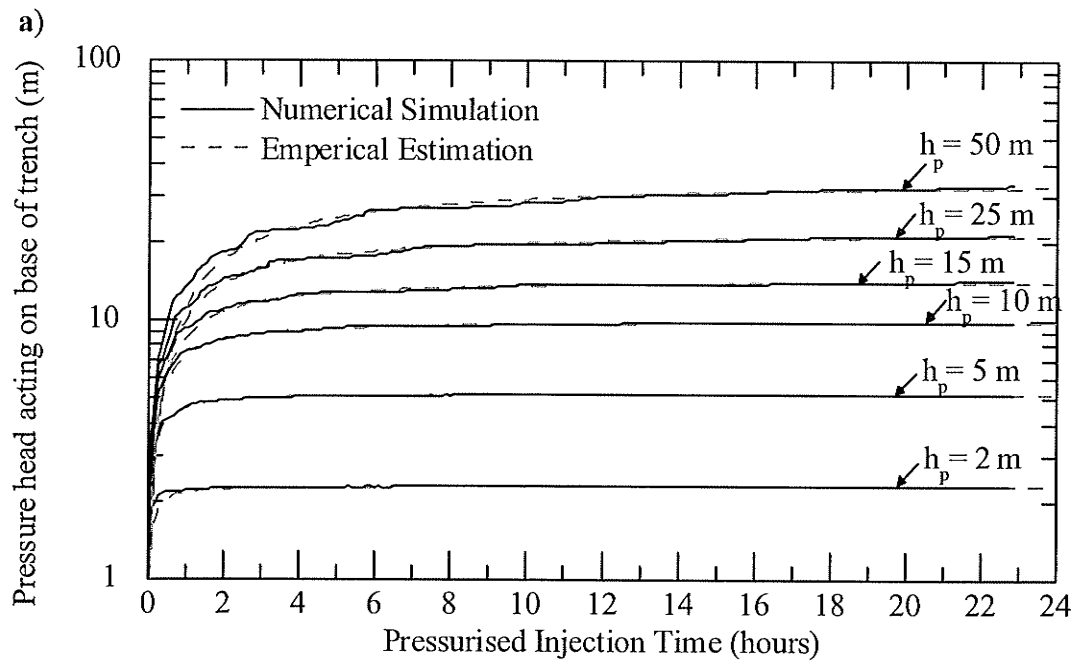


Figure B.1: Simulated and predicted a) pressure head at the trench base and b) volume injected for liquid injection into a saturated refuse hydraulic conductivity of 10^{-6} m/s, a normalized model perforation discharge of 5×10^{-5} $\text{m}^3/\text{s}/\text{m}$, and an inlet hydraulic head of 2 to 50 m.

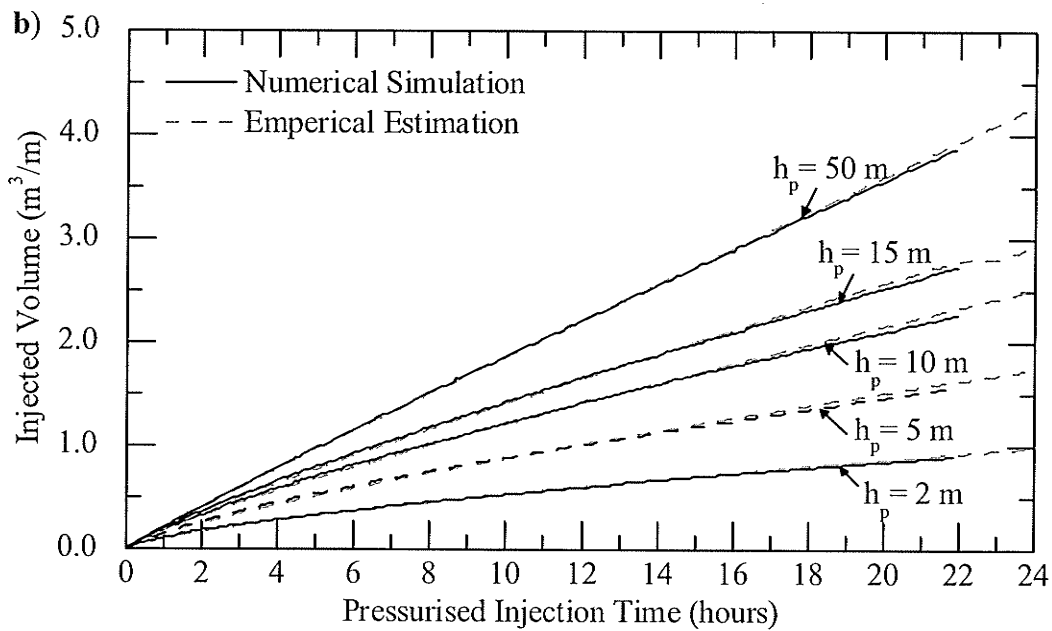
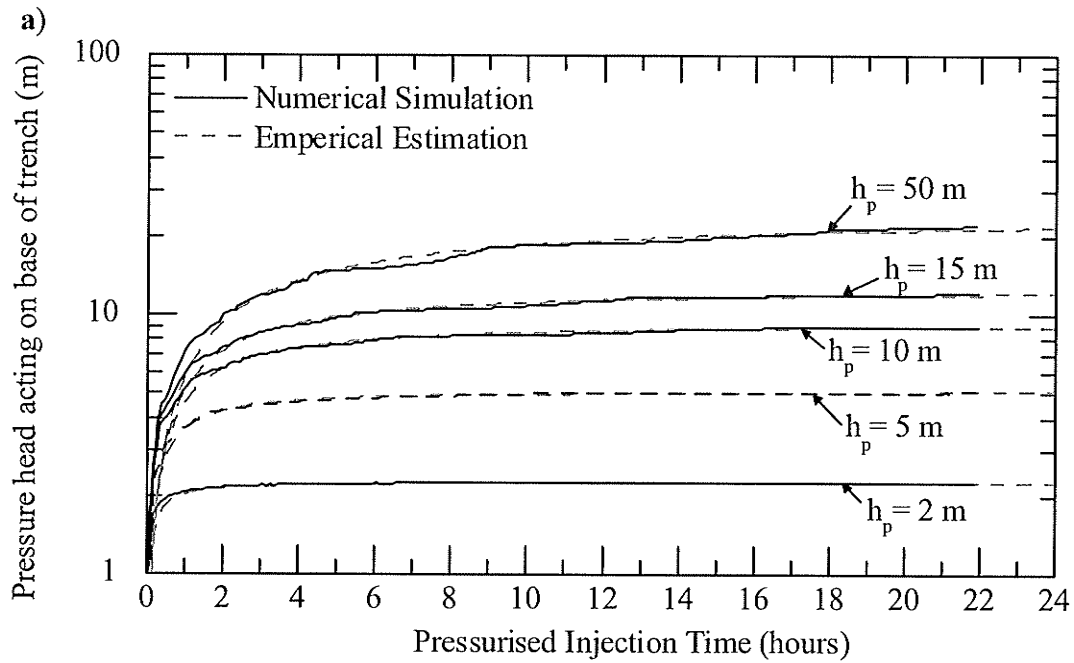


Figure B.2: Simulated and predicted a) pressure head at the trench base and b) volume injected for liquid injection into a saturated refuse hydraulic conductivity of 10^{-6} m/s, a normalized model perforation discharge of 3×10^{-5} $m^3/s/m$, and an inlet hydraulic head of 2 to 50 m.

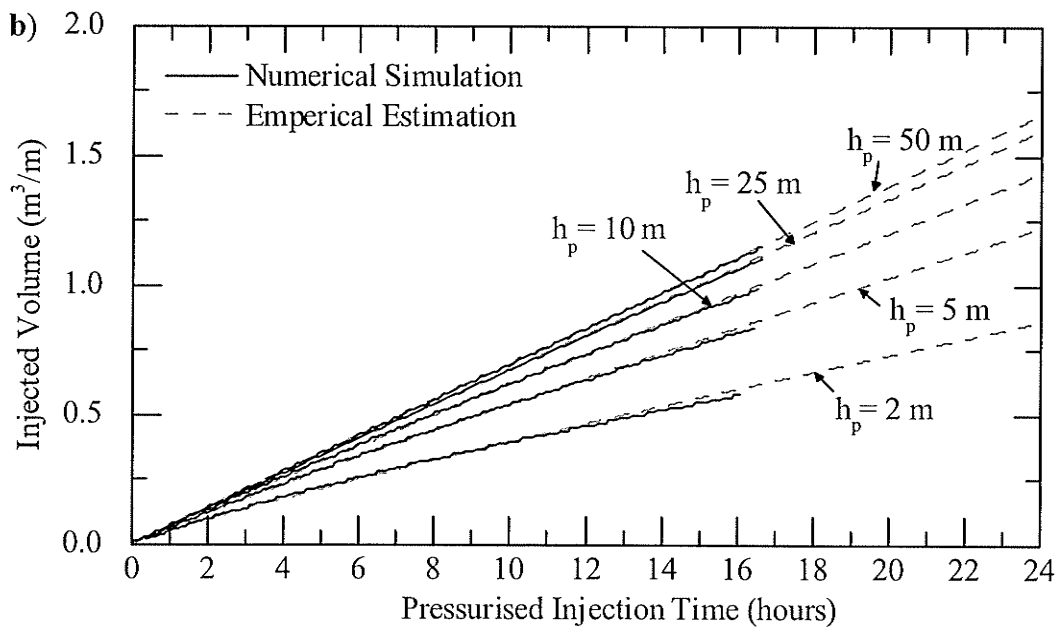
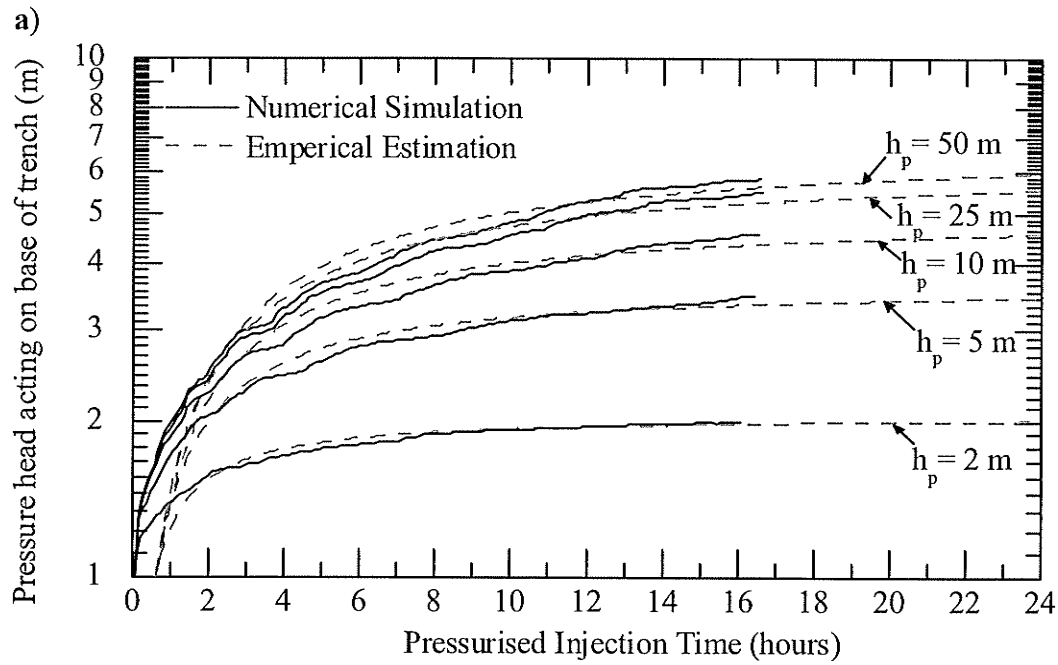


Figure B.3: Simulated and predicted a) pressure head at the trench base and b) volume injected for liquid injection into a saturated refuse hydraulic conductivity of 10^{-6} m/s, a normalized model perforation discharge of 1×10^{-5} $m^3/s/m$, and an inlet hydraulic head of 2 to 50 m.

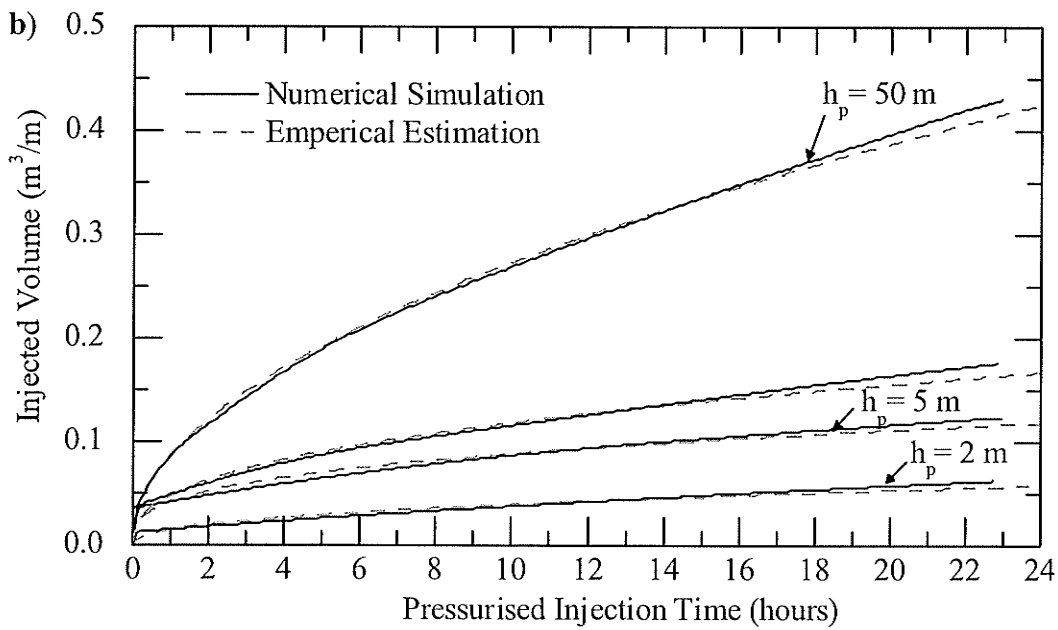
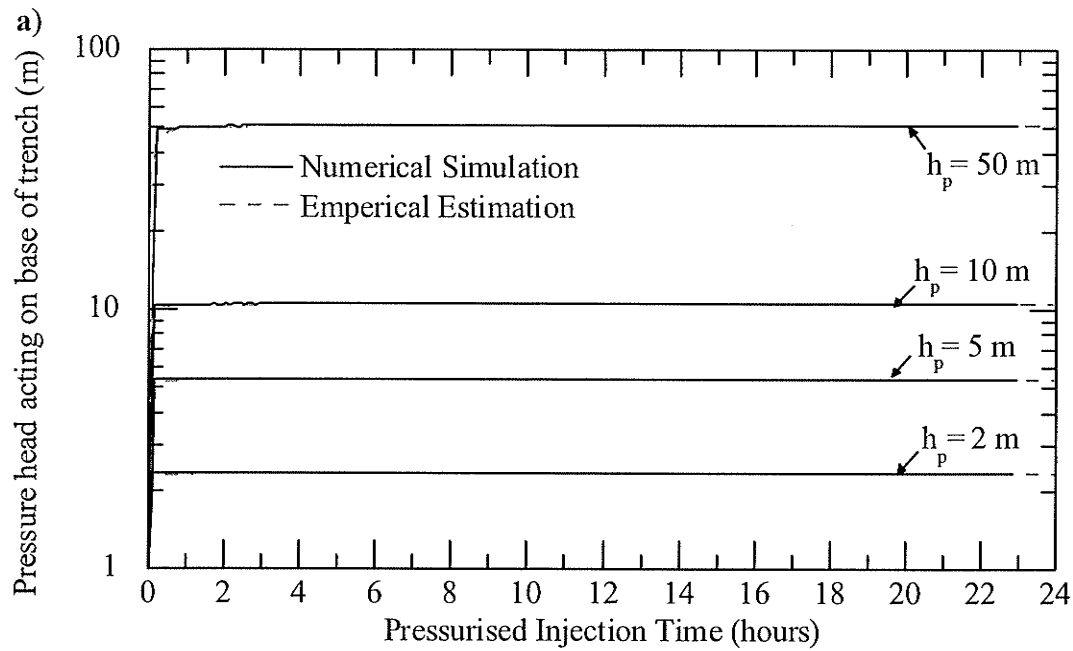


Figure B.4: Simulated and predicted a) pressure head at the trench base and b) volume injected for liquid injection into a saturated refuse hydraulic conductivity of 10^{-8} m/s, a normalized model perforation discharge of 5×10^{-5} $m^3/s/m$, and an inlet hydraulic head of 2 to 50 m.

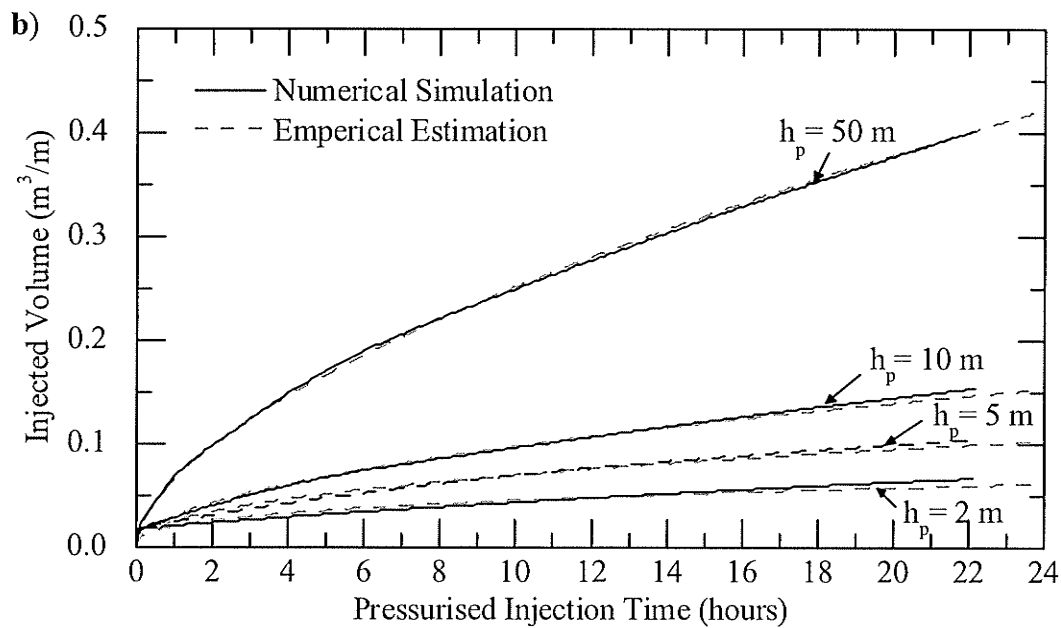
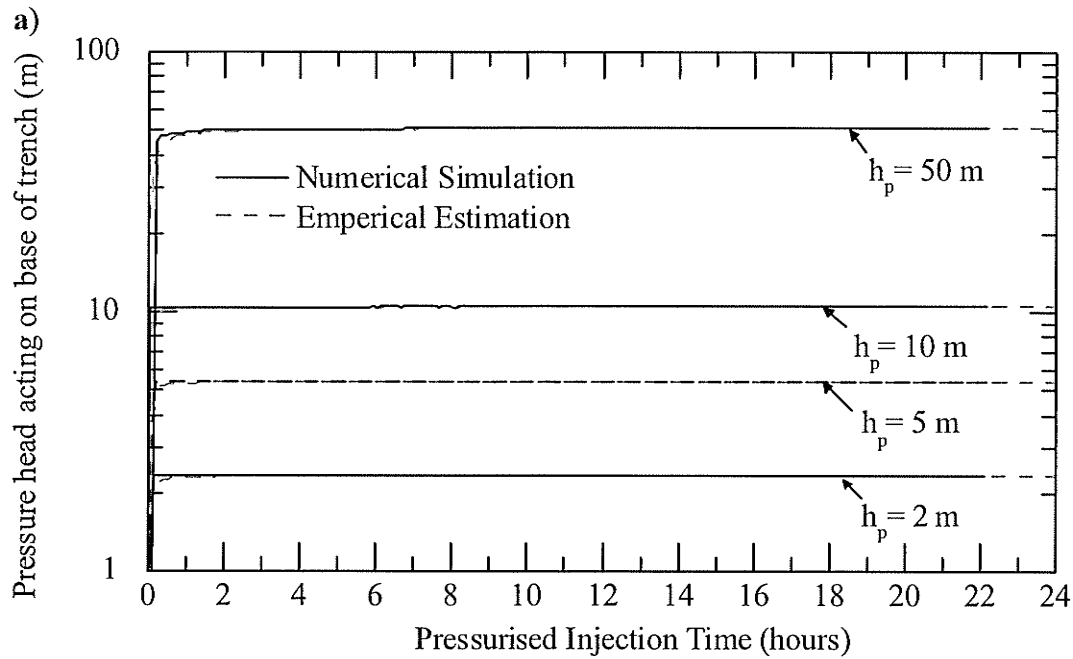


Figure B.5: Simulated and predicted a) pressure head at the trench base and b) volume injected for liquid injection into a saturated refuse hydraulic conductivity of 10^{-8} m/s, a normalized model perforation discharge of 3×10^{-5} m³/s/m, and an inlet hydraulic head of 2 to 50 m.

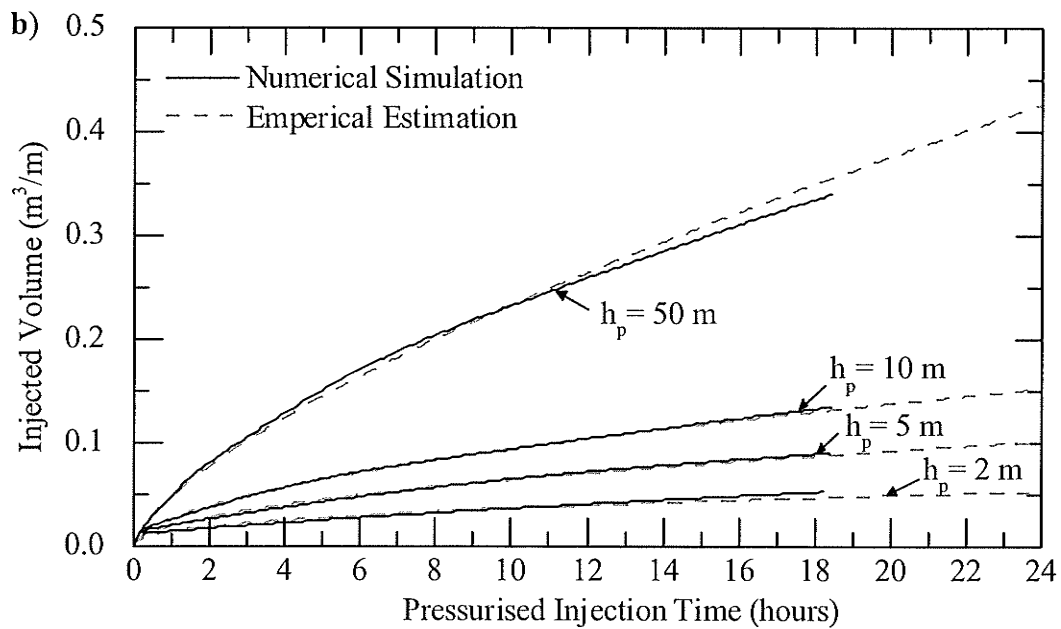
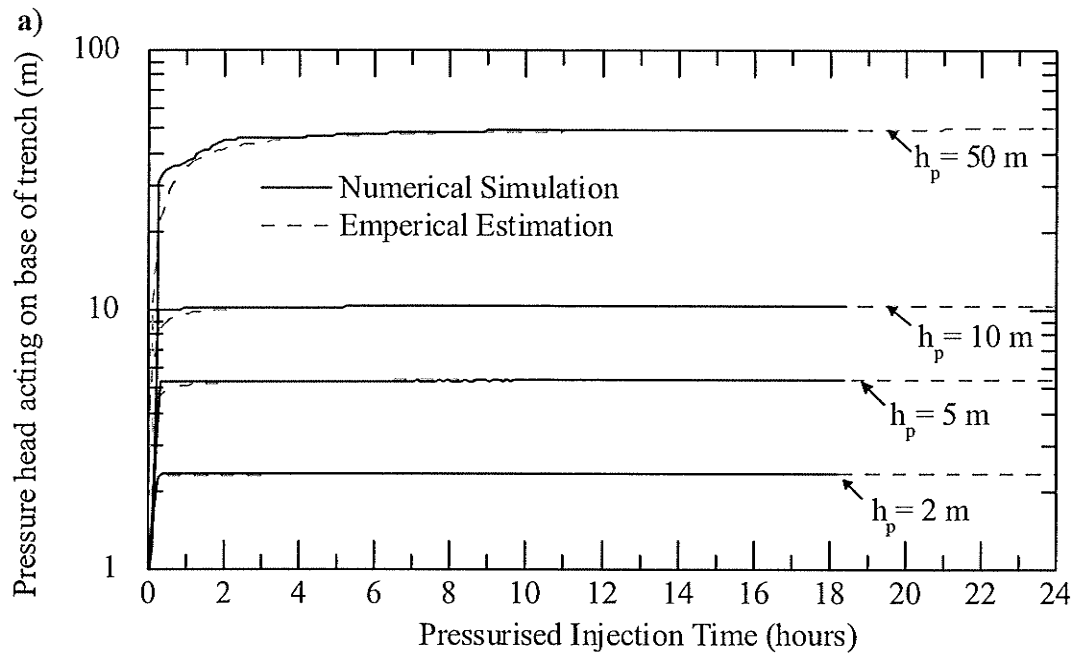


Figure B.6: Simulated and predicted a) pressure head at the trench base and b) volume injected for liquid injection into a saturated refuse hydraulic conductivity of 10^{-8} m/s, a normalized model perforation discharge of 1×10^{-5} $m^3/s/m$, and an inlet hydraulic head of 2 to 50 m.

APPENDIX C BRADY ROAD LANDFILL FIELD STUDY SURVEY

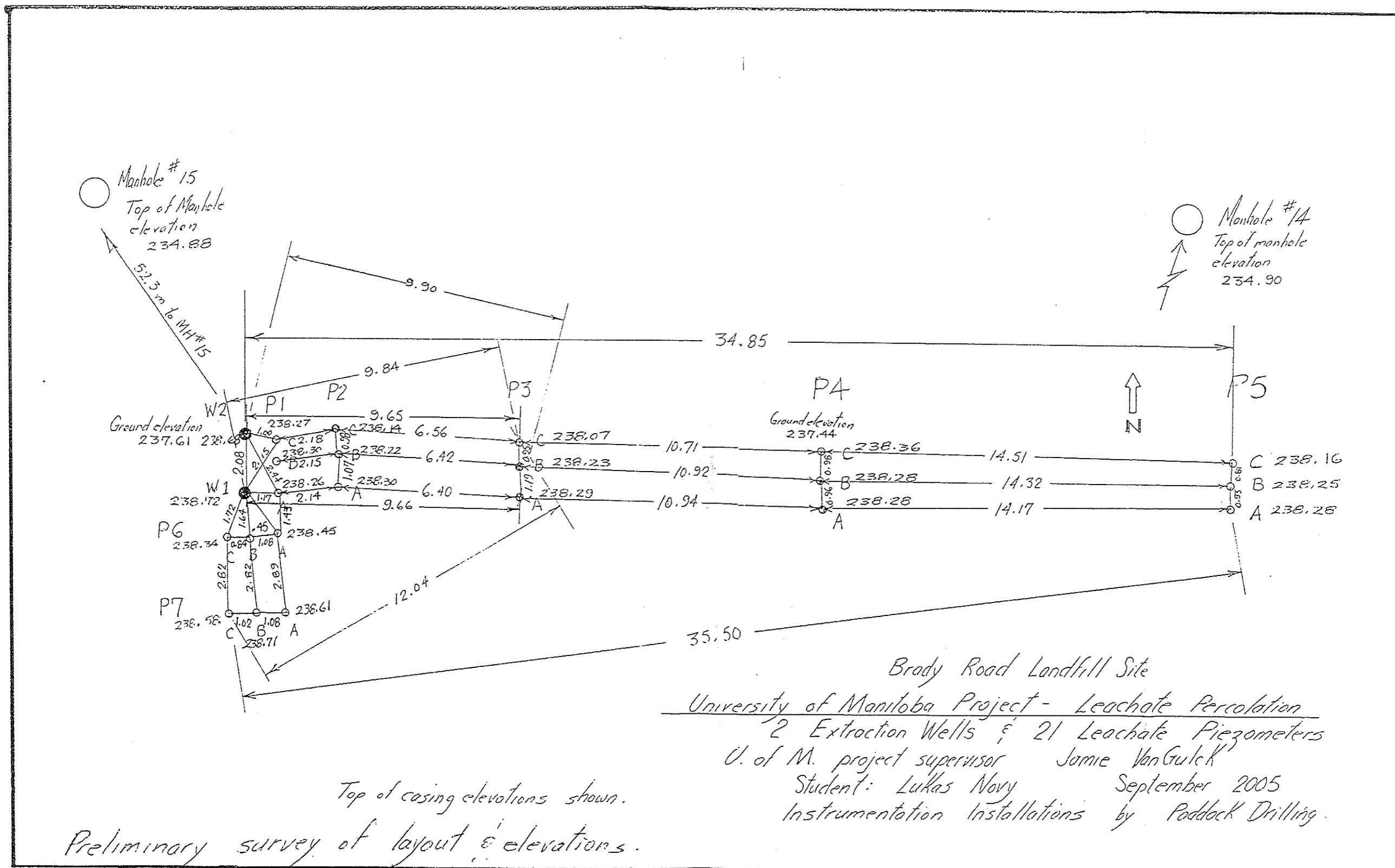


Figure C.1: Survey of Site Layout and elevations conducted by the City of Winnipeg, Solid Waste Division

BRADY ROAD LANDFILL - UNIVERSITY OF MANITOBA PROJECT
 EXTRACTIONS WELLS & LEACHATE PROBES / PIEZOMETERS 2005
 LOCATION - NORTH BOUNDARY - NORHT OF MANHOLES #14 & 15
 USE MANHOLES #14 & 15 AS BENCHMARKS

STA	BS	HI	FS	ELEV
MH#15	4.37	239.25		234.88
W1			0.530	238.72
W2(joint)			1.155	238.10
W2 (new top)				238.68
GS(W2)			1.640	237.61
P1C			0.980	238.27
P1B			0.950	238.30
P1A			0.995	238.26
P6A			0.805	238.45
P6B			0.805	238.45
P6C			0.915	238.34
P7A			0.640	238.61
P7B			0.545	238.71
P7C			0.675	238.58
P2A			0.950	238.30
P2B			1.030	238.22
P2C			1.110	238.14
P3A			0.965	238.29
P3B			1.020	238.23
P3C			1.180	238.07
P4A			0.975	238.28
P4B			0.975	238.28
P4C			0.895	238.36
GS(P4C)			1.81	237.44
P5A			0.975	238.28
P5B			1.000	238.25
P5C			1.095	238.16
MH#14			4.360	234.89
MH#15			4.365	234.89

234.90
 234.88

Figure C.2: Summary of piezometer and extraction well elevations, conducted by the City of Winnipeg, Solid Waste Division

APPENDIX D ANALYTICAL SOLUTIONS FITS

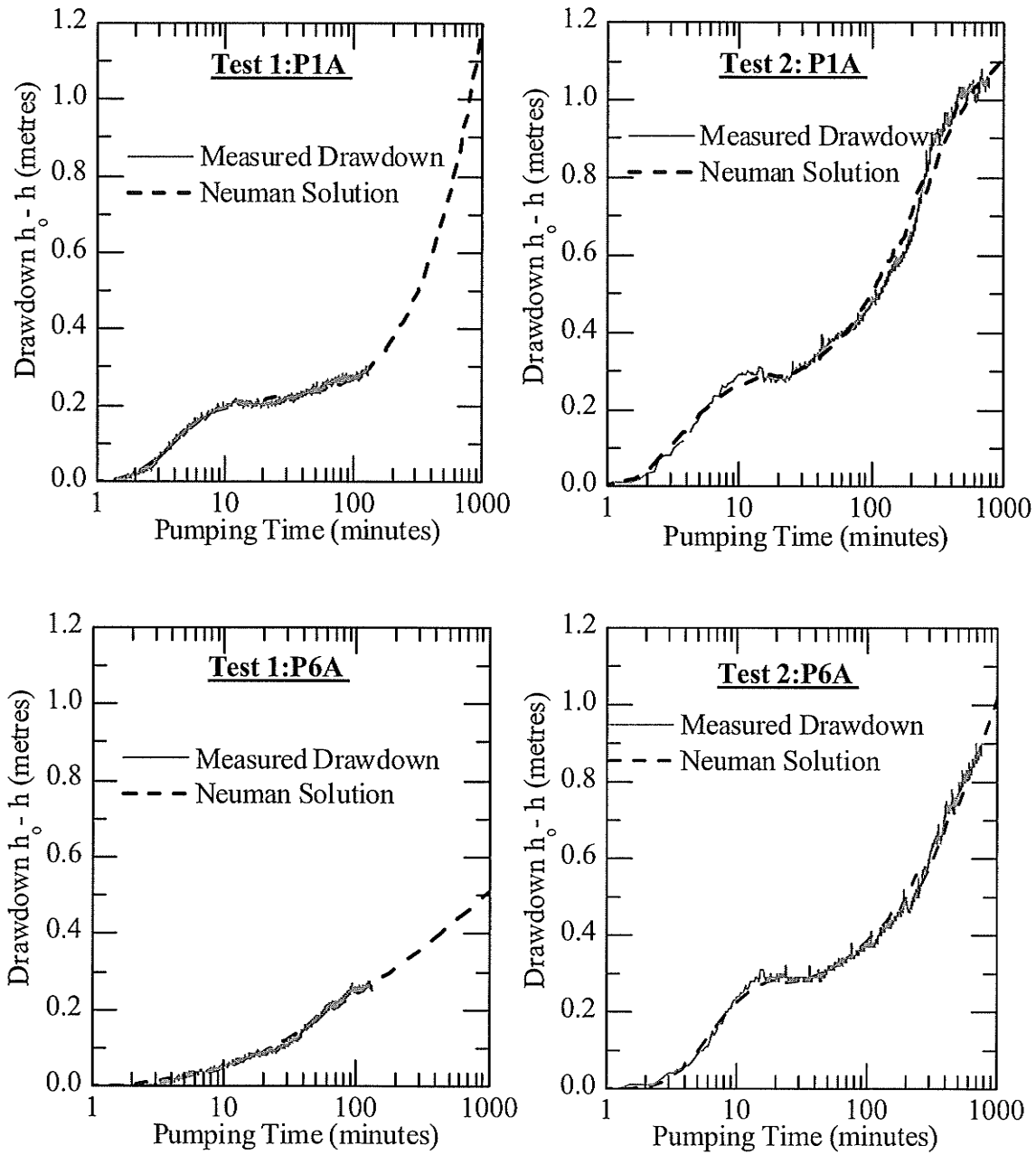


Figure D.1: Generated Neuman (1974) solution fit to measured drawdown data for piezometers at locations P1A and P6A.

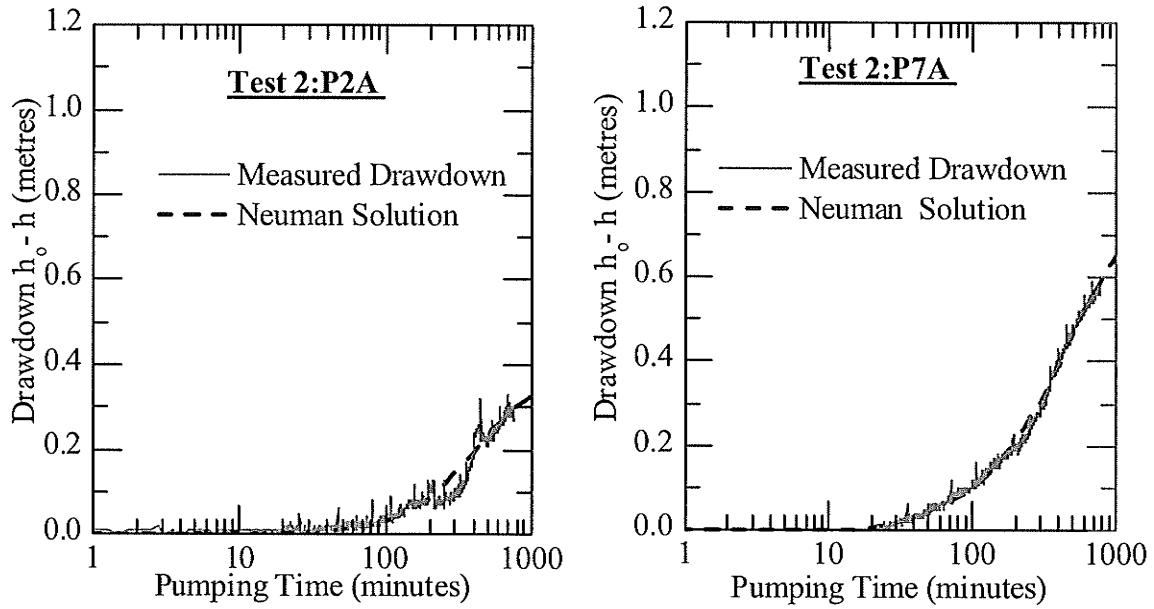


Figure D.2: Generated Neuman (1974) solution fit to measured drawdown data for piezometers at locations P2A and P7A.

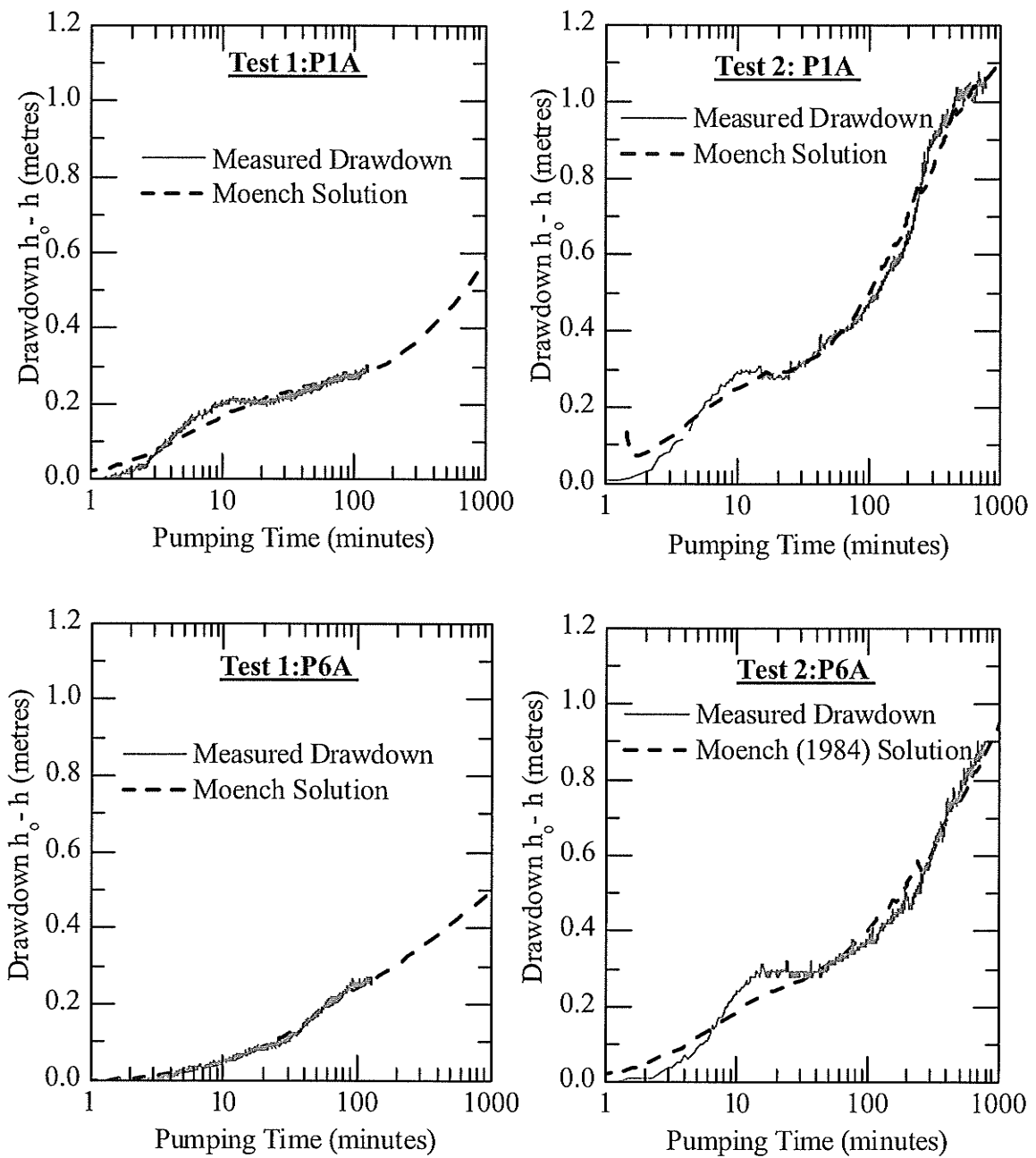


Figure D.3: Generated Moench (1984) solution fit to measured drawdown data for piezometers at locations P1A and P6A.

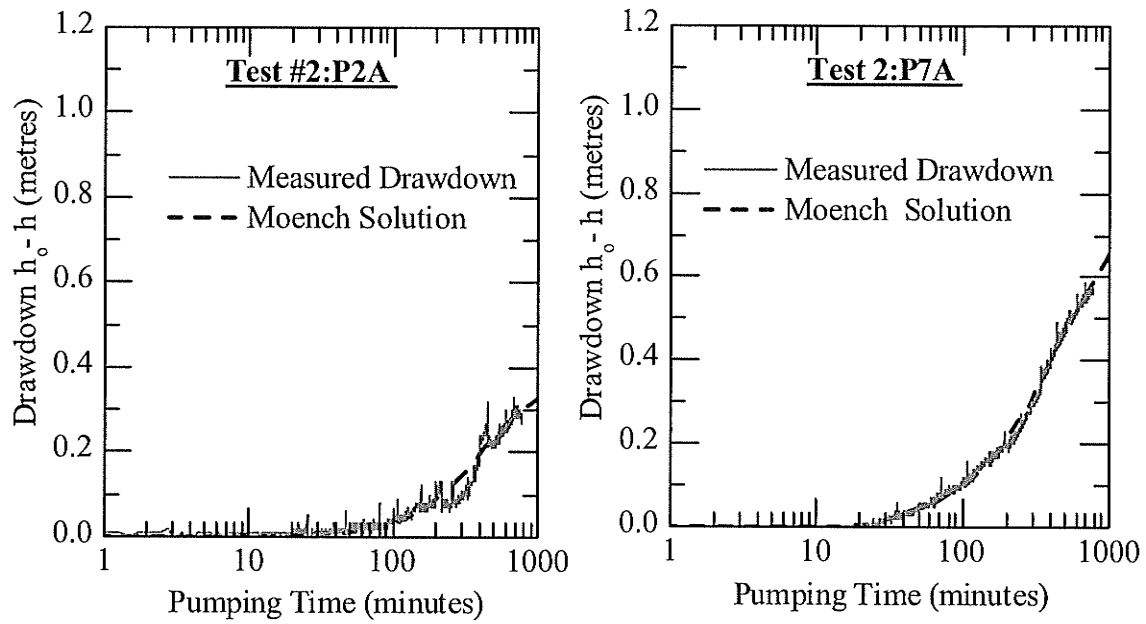


Figure D.4: Generated Moench (1984) solution fit to measured drawdown data for piezometers at locations P2A and P7A.

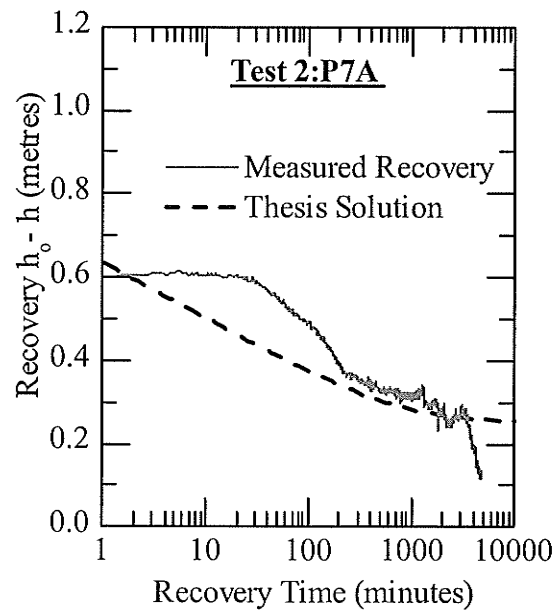
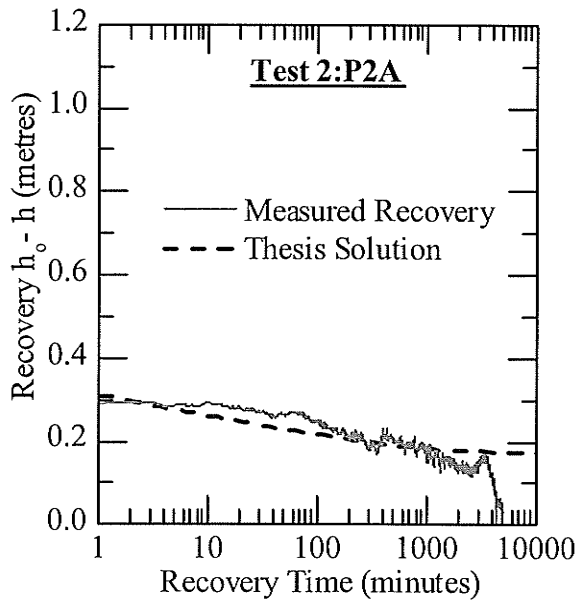
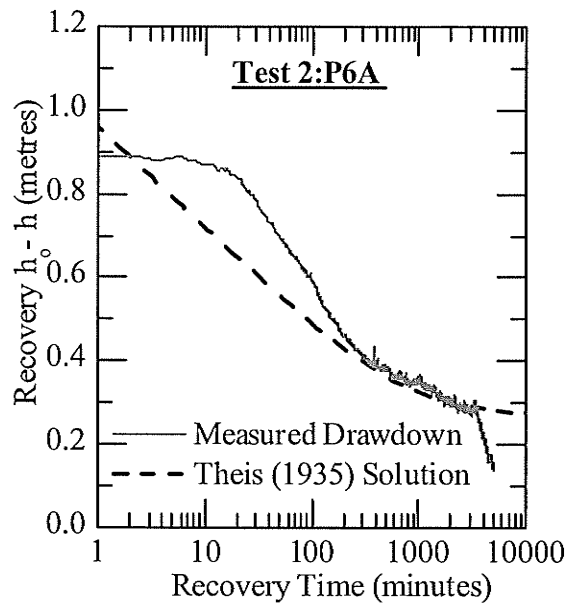
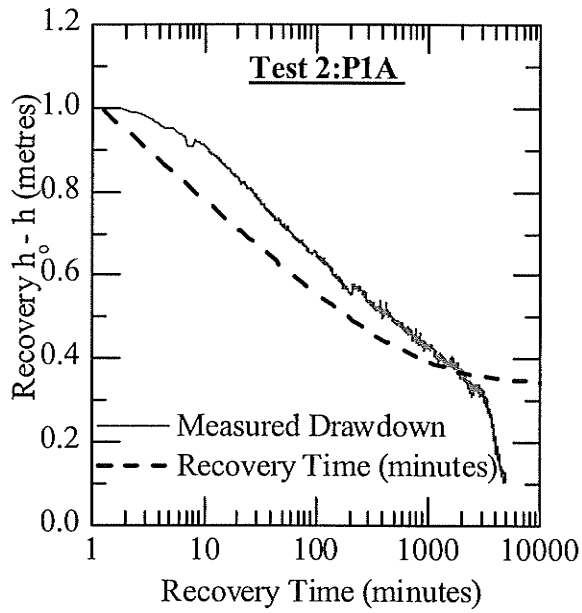


Figure D.5: Generated Theis (1935) solution fit to measured recovery data for piezometers at locations P1A, P2A, P6A and P7A.

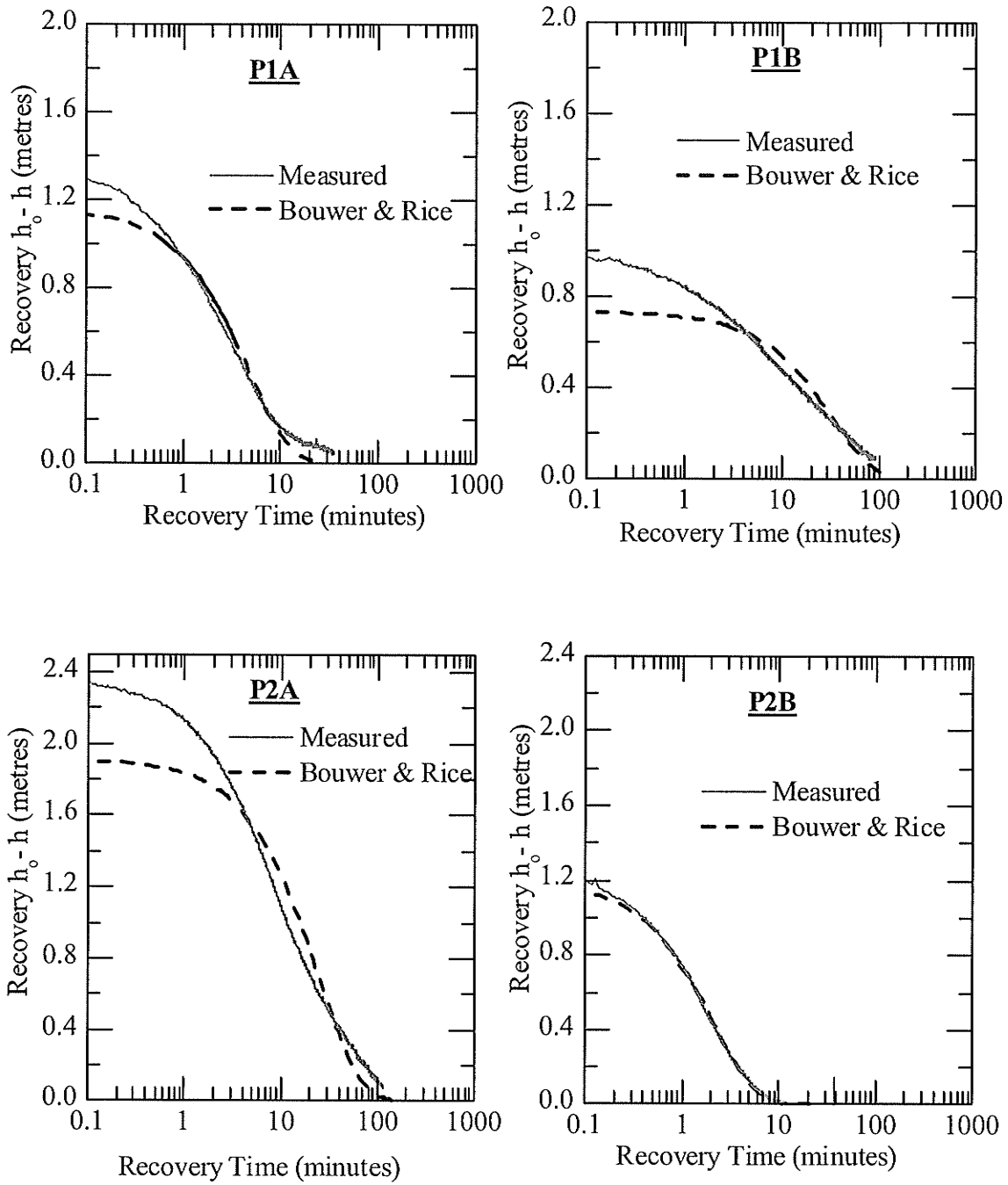


Figure D.6: Generated Bouwer and Rice (1976) solution fit to measured slug recovery data for piezometers at locations P1A,P1B, P2A and P2B.

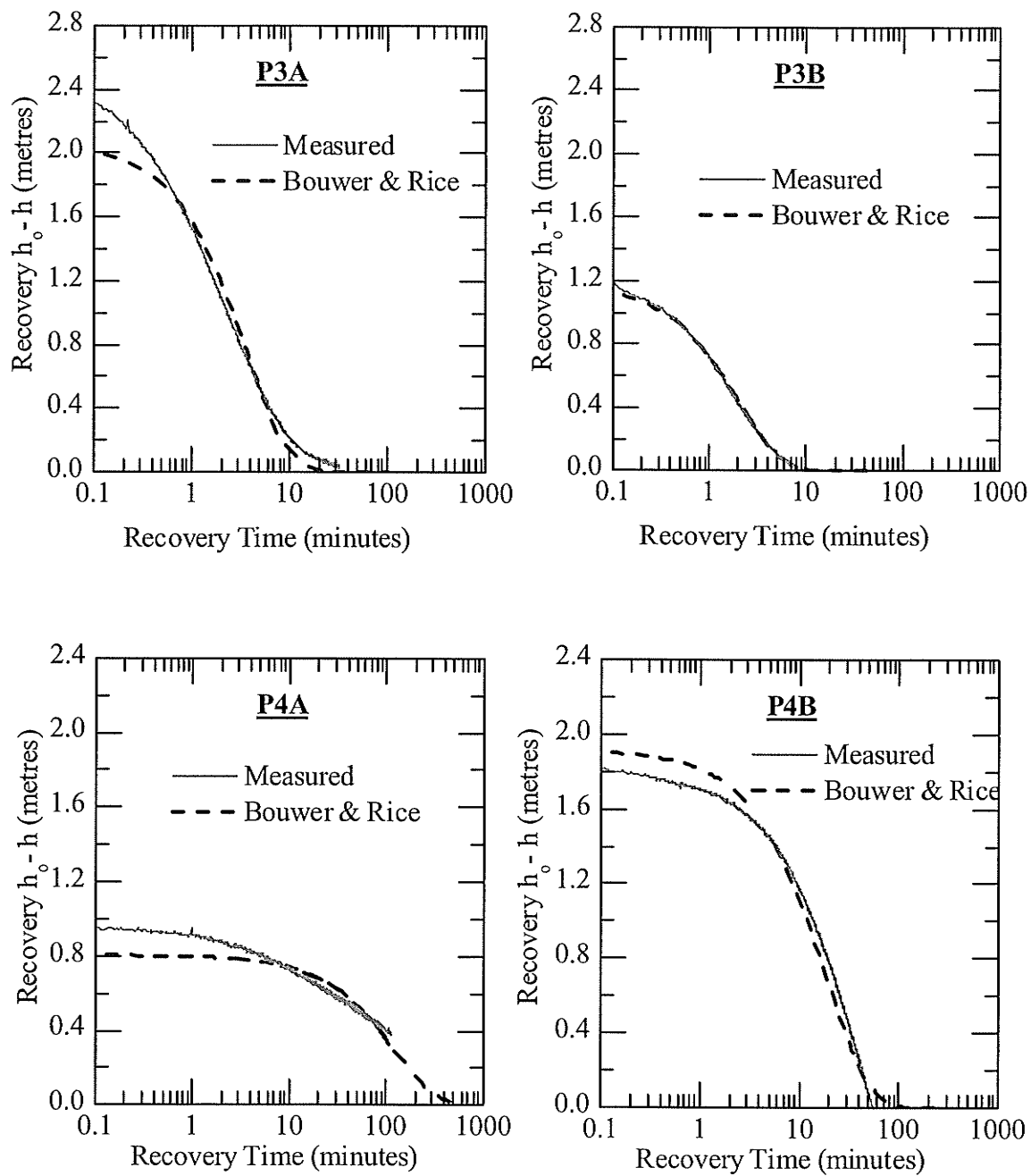


Figure D.7: Generated Bouwer and Rice (1976) solution fit to measured slug recovery data for piezometers at locations P3A, P3B, P4A and P4B.

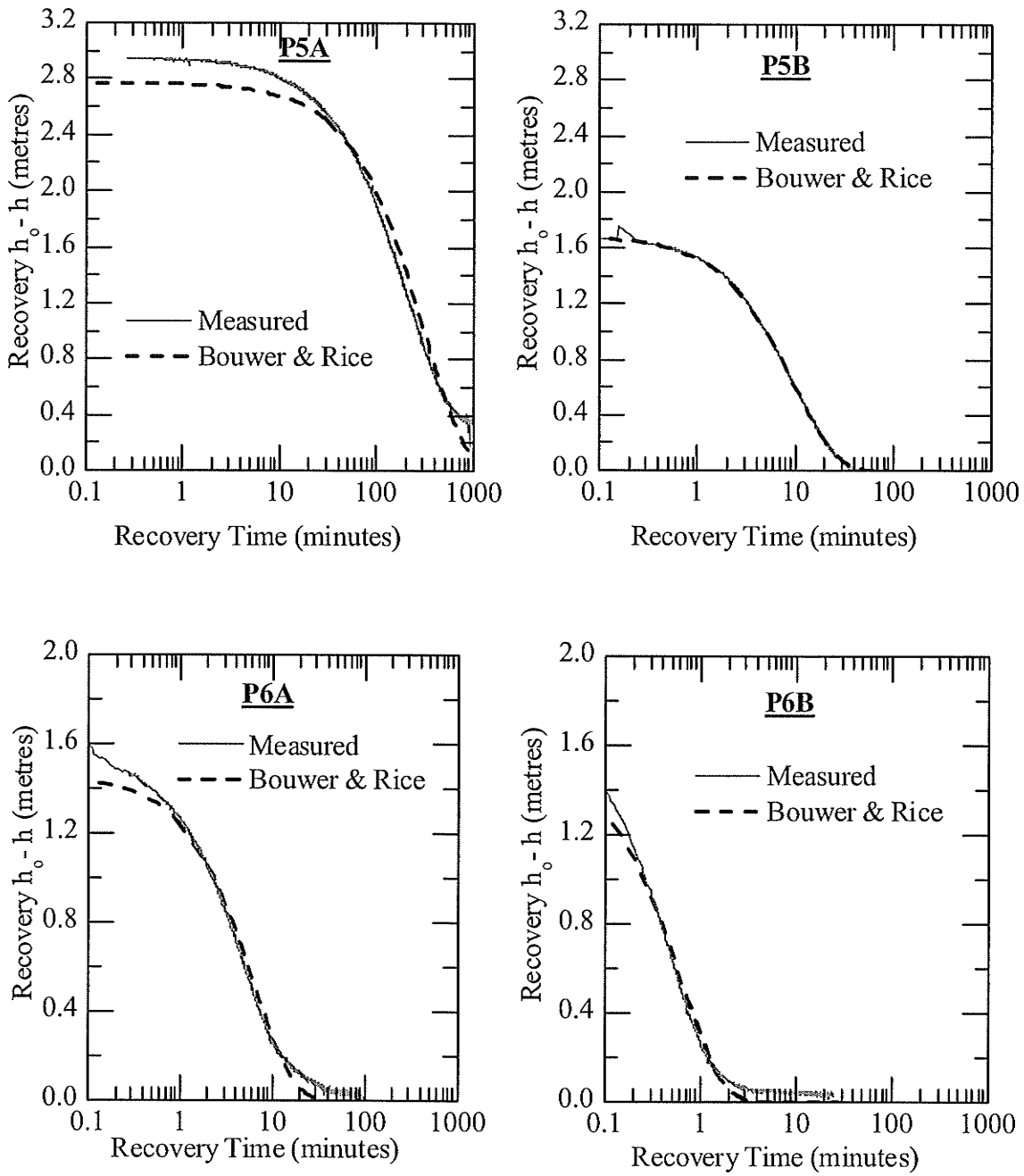


Figure D.8: Generated Bouwer and Rice (1976) solution fit to measured slug recovery data for piezometers at locations P5A, P5B, P6A and P6B.

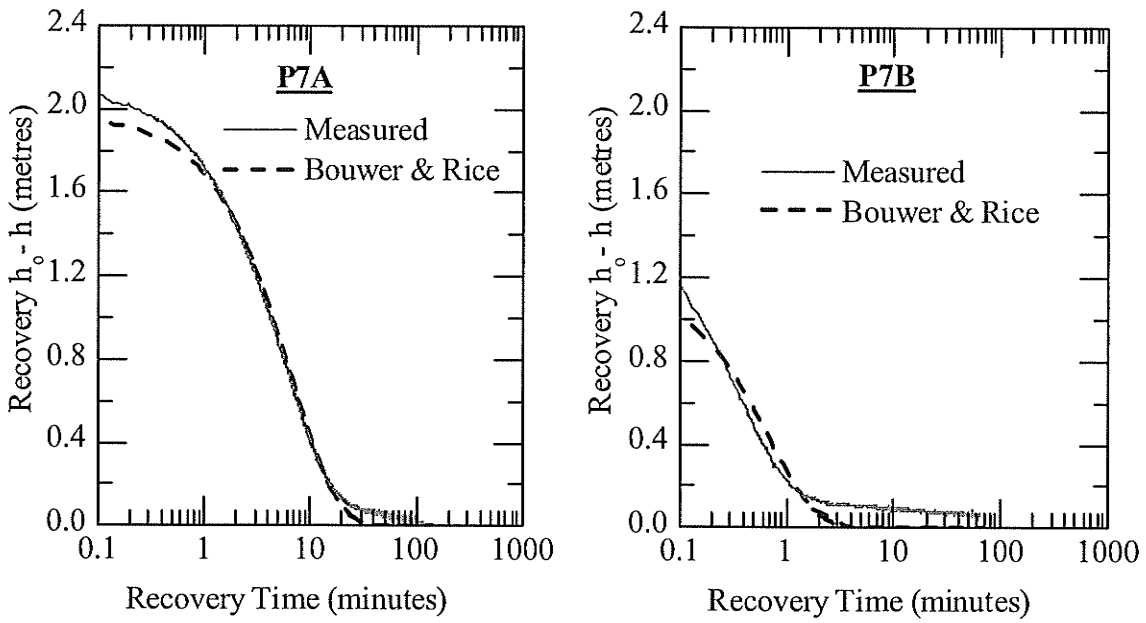


Figure D.9: Generated Bouwer and Rice (1976) solution fit to measured slug recovery data for piezometers at locations P7A, and P7B, P6A.

APPENDIX E EXTRACTION WELL NUMERICAL ANALYSIS

E.1 REFUSE ANISOTROPY NUMERICAL ANALYSIS

Average liquid elevation measurements have indicated the presence of a vertical gradient with depth at Brady Road Landfill, additionally it is hypothesized that the vertical gradient is being maintained due to liquid recharge from the higher cell elevation. A vertical gradient at the test site conflicts with the assumption of initial hydro static conditions in the Neuman (1974) solution for an unconfined aquifer. Transient saturated modeling of liquid movement from refuse to a vertical leachate extraction well using SEEP/W was conducted to investigate the anisotropy ratio outputted by the Neuman (1974) solution. The model domain and boundary conditions were selected as to match the Brady Road Field Tests. The refuse hydraulic properties were obtained from the deduced range of values using the Neuman (1974) solution for an unconfined aquifer system.

E.1.1 Model Domain and Boundary Conditions

A 2-D cross section in radial coordinates of the problem domain and also the model boundary conditions is depicted in Figure E.1. An artificial no flow ground water divide occurs at the center of the extraction well and therefore a no flow boundary is implemented at the middle of the trench and the refuse. In order to isolate the movement of liquid through the refuse only, a no flow boundary condition was assumed at the top and bottom of the refuse. A constant head boundary condition with a value of 14 m was imposed at a 35 meter distance from the center line of the extraction well. The constant head boundary condition of 14 m enforced an initial saturated thickness of 14 m across the 2-dimensional model domain; a value of 14 m was selected such that it would be of

sufficient large distance away from the imposed no flow boundary condition at the bottom of the domain. The selection of the 35 m later distance away from the extraction well center line, the 8.8 m extraction well depth, and 2 m screen length were obtained directly from the Brady Road Field Study. The collected well extraction rate with time from Test#2 was inputted as time dependent flux boundary condition across series of 9 nodes (2 meters in length) to simulate liquid extraction from refuse to a well screen.

E.1.2 Refuse Hydraulic Properties

Two anisotropy ratios of $K_H = 0.04K_V$ and $K_H = 0.19K_V$ were selected from the deduced range using the Neuman method, additionally an isotropic condition $K_H = K_V$ and a value of $K_H = 4K_V$ based from previous studies (Landva *et al.*, 1998 and Hudson *et al.*, 1999) was selected. The selected model simulations hydraulic conductivity values of 6.3×10^{-7} and 1.5×10^{-7} m/s were calculated were from the deduced high (8.9×10^{-6} m²/day) and low (2.0×10^{-6} m²/day) transmissivity range and a assumed refuse saturated thickness of 14 m. The refuse storativity was incorporated into the model through the m_w term which is used to define the compressibility of an aquifer system due to a change in pore water pressure. The m_w is related to storativity as follows:

$$m_w = \frac{S}{\gamma_w D} \quad [E.1]$$

where γ_w is the unit weight of water in, S is storativity, and D is the saturated aquifer thickness

The refuse compressibility values of 7.3×10^{-6} and 5.5×10^{-5} were calculated from the deduced storativity range of 1×10^{-3} to 8×10^{-3} and aquifer thickness of 14 m. To model the movement of gravity drainage from the saturated zone of refuse the relationship between the change in water content with suction was represented through the empirical parameters of Clapp and Hornberger (1978). The b empirical fitting parameter was chosen to equal to 7 and the saturated water content equal to 0.54 (See Chapter 3: Refuse and Hydraulic Properties for a detailed explanation of the selection of the b empirical parameter and saturated water content).

E.1.3 Vertical Extraction Well Numerical Simulations

The deduced anisotropy values from the Neuman (1974) method for an unconfined aquifer were analyzed through a set of vertical extraction well numerical simulations (see Table E.1 for summary). The simulated pressure responses at a 1m radial distance from the extraction well at a refuse depth of 8.8 m were compared to the measured drawdown response of pump test #2 at the P1A piezometer location at the Brady Road Field Study. The simulated pressure response for an anisotropy ratio range of 0.04 to 1 and refuse compressibility of $7.3 \times 10^{-6} \text{ kPa}^{-1}$ and $5.5 \times 10^{-5} \text{ kPa}^{-1}$ are displayed in Figure E.2 and Figure E.3 for refuse hydraulic conductivity values of $1.5 \times 10^{-7} \text{ m/s}$ and $6.3 \times 10^{-7} \text{ m/s}$ respectively. From the numerical simulations the observations on the influence of refuse anisotropy refuse hydraulic conductivity, and refuse compressibility on the drawdown behaviour were as follows:

- An increase in the refuse horizontal to vertical hydraulic conduction anisotropy ratio resulted in an overall larger drawdown response; however the initial drawdown response time was not greatly affected

- A decrease in the refuse hydraulic conductivity resulted in an overall larger drawdown response, and a longer duration for an initial drawdown response.
- A decrease in refuse compressibility resulted in a quicker initial response and rate of drawdown response however the magnitude of drawdown at late pump time (600- 700 minutes) was not greatly affected.

An anisotropy ratio of 0.04 was unable to simulate the observed field pressure responses as all simulations resulted in an overall underestimation of the drawdown magnitude when compared to measured values. Simulations with a anisotropy ratio of 0.19, a refuse compressibility of $7.3 \times 10^{-6} \text{ kPa}^{-1}$ and a low refuse hydraulic conductivity value of $1.5 \times 10^{-7} \text{ m/s}$ predicted the measured medium to late time (10 m to 800 min) responses fairly accurately, however the initial drawdown response occurred at a later time. The observed pressure responses with literature reported values of anisotropy ratio of 1 and 4 were best simulated with a refuse compressibility value of $5.5 \times 10^{-5} \text{ kPa}^{-1}$ and a high refuse hydraulic conductivity of $6.3 \times 10^{-7} \text{ m/s}$. The above mentioned simulations resulted in equal initial response time and a similar drawdown value at the end of pumping when compared to the measured values, however both anisotropy ratios resulted in an overestimation of the drawdown rate throughout the majority of the simulated pumping. A larger rate of drawdown than observed in the above mentioned solutions could be due to the numerical model not accounting for the possible effects of groundwater recharge. It is hypothesized that the addition of ground water recharge process in the numerical model could lead to a decrease in rate of drawdown for a high refuse hydraulic conductivity.

E.2 REFERENCES

- Clapp, R.B and Hornberger (1978) Empirical Equations for Some Soil Hydraulic Properties, *Water Resources Research*, 14(4).
- Hudson, A.P., Beaven, R.P. and Powrie, W. (1999) Measurement of the horizontal K of household waste in a large scale compression cell, *Proceedings Sardinia 99, Sixth International Landfill Symposium*, S. Margherita di Pula, Cagliari, Italy.
- Landva, A.O., Pelkey, S.A. and Valsangkar, A.J. (1998) Coefficient of Permeability of Municipal Refuse, *Proceedings, 3rd International Congress on Environmental Geotechnics*, Lisbon, Portugal, 1: 63-68
- Neuman, S.P. (1974) Effect of partial penetration on flow in unconfined aquifers considering delayed gravity response, *Water Resources Research*, 10(2): 303-312.

Table E.1: Summary of selected anisotropy ratio, refuse hydraulic conductivity, and aquifer compressibility for the conducted vertical extraction numerical simulations.

Anisotropy Ratio # K_{hor.}: K_{ver.}	Refuse Hydraulic Conductivity K (m/s)	Refuse Compressibility m_w (KPa⁻¹)
0.04	1.5 x 10 ⁻⁷	7.3 x 10 ⁻⁶
0.04	1.5 x 10 ⁻⁷	5.5 x 10 ⁻⁵
0.04	6.3 x 10 ⁻⁷	7.3 x 10 ⁻⁶
0.04	6.3 x 10 ⁻⁷	5.5 x 10 ⁻⁵
0.19	1.5 x 10 ⁻⁷	7.3 x 10 ⁻⁶
0.19	1.5 x 10 ⁻⁷	5.5 x 10 ⁻⁵
0.19	6.3 x 10 ⁻⁷	7.3 x 10 ⁻⁶
0.19	6.3 x 10 ⁻⁷	5.5 x 10 ⁻⁵
1	1.5 x 10 ⁻⁷	7.3 x 10 ⁻⁶
1	1.5 x 10 ⁻⁷	5.5 x 10 ⁻⁵
1	6.3 x 10 ⁻⁷	7.3 x 10 ⁻⁶
1	6.3 x 10 ⁻⁷	5.5 x 10 ⁻⁵
4	1.5 x 10 ⁻⁷	7.3 x 10 ⁻⁶
4	1.5 x 10 ⁻⁷	5.5 x 10 ⁻⁵
4	6.3 x 10 ⁻⁷	7.3 x 10 ⁻⁶
4	6.3 x 10 ⁻⁷	5.5 x 10 ⁻⁵

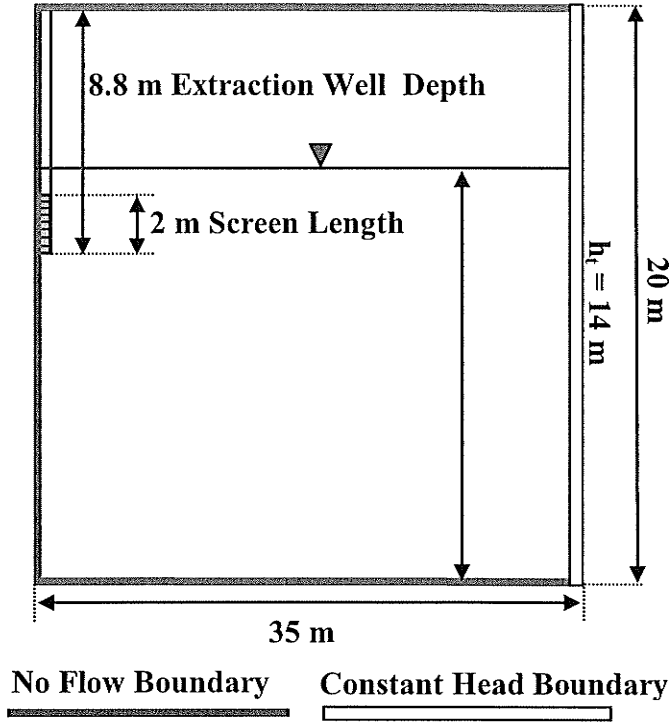


Figure E.1: Numerical model boundary conditions and problem domain for vertical extraction well analysis.

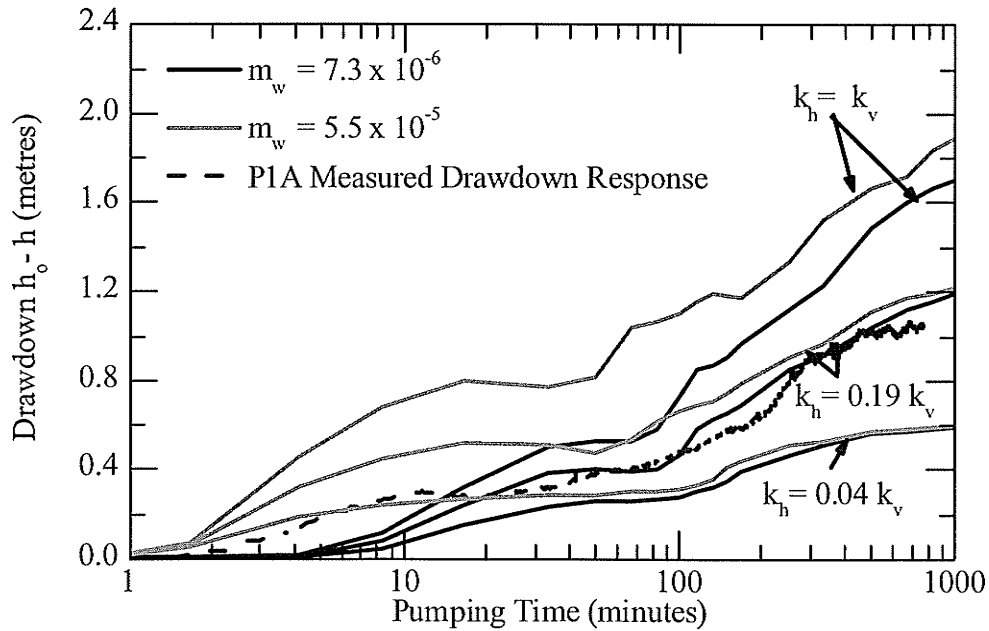


Figure E.2: Simulated drawdown response at radial distance of 1 m and refuse depth of 8.8 m for a refuse hydraulic of $1.5 \times 10^{-7} \text{ m/s}$ and vertical to hydraulic anisotropy ratios of 0.04, 0.19 and 1.

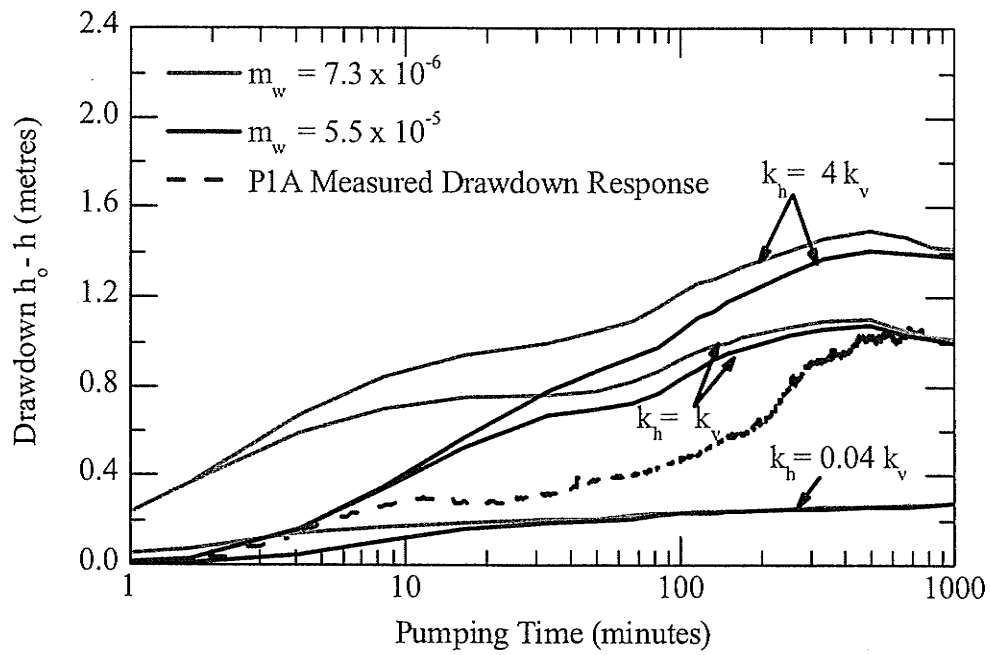


Figure E.3: Simulated drawdown response at radial distance of 1 m and refuse depth of 8.8 m for a refuse hydraulic of 6.3×10^{-7} m/s and vertical to hydraulic anisotropy ratios of 0.04, 1 and 4.